Role of Bacterial Biofilms and Extracellular Polymeric Substances in the Colloidal Stability and Transport of Hematite Nanoparticles in Synthetic Porous Media

Dissertation

zur Erlangung des akademischen Grades doctor rerum naturalium

(Dr. rer. nat.)

vorgelegt dem Rat der Chemisch-Geowissenschaftlichen Fakultät der Friedrich-Schiller-Universität Jena

von Sneha Pradip Narvekar

geboren am 19 December 1985 in Dombivli, Mumbai, India.

Gutachter:

1. Prof. Dr. Kai Uwe Totsce .

2. Prof. Dr. Kögel Knabner

Tag der Verteidigung: 17/01/2017

Dedicated to the five pillars of my life

Dada, Mothiaie, Baba, Aie and Nilesh

Abstract

The heterogeneous physicochemical properties of biofilm and extracellular polymeric substances (EPS) play an important role in deciding the fate of transport of nanoparticles in subsurface. However, contrasting results have been observed for the mobility of different nanoparticle transport in porous media coated with biofilms. Also, no comparative studies have been done linking the effect of biofilms on colloidal stability and mobility of colloids to date.

Laboratory scale experiments were conducted to obtain insights into different ways bacterial biofilms and EPS can influence the transport of nanoparticles in porous media. Using complementary experimental approaches, we investigated (1) the effect of microbial EPS on the colloidal stability of nanoparticles, (2a.) the transport of uncoated colloidal nanoparticles in biofilm and EPS-coated porous media, (2b.) the transport of EPS-coated colloidal nanoparticles in uncoated porous media (2c), the combined transport of EPS-coated colloids in biofilm and EPS-coated porous media, and finally (3) the remobilization of deposited colloidal nanoparticles by EPS. Laboratory synthesized hematite nanoparticles (HNP) and *Bacillus subtilis 168 (DSM 402)* were used as nanoparticles and biofilm forming bacterium respectively.

To study the effect of EPS on the colloidal stability, HNP were amended with three increasing concentrations of EPS (20, 200 and 500 mg/l carbon) resulting in carbon:iron ratios 1:5, 2:1 and 5:1, respectively. The zeta potential (ZP), the shift in isoelectric point and the change in the critical coagulation concentration (CCC) for NaCl and $CaCl_2$ showed formation of colloidally stable organo-mineral colloids at higher concentrations of EPS (200 mg/l and 500 mg/l of carbon, HNP2:1, HNP 5:1). However, lower concentrations of EPS (20 mg/l carbon, HNP 1:5) resulted into aggregation of HNP.

The transport of uncoated and EPS-coated HNP colloids at environmental pH was studied with closed flow columns experiments in three different synthetic porous media, i.e., uncoated, biofilm-coated, and EPS-coated glass beads. No drastic change was observed in the pH and the electrical conductivity of the system during the transport experiments. However, a constant amount of organic matter and bacterial cells were continuously released from the porous media coatings.

In the first scenario, positively charged uncoated HNP were immobile and retained in uncoated-glass bead porous media. Contrary, a mobile fraction of negatively charged HNP was observed in biofilms and EPS-coated porous media. The charge reversal of HNP during transport is due to adsorption of organic matter released from the coatings forming organo-mineral associations of HNP and components of the biofilm or EPS.

Transport of EPS-coated HNP in coated and uncoated porous media highlighted the role of colloidal stability in transport under saturated conditions. A mobile fraction of colloidally stable EPS-coated HNP (HNP 2:1 and HNP 5:1) persists in all three porous media due to electro-steric repulsion between like charged surfaces. However, colloidally unstable EPS-coated HNP (HNP 1:5) are immobile in uncoated and EPS-coated porous media. Interestingly, in biofilm-coated porous media, a fraction of colloidally unstable EPS-coated HNP (HNP 1:5) were transformed to colloidally stable nanoparticles (|ZP|>20 mV) and were mobile. This transformation in colloidal stability may be due to the excess organic matter released from the biofilm-coated surfaces conferring colloidal stability.

Last, the remobilization studies with EPS solutions showed desorption of HNP previously retained in the uncoated porous media. This was attribute to the strong affinity of EPS to HNP resulting in the formation of negatively charged organo-mineral EPS-HNP colloids.

In conclusion, biofilms and EPS influences mobility of HNP where normally HNP would be immobile in absence of biofilms. This study highlights the significance of biofilms and EPS in the transformation of nanoparticles to form organo mineral colloids and influencing colloidal stability and transport of nanoparticles. Such transformations will also have environmental implication on colloid facilitated transport of contaminants, which are associated with HNP.

Zusammenfassung

Mikrobielle Biofilme sind aufgrund ihrer vielfältigen Interaktionen mit mobilen Kolloiden und mit immobilen Oberflächen und den daraus entstehenden organo-mineralischen Verbindungen von sehr großer Bedeutung für den Transport von anorganischen Kolloiden durch den porösen Untergrund. In dieser Arbeit wurden Experimente auf Laborskala durchgeführt, um die verschiedenen Möglichkeiten zu untersuchen, wie mikrobielle Biofilme und extrazelluläre polymere Substanzen (EPS) den Transport von Nanopartikeln durch poröse Medien beeinflussen. Mit komplementären experimentellen Ansätzen wurde dabei (1) der Effekt von mikrobiellen EPS auf die Kolloidstabilität von Nanopartikeln, (2a.) der Transport von EPS-freien Nanopartikeln durch Biofilm-beschichtete und EPS-beschichtete poröse Medien, (2b.) der Transport von EPS-beschichteten Nanopartikeln durch ein unbeschichtetes poröses Medium, (2c.) der Transport von EPS-beschichteten Kolloiden durch Biofilm- und EPS-beschichteten porösen Medien und (3) die Remobilisierung von abgelagerten Kolloiden durch EPS untersucht. Dafür wurden synthetischer Hämatit als Nanopartikel (HNP) und *Bacillus subtilis 168 (DSM 402)* als Biofilm-produzierende Mikroorganismen ausgewählt.

In den Untersuchungen des EPS-Effekts auf die Kolloidstabilität wurden HNP mit drei EPS-Konzentrationen (50, 200, 500 mg C/l) behandelt. Das entsprach EPS:HNP-Verhältnissen von 1:5 (HNP 1:5), 2:1 (HNP 2:1) beziehungsweise 5:1 (HNP 5:1). Die jeweiligen Zeta-Potentiale (ZP) und Verschiebungen des isoelektrischen Punkts und der kritischen Koagulationskonzentration (CCC) unter Zugabe von NaCl und $CaCl_2$ deuteten auf die Bildung von stabilen organo-mineralischen Kolloiden in den HNP 2:1- und HNP 5:1-Behandlungen hin. Geringere EPS-Konzentrationen (HNP 1:5) begünstigten jedoch eine Aggregation der HNP.

Mittels Kreislauf-Säulenexperimenten wurde der Transport von unbeschichteten und EPS-beschichteten HNP bei bodentypischen pH-Bedingungen in drei künstlichen porösen Medien untersucht (unbeschichtete, Biofilm-beschichtete und EPS-beschichtete Glaskugeln). Es wurden keine drastischen Änderungen im pH-Wert und der elektrischen Leitfähigkeit während der Transportexperimente festgestellt. Allerdings wurde eine konstante Menge an organischer Substanz und Bakterienzellen kontinuierlich aus den Glaskugelbeschichtungen freigesetzt. Positiv geladene, unbeschichtete HNP wurden durch die unbeschichteten Glaskugeln zurückgehalten und dadurch immobilisiert. Im Gegensatz dazu wurde eine mobile Fraktion von negativ geladenen HNP in den Experimenten mit Biofilm- und EPS-beschichteten Glasperlen beobachtet. Die aus den Beschichtungen freigesetzten organischen Substanzen adsorbierten dabei an den HNP, was in einer Umkehrung der Netto-

Oberflächenladung und damit zur Bildung von negativ geladenen, organo-mineralischen HNP resultierte.

Die Mobilität von EPS-beschichteten HNP sowohl in beschichteten als auch in unbeschichteten porösen Medien unterstrich die Bedeutung der Kolloidstabilität für den Transport unter wassergesättigten Bedingungen. Durch elektrostatische Abstoßungskräfte zwischen gleichgeladenen Oberflächen war eine Fraktion von stabilen, EPS-beschichteten HNP (HNP 2:1 und HNP 5:1) dauerhaft mobil in den drei untersuchten porösen Medien. Im Gegensatz dazu waren instabile, EPS-beschichtete HNP (HNP 1:5) immobil in unbeschichteten und EPS-beschichteten porösen Medien. Diese instabilen HNP waren jedoch teilweise mobil im porösen Biofilm-beschichteten Medium, da ein Teil dieser Partikel zu stabilen Kolloiden umgewandelt wurde ($|ZP| > 20$ mV). Diese Änderung in der kolloidalen Stabilität könnte aus dem Überschuss an organischen Substanzen resultieren, welche von den Biofilm-beschichteten Oberflächen freigesetzt wurden.

Die Experimente bezüglich der Remobilisierung von HNP durch EPS-haltige Lösungen zeigten eine Desorption von HNP, welche vorher an unbeschichteten Glaskugeln zurückgehalten wurden. Diese Beobachtung wird mit der hohen Affinität von EPS für HNP erklärt, was zur Bildung von negativ geladenen, organo-mineralischen EPS-HNP-Kolloiden führte.

Schlussfolgernd beeinflussen Biofilme und EPS die Mobilität von HNP. Diese HNP wären immobil bei Absenz von Biofilmen. Diese Arbeit unterstreicht damit die Signifikanz von Biofilmen und EPS hinsichtlich der Transformation von Nanopartikeln zu organo-mineralischen Kolloiden, was deren kolloidale Stabilität und damit ihr Transportverhalten bestimmt. Solche Transformationen haben demnach ebenfalls eine Umweltrelevanz hinsichtlich des kolloid-gekoppelten Transports von Kontaminanten.

Table of Contents

List of Figures

List of Tables

List of Abbreviations

Atomic force microscopy	AFM
Colloidal filtration theory	CFT
Confocal laser scanning microscopy	CLSM
Critical coagulation concentration	CCC
Derjaguin-Landau-Verwey-Overbeek theory	DLVO
Diffusion-limited aggregation	DLA
Dissolved organic carbon	DOC
Dynamic light scattering	DLS
Electrical double layer	EDL
Extended Derjaguin-Landau-Verwey-Overbeek theory	EDLVO
Extracellular polymeric substances	EPS
Fourier transform infrared spectroscopy	FTIR
Hematite nanoparticles	HNP
Isoelectric point	pH_{IEP}
Lewis acid base	AB
Luria-Bertani media	LB
Polyvinyls pyrrolidone	PVP
Reaction-limited aggregation	RLA
Scanning electron microscopy	SEM
X-ray diffraction	XRD
Zeta potential	ZP

1 Introduction

1.1 Colloids and nanoparticles

Colloids and nanoparticles have been present on the earth for billions of years. However, recently they have been a subject of intense research due to easy synthesis and multiple uses. Colloidal particles are defined as particles smaller than 1 μm in at least one dimension with a high specific surface area (10-800 m^2/g) (Hochella, 2008; Kretzschmar & Schafer, 2005; Theng & Yuan, 2009). Nanoparticles are a subset of colloidal particles and are defined as particles smaller than 100 nm in at least one dimension (Figure 1.1). Particles with size smaller than 100 nm in one, two or three dimensions are classified as nanofilms, nanorods and nanominerals respectively (Hochella, 2008). Minerals that exist only in nano size range are termed nanominerals (example: ferrihydrite) while; mineral nanoparticles are minerals that also exist in larger sizes (Hochella, 2008).

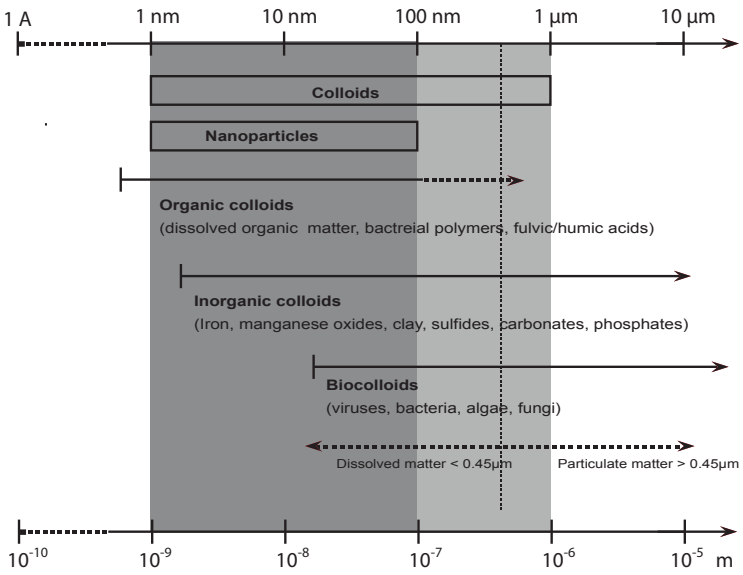

Figure 1.1 Size chart for nanoparticles and colloids (Modified from Christian et al. (2008))

For colloids and nanoparticles, size matters the most. Various properties like chemical, optical, thermodynamic vary as a function of size. Due to the extremely small size and similarity in the composition to the soil matrix, natural colloids exhibit a high mobility in the environment (Mccarthy & Zachara, 1989). They are also more reactive than their larger counterpart due to a larger surface area (Waychunas & Zhang, 2009). This effect is even more pronounced for particles smaller 10 nm. The surfaces of the colloids contain a high proportion of functional groups, which enable sorption to various heavy metals, organic pollutants and nutrients. The colloids thus constitute an important carrier phase for metal/contaminant transport in the environment. This is termed as colloid facilitated transport. The transport of colloids and nanoparticles in the environment has been studied with different objectives such as its effect on the transport of engineered nanoparticles in environment (G. Chen et al., 2012; K. L. Chen & Elimelech, 2008; Jiang et al., 2012; Mitzel & Tufenkji, 2014), waste-water treatment management (Khaydarov & Gapurova, 2010; Nashaat 2013), groundwater contamination (Baumann, 2010; Lanphere et al., 2014) and also remediation purposes (Fu et al., 2014).

1.2 Natural colloids

Natural colloids are ubiquitous in soil and aquatic environments. A large fraction of minerals occurs as nanoparticles in the environment (Christian et al., 2008). They generally consist of clay minerals, mineral precipitates (e.g. Fe, Al, Mn or Si oxides and hydroxides, carbonates, phosphates) and organic biopolymers (e.g. humic acid fulvic acid and extracellular polymers) (Table 1.1). The concentration of natural colloids depends mainly on the environment they are formed and present in.

The colloids are generally formed by biotic, abiotic processes or anthropogenic process. In fact, the rates of biotic mineralization are higher than abiotic factors

(Lüttge et al., 2005). Erosion by wind, dust, water currents are few of the abiotic process documented for formation of colloids (Hochella, 2008). In acid mine drainage systems, iron nanoparticles are known to be precipitated as nanoscale iron hydroxides /oxides /oxyhydroxides. This due to the high solubility of oxygen, low solubility of iron, and faster oxidation kinetics that leads to rapid precipitation of nanoparticles (Banfield & Zhang, 2001).

Table 1.1 Categorization of colloids (modified from (Christian et al., 2008))

Natural colloids		**Engineered nanoparticles**
Inorganic colloids	**Organic colloids**	
	Macromolecules	Polymers
	Humic acids	Polystyrene latex particles
Silicates	Fulvic acids	Surfactants
Mica	Extracellular polymeric	Dyes and pigments
Kaolinite	substances	Metals (Au,Ag, Fe, Zero
Montmorillonite	Polysaccharides	valent Fe)
Oxides/hydroxides of Fe, Mn	Proteins	Metal oxides (oxides of Ti,
and Al	Cellular debris	Zn, Zr, Ce)
Carbonates	Coal/black carbon	Fullerenes
Phosphates	**Bio-colloids**	Quantum dots
Metal sulfides	Bacteria	Functionalized materials
	Viruses	
	fungi	

Colloids of Fe, Al and trace metals are also formed by the natural mixing of acidic, sulphate-rich acid mine drainage water with near-neutral surface waters (Zänker et al., 2002). Moreover, hydrothermal vents are considered to be "nanoparticle factories" in marine environments as since they lead to formation of polymetallic sulphide nanoparticles (Yucel et al., 2011). Biotic factors mainly include bio-mineralization by microorganisms. Microorganisms lead to bio-mineralization either to prevent itself from toxicity of the metals or as storage granules for micronutrients. Microorganism can also accumulate metal cations, which then combine with anions (carbonate,

phosphate, silicate) from the surrounding medium to form a variety of nanosized minerals (Labrenz et al., 2000). Lastly, anthropogenic activities such as waste combustion or wear and tear of man-made products can also lead to formation of colloids.

1.3 Engineered nanoparticles

Engineered nanoparticles have many applications in diverse consumer products such as personal-care products, food storage containers, cleaning supplies, bandages, and clothing. Increased use of nanoparticle containing products has resulted in an increase in released of engineered nanoparticles into the environment. Many studies are focused to study the implications of such nanoparticles introduced into the environment (Eg: (Braydich-Stolle et al., 2009; Gwinn & Vallyathan, 2006; Soni et al., 2015; Wagner et al., 2014)).

Apart from used in manufactured products, certain nanoparticles are deliberately introduced into the environment. Silver, TiO_2, and ZnO_2 and carbon nanotubes nanoparticles have antimicrobial properties and are used in drinking water treatments (Gehrke et al., 2015). Also, zero valent iron is used for remediation of contaminants due to their high reactivity to heavy metal and organic pollutants (Fu et al., 2014).

1.4 Colloidal stabilization of nanoparticles

An important property of colloids is their aggregation, which also plays an important role in transport of colloids. A colloidal system consists of a dispersing medium and a dispersed colloidal phase. The dispersing medium can be gas, liquid or a solid. However, in soil and aquatic environments, the medium is mainly water while the nanoparticles can be inorganic or organic or a mixture of both (MacKay & Gschwend, 2001). When dispersed in a medium, nanoparticle either aggregate or remain as single particles (The latter state is called “colloidal stable”). Colloidal stabilization depends

on the force balance of attractive and repulsive forces in between the individual particles. The colloidal stability of nanoparticles in a medium is controlled by three major mechanisms: electrostatic stabilization, steric stabilization and electrosteric stabilization.

1.4.1 Electrostatic stabilization

In electrostatic stabilization, the attractive van der Waals forces are counterbalanced by the repulsive Coulomb forces acting between the charged colloidal particles. When a charged surface of the nanoparticles is suspended in a medium, a layer of counter ions and the solvent molecules is formed around the particles, called a stern layer. The stern layer causes repulsion of like charges according to coulomb's law preventing aggregation of nanoparticles (Hiemenz & Rajagopalan, 1997).

1.4.2 Steric stabilization

High molecular weight polymers sorb on the surfaces of minerals forming layers 10 to 20 nm in thickness (Grasso et al., 2002; K. Li & Chen, 2012). The adsorbed polymers can extend out from the surface into solution, and may rearrange their position on the surfaces in response to the environment. The configuration and osmotic effect and the volume restriction by the polymers result in steric forces (Hiemenz & Rajagopalan, 1997; Tadros, 2006).

1.4.3 Electrosteric stabilization

More recently, Fritz et al. (2002) described electrosteric stabilization for charged polymers which includes both; electrostatic stabilization by charged ions and steric stabilization by polymer brushes (Fritz et al., 2002).

1.5 The DLVO and EDLVO theory

The interactions between the colloidal particles and their aggregation behavior is described by Derjaguin-Landau-Verwey-Overbeek (DLVO) theory. This theory

defines the net surface interaction energy between colloids (Israelachvili, 1982). The aggregation kinetics of colloids (polymer coated and uncoated) has been commonly interpreted using the DLVO theory by many researchers (K. L. Chen & Elimelech, 2007; K. L. Chen et al., 2006; Di Marco et al., 2007; Hu et al., 2010; Huynh & Chen, 2011). According to the DLVO theory, the net surface interaction energy is equal to the sum of the inter-actions between electrical double layer (EDL) and van der Waals forces, which vary with the separation distance between colloids.

Classical DLVO assumes the particle surfaces are chemically inert (Perni et al., 2014). However, most mineral nanoparticles and organic polymers have a chemically active surface. Hence simple implementation of DLVO theory is often inadequate to describe the interfacial interactions of colloidal solutions. Recently, the Extended DLVO (EDLVO) has been used to explain the interaction between the colloidal particles using acid-base and steric interactions (Huang, 2012; K. Li & Chen, 2012; Romero-Cano et al., 2001). Lewis acid–base (AB) interaction account for hydrogen bonding on approach of nanoparticles and the suspending medium. Based on the hydrophobic/hydrophilic property of nanoparticles and the suspending medium, these interactions could be attractive (hydrophobic attraction) or repulsive (hydrophilic repulsion or hydration effects), and can be up to 10–100 orders of magnitude higher than electrostatic or van der Waals interactions (Azeredo et al., 1999). Similarly, the steric force can also be attractive or repulsive based on the charge, concentration and the configuration of the polymers (Grasso et al., 2002; Tadros, 2006). However, Huynh and Chen (2011) have shown that steric forces dominate the interaction of colloids only if the adsorbed layer thickness is larger than the Debye length. Flat adsorbing molecules show a weak steric hindrance while molecules that extend from

the surface show a strong steric hindrance (Huynh & Chen, 2011; Philippe & Schaumann, 2014).

1.6 Transport of colloids in the porous media

The transport of colloids and nanoparticles mainly depend on the stability and mobility of the colloids and its interactions with the surrounding milieu (Mccarthy & Zachara, 1989). A few factors are identified based on the physical, chemical and biological processes/interactions between the colloids and its surrounding (Figure 1.2) (Kretzschmar & Schafer, 2005; Mccarthy & Zachara, 1989). Particularly, colloidal stability/ the aggregation-deposition of the colloids at the given environmental conditions dominants the transport of the colloids.

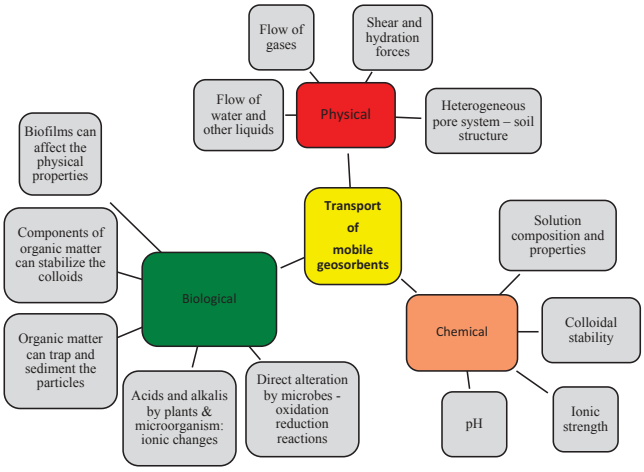

Figure 1.2 Physical, chemical and biological factors affecting the transport of colloids in the porous media

The rate of aggregation and deposition are controlled by the balance between attractive van der Waals force and electrostatic force (attractive or repulsive, depending on surface charge) acting upon colloid–colloid and colloid–porous media surface collisions. Thus, colloids with opposite charge than the porous media are more likely to deposit in the porous media. While, colloids with similar charge as the

porous media are easily mobile due to repulsion between like charge. However, other factors such as screening of surface charges with ions, presences of organic polymers can affect the repulsive forces resulting in aggregation.

1.7 Implication for colloid transport

As mentioned earlier, nanoparticles act as transport vectors that can sorb contaminants and carry them through porous media over long distances. Colloidal transport plays an important role in solubility and mobility of pollutants like heavy metals, radionuclides, polycyclic aromatic hydrocarbons and trace metals (Kaste et al., 2006; Kretzschmar & Schafer, 2005; MacKay & Gschwend, 2001; Novikov et al., 2006; Totsche et al., 2007). Mineral nanoparticles are also used for various bioremediation processes to degrade or immobilize contaminations. For example, stabilized zero-valent iron nanoparticles have been studied for immobilization of Cr(VI) in water (Xu & Zhao, 2007).

Transport of bio-colloids has also received a considerable attention due to its direct implication on human health. Many studies focus on transport of pathogenic microorganisms in the subsurface and in ground water (G. Chen & Walker, 2012; Fontes et al., 1991; Herbold-Paschke et al., 1991; Matthess et al., 1988; Nevers & Boehm, 2011; Redman et al., 2001; Zhao et al., 2014). Bio-colloids also play a role in transport of contaminants (Francis et al., 1998; Pang et al., 2005) and bioremediation of contaminant sites (Allard & Neilson, 1997; Ebihara & Bishop, 2002; Wilson & Jones, 1993). Additionally, extracellular polymeric substances (EPS) act as organic colloids and are mobile in the porous media. They also have a high sorption to heavy metals and organic pollutants and can mobilization of contaminants in the porous media (J. H. Chen et al., 1995). The transport of bio-colloids is more complicated than the inorganic colloidal transport due to the presence of living microorganism which

more susceptible to factors such as physical straining or filtration (Keller & Auset, 2007).

1.8 Bacterial biofilm

Biofilms are communities of surface associated microorganism encased in self-produced extracellular matrix (Vlamakis et al., 2013). Biofilms are found on almost all natural and artificial surfaces including the soil and the rock surfaces, stone monuments, murals, water pipes, sewage treatment plans and also human teeth (Costerton et al., 1987; Hall-Stoodley et al., 2004). The thickness and the composition of the biofilm vary with the environmental conditions and the nutrients present (Hall-Stoodley et al., 2004).

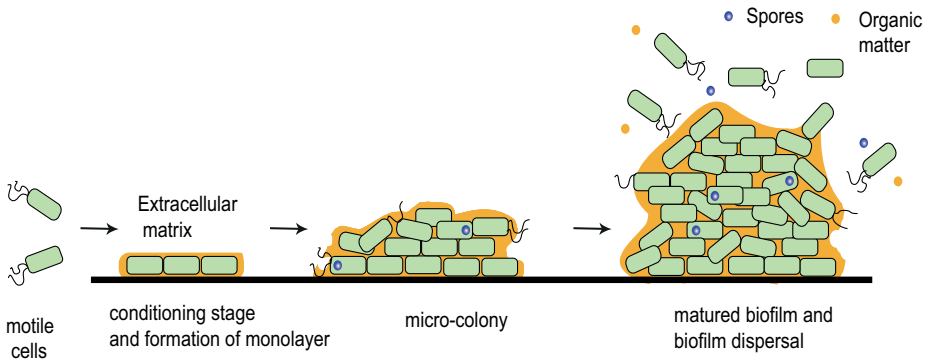

Figure 1.3 Formation and development of *Bacillus subtilis 168 (DSM 402)* biofilm (Vlamakis et al., 2013)

The formation of a biofilm starts with the "conditioning stage", where a single bacterium makes the first contact to the surface (Figure 1.3). Most bacterium have a net negative surface potential which makes it unfavorable to attach on many mineral surfaces which are also negatively charged. Bacterium secrets a condition film composed of extracellular polymers, which makes it favorable for adhesion on the mineral surface. This is followed by the formation of a monolayer of bacteria, which progresses to a micro-colony with multi-layer cells, ultimately forming a matured

biofilm. Environmental changes such as pH, temperature, ionic conditions, flow velocity of the air/solute the biofilm is in contact with, results in mechanical stress. This leads to detachment of cells, EPS or organic matter from time to time (O'Toole et al., 2000; Vlamakis et al., 2013). The detached components of the biofilm are termed as bio-colloids (cells) and organic colloids (EPS/organic matter) of microbial origin (Cullimore, 2010; Keller & Auset, 2007).

1.9 Extracellular polymeric substances

EPS are a physicochemically complex highly hydrated gel-like matrix of interlinked charged polymers, which surround cells in biofilm (Hall-Stoodley et al., 2004; Spath et al., 1998). They play a vital role in maintaining the structural integrity of biofilm, protection from environmental factors, sequestration and degradation of harmful compounds and nutrition (Flemming & Wingender, 2010). EPS consist a mixture of polysaccharides, proteins, lipids, lipopolysaccharides, glycolipids, peptides and nucleic acids; which surrounds microbial cells (Bazaka et al., 2011; Flemming & Wingender, 2010; Hall-Stoodley et al., 2004; Marvasi et al., 2010; Spath et al., 1998). The chemical composition, the charge and number of linkages between adjacent polymer chains of the EPS depends on the genetics of the microorganism and the environment in which they are synthesized and vary from bacterium to bacterium (Marvasi et al., 2010; Wang et al., 2012). EPS exists in various forms. It can occur as cell bound which is tightly bound to the cell surfaces, as free EPS that is loosely associated with the bacteria (Flemming & Wingender, 2010; Omoike & Chorover, 2004) or as free dissolved organic matter (Bhaskar & Bhosle, 2005). The cell-bound EPS are closely associated with the bacterial cells. It helps in formation of a distinct cell structure and protects the bacteria from environmental elements. The cell-bound EPS are released only after bacterial lysis (Bazaka et al., 2011). In contrast, the free

EPS are loosely associated with the bacterial cell and mitigates bacterial attachment to mineral surfaces by conditioning them (Bazaka et al., 2011; Omoike & Chorover, 2004).

EPS are synthesized by the biofilms for multiple functions. They mainly serve in attachment of bacteria to mineral surfaces or as signaling molecules. They also are used as energy and nutrient reserves and can serve as enzymes. EPS are known to play an important role in various geochemical processes such as bio mineralization (Miot et al., 2009), bioleaching (Kinzler et al., 2003; Sand & Gehrke, 2006), and heavy metal accumulation (Fang et al., 2011; Tourney & Ngwenya, 2014; Wei et al., 2011). Due to its complex structure and heterogonous composition, it is not possible to determine the exact composition of EPS. Hence, EPS are relatively poorly studied with respect to the matrix composition in natural environments (Marvasi et al., 2010).

1.10 Biofilms in porous media

Accumulation of nutrients and large surface area provide favorable condition for the growth of micro colonies and bacterial biofilms in soils. A great deal of research is focused on the biofilm in the subsurface porous media (Rittmann, 1993), although the focus of study has been varied. These include detection of subsurface biofilms (Burmolle et al., 2007; Kirkland et al., 2015), biofilm barriers for bioremediation (Cunningham et al., 2003), change in the physical properties of porous media (Brydie et al., 2005; Cunningham et al., 1991) and transport of colloids (Coombs et al., 2010; Kone et al., 2014; Strathmann et al., 2007).

Biofilm are a potential sink for various colloidal nanoparticles due to their high sorption to different mineral surfaces (Spath et al., 1998). Biofilm also aid in the biotransformation of colloids and contaminants and degradation of colloidal nanoparticles and the contaminants associated with it. Moreover, biofilm can also

affect the architecture and the hydrodynamic properties of the soil matrix (Coombs et al., 2010). For example: Levan a polysaccharide secreted by Paenibacillus (formerly Bacillus) polymyxa CF43 found in the rhizosphere of wheat leads to aggregation of soil in the roots of the plant (Marvasi et al., 2010). The thickness and the type of biofilm growth (patchy/complete) can have a significant impact on the porosity and permeability of fractures and the porous media (Cunningham et al., 1991). Biofilm are filamentous and hence can divide the pores space into smaller pore spaces (Brydie et al., 2005; Coombs et al., 2010). Older biofilm (Mitzel & Tufenkji, 2014), excessive growth of biofilm (Cunningham et al., 1991; Taylor & Jaffe, 1990; Thullner et al., 2002), increased trapping and sequestering of harmful mineral nanoparticles (Hama, 1997) or transport of bio-colloids (Coombs et al., 2010) can further reduce the internal pore size or cause clogging of the porous media.

1.11 Influence of biofilms on nanoparticle transport: Complex interaction between the nanoparticles and porous media

The fate and mobility of nanoparticles in the environment will depend not only on the physical and chemical character of the nanoparticle, but also on the characteristics of the receiving environment (K. L. Chen & Elimelech, 2008; Saleh et al., 2008). Under favorable conditions, biofilm flourish and can cover the surfaces of the rocks/porous media thus changing the surface properties of the host rock/porous media. Moreover, the heterogeneity in the chemical and physical properties of the biofilm and EPS can also alter the transport of colloidal nanoparticles by deposition of nanoparticles, transformation by various microbial processes or remobilization.

To study the holistic influence of biofilms on transport of nanoparticles three situations must be considered (Figure 1.4)

1. Biofilm present on the porous media: Biofilms can change the surface properties of the porous media
2. EPS/organic matter from biofilms can sorb on the surface of nanoparticles: EPS/organic matter alter charge and hydrophobicity of nanoparticles
3. A combination of 1 and 2. Both porous media and nanoparticles are coated with biofilm/EPS.

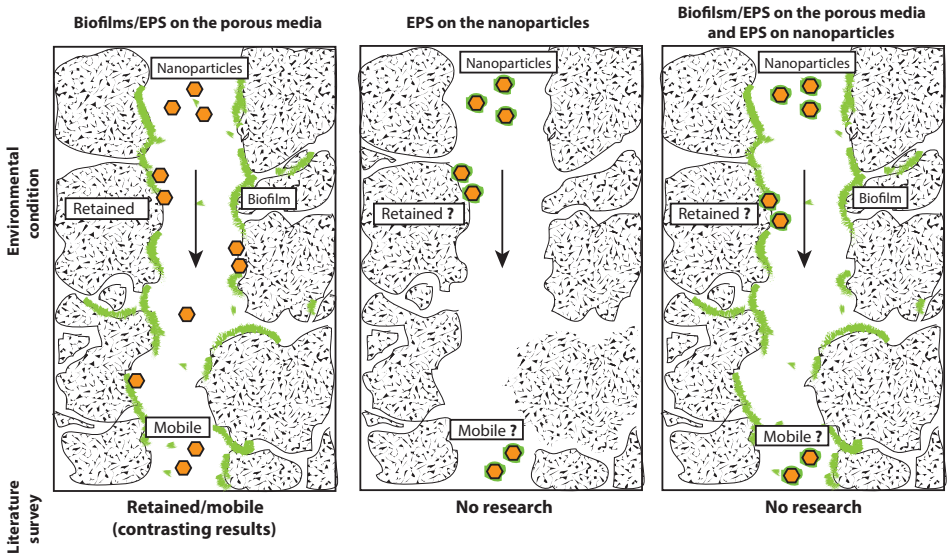

Figure 1.4 Influence of biofilms on nanoparticle transport

The first scenario i.e. the effect of biofilms present on the porous media on the transport of nanoparticles has been studied since last decade with contrasting results (Basnet et al., 2016; Golmohamadi et al., 2013; Jian-Zhou et al., 2015; Leon-Morales et al., 2004; Lerner et al., 2012; Mitzel & Tufenkji, 2014; Tripathi et al., 2012). Most studied engineered nanoparticles, e.g. zero valent iron, graphene, zinc sulfate-functionalized polystyrene latex particles, titanium oxide, cerium oxide nanoparticles, exhibit a retarded mobility in biofilm-coated porous media with the biofilm acting as "traps" (collectors) for nanoparticles (Jian-Zhou et al., 2015; Kurlanda-Witek et al., 2015; Tong et al., 2010; Tripathi et al., 2012). Retention of the nanoparticles in the

biofilms is attributed to the binding affinity of nanoparticles to functional groups in the biofilm EPS (Kurlanda-Witek et al., 2015), surface roughness of the biofilm (Jian-Zhou et al., 2015) and interaction between the surface coating of the nanoparticles and the biofilms (Tripathi et al., 2012). However, certain nanoparticles such as silver nanoparticles coated with polyvinyls pyrrolidone (PVC), laponite are mobile in the biofilm-coated porous media (Leon-Morales et al., 2004; Mitzel & Tufenkji, 2014; Xiao & Wiesner, 2013). Factors such as hydrophobicity (Xiao & Wiesner, 2013), steric repulsion by the polymer coating applied for maintaining colloidal stability (Mitzel & Tufenkji, 2014) and colloidal stability of nanoparticles in different salt solutions (Leon-Morales et al., 2004) have been credited to enhanced mobility of nanoparticles.

For the second scenario, the effect of EPS present on the nanoparticles on transport has not been studied so far. Transport, reactivity and bioavailability of nanoparticles are broadly controlled by their colloidal stability (Hochella, 2008; Kimball et al., 1995). The colloidal stability of nanoparticles depends on the environmental conditions like pH, ionic strength, temperature, and presence of organic matter. A few studied have shown the change in colloidal stability of fullerene, hematite and magnetite nanoparticles on sorption of humic acids (K. L. Chen & Elimelech, 2007; Hassellov & von der Kammer, 2008; Illes & Tombacz, 2006; Kretzschmar & Sticher, 1997; Mylon et al., 2004). Organic matter from bacteria such as EPS also have a high affinity to mineral surfaces (Spath et al., 1998; Tourney & Ngwenya, 2014). When released into the environment, EPS might potentially sorb to naturally occurring mineral surfaces by various interactions such as ionic bonding, steric interaction, dipole interaction, inner sphere complexation and hydrophobic bonding (Cao et al., 2011). Due to the presence of various functional groups, EPS can also modify the

charge and surface chemistry of the mineral (Cao et al., 2011; Jain et al., 2015) thus altering the stability and aggregation kinetics. This can also result in new reactive sites on the mineral surfaces. Bacterial EPS comprises a varied concentration of proton-active functional groups charged as a function of pH (Tourney & Ngwenya, 2014). Moreover, high molecular polymers can exert steric stabilization on the engineered nanoparticles on sorption (Kleshchanok & Lang, 2007). Hence, it is reasonable to assume that EPS sorption on nanoparticles will affect the colloidal stability and reactivity of EPS: nanoparticle association to other minerals or contaminants. Yet, not much is known about the effect of EPS on the stability of colloidal nanoparticles. Only few studies are available that report on the increase in colloidal stability of silica, hematite, fullerene and acrylic latex particles in the presence of alginate and gelatin, both components of EPS from algae (Abe et al., 2011; K. L. Chen & Elimelech, 2008; K. L. Chen et al., 2006; Likos et al., 2000).

Also, the combined effect of biofilms/EPS present on the porous media and EPS present on the nanoparticles has not been tested so far. However, Mitzel and Tufenkji (2014) have reported a low retention of poly(vinylpyrrolidone) (PVP) stabilized silver nanoparticles in biofilm-coated porous media due to steric repulsion between the nanoparticles and the coated surfaces. However, EPS are a complex mixture of polymers with both positive and negative charged functional groups and hence it is difficult to predict the fate of nanoparticles in biofilm/EPS-coated porous media.

1.12 Aim and objectives of the work

The main aim of this study was to investigate the effect of biofilms on the transport of colloids. To get a holistic view of the effect of biofilms on the transport of nanoparticles, the three situations mentioned in section 1.9 were systematically studied.

1. Biofilm/EPS present on the porous media and bare nanoparticles
2. EPS present on the nanoparticles and bare porous media
3. Biofilm/EPS present on porous media and EPS sorbed on nanoparticles

Hematite nanoparticles were choosen as model natural colloids. Hematite are commonly found iron oxides in soils, acid mine drainage and in river water. Hematite nanoparticles (HNP) exhibit a large surface area and show a presence of surface defects due which they are reactive towards other solution components. Moreover, they are well-known mobile sorbents that transport various pollutants including heavy metals (Kaste et al., 2006; Novikov et al., 2006), radionuclides (Simmons & Neymark, 2012) and trace metals (Kretzschmar & Schafer, 2005) in soil and river systems. *Bacillus subtilis 168 (DSM 402)* was used as a model for soil biofilm forming microorganism. Though pure biofilms are not ideal representative of natural biofilms, they offer an ease of reproducibility and are model for lab study.

As mentioned earlier, the effect of biofilm/EPS present on the porous media has been studied before. However, the role of EPS in transport of colloids is not much studied. Based on the literature survey we made the following hypothesis for the three situations tested:

1. "Biofilm on the porous media will act as trap and reduce the mobility of uncoated HNP, due to the electrostatic attraction between the positively charged hematite and negatively charged biofilm surfaces"
2. "EPS can attach to HNP and can colloidally stabilize them, thus increase their mobility in uncoated porous media under saturated condition.
3. “EPS-coated particles will experience enhanced mobility in biofilm/EPS-coated porous media due to the presence of similar surface coating on the porous media and nanoparticles."

To test the hypothesis experiments were planned with the following objectives:

1. Synthesize and characterize colloidal hematite nanoparticles and isolate and characterize EPS from *Bacillus subtilis 168 (DSM 402)*
2. Study the effect of biofilms/EPS present on the porous media on transport of hematite nanoparticles
3. Determine the effect of increasing loadings of EPS on colloidal stability of hematite nanoparticles
4. Determine the transport of EPS-coated hematite nanoparticles in uncoated porous media
5. Determine the transport of EPS-coated hematite nanoparticles in biofilm/EPS-coated porous media
6. Demonstrate remobilization of sorbed hematite nanoparticles by EPS

For the ease of writing this thesis, the experiments designed to achieve the above aims were divide in to sections to separated batch experiments from column transport experiments. Hence forth, the materials and methods and the results and discussion of all the above aims are described in separate sections:

Section 1: Synthesis and characterization of Hematite nanoparticles and EPS from *Bacillus subtilis*

Section 2: Colloidal stability and aggregation kinetics of HNP coated with EPS

Section 3: Closed-flow column transport experiments

A) Transport of uncoated HNP in uncoated, biofilm and EPS-coated porous media

B) EPS-coated HNP (HNP 5:1, HNP 2:1, HNP 1:5) in uncoated, biofilm and EPS-coated porous media

C) Remobilization of HNP in uncoated porous media with EPS

The effect of EPS coating on colloidal stability of hematite was studied by coating the colloidal hematite particles with increasing concentrations of EPS, and measuring its effect on the colloidal stability. Time-resolved dynamic light scattering experiments were conducted on all the mixtures of EPS-hematite over a wide range of NaCl and $CaCl_2$ concentrations. Colloidal properties such as isoelectric point (pH_{IEP}) and critical coagulation concentration (CCC) were used to compare the effect of EPS on the colloidal stability of HNP. The DLVO and EDLVO were used to explain the results.

The transport of the colloids was studied using closed flow column experiments over a period of 20 days till an equilibrium state of transport was achieved. Three porous media: uncoated, biofilm-coated and EPS-coated were tested. In the closed flow mode, the outflow solution is redirected to the columns via a mixing vessel after passing through the porous medium. Thus, only the mobile fraction of the solute can be exhaustively determined. Also, this type of column experiments allows a full establishment of equilibrium, while at the same time conserving the total mass of the system and minimizing experimental artifacts (Ritschel & Totsche, 2016a). The mobility of the colloids was measured by monitoring the concentration in the mixing vessel. The transport of the EPS:HNP suspensions was interpreted using Colloidal filtration theory (CFT) model modified by Tufenkji and Elimelech (2004).

The results from this research will serve in understanding the transport of mineral nanoparticles in water-saturated areas with high microbial biomass such as river/lake

sediments, or events of water logging and epiphreatic zone with karst hydrogeology. Such regions have reported existence of biofilms and EPS that can alter the transport of colloidal geosorbents into groundwater (Brannen-Donnelly & Engel, 2015; Farnleitner et al., 2005; Shabarova et al., 2014).

2 Material and Methods

Section 1. Synthesis and characterization of hematite nanoparticles and EPS from *Bacillus subtilis*

2.1 Synthesis of hematite nanoparticles

Hematite nanoparticles were synthesized by the method described by Sorum (1928). The method involved the synthesis of hematite by transformation of ferrihydrite in aqueous solution. Particles were synthesized by adding 400 ml of 1 M $Fe(N0_3)_3$ into boiling distilled water at a rate of 0.05 ml/min. The temperature was specifically kept above 80°C to avoid co-precipitation of goethite. The suspension was cooled overnight and washed with distilled water. Finally, the particles were purified by dialysis (molecular weight cutoff: 1 kDa; Spectra/Por7, Spectrum Labs, USA) till the electric conductivity of the water was around 2 μS/m. The concentrated hematite nanoparticle stock suspension was then stored at 4°C.

2.2 Characterization of synthesized hematite nanoparticles

2.2.1 Structural characterization of hematite nanoparticles

The particle structure and purity of the synthesized HNP were described using X-ray diffraction (XRD), Fourier transform infrared spectroscopy (FTIR) and Scanning electron microscopy (SEM). Freeze dried HNP were used XRD and FTIR analysis.

For XRD, the X-ray diffractograms were obtained with D8 Advance DaVinci diffractometer (Bruker AXS, Germany) using Cu Kα radiation (λ = 0.15418 nm) at 40 kV and 40 mA. The resultant diffractograms were compared with reference hematite (Maslen et al., 1994) from The American Mineralogist Crystal Structure Database (Downs & Hall-Wallace, 2003).

Fourier-transform IR spectra were recorded with a Nicolet iS10 spectrometer (Thermo Fisher Scientific, Germany). Freeze dried samples mixed with KBr were pressed into pellets and measured in the transmission mode to obtain the resultant spectra.

Particle morphology and size distribution were determined by a ULTRA plus field emission scanning electron microscope (Zeiss, Germany). The samples were prepared by placing a drop of hematite suspension on a silica plates and allowed to dry overnight.

2.2.2 Colloidal characterization

The hydrodynamic diameter and the zeta potential of the colloidal HNP were measured by dynamic light scattering (DLS) (Nano ZS, Malvern Instruments, UK).

2.2.3 Chemical characterization

The hematite concentration was measured as the total iron concentration by a spectroscopic method using phenanthroline (Saywell & Cunningham, 1937). Prior to the estimation of the iron concentration, the HNP were dissolved by protonation using equal volumes of concentrated HCl.

2.3 EPS isolation and characterization

Free EPS were isolated from *Bacillus subtilis 168 (DSM 402)* by the method of Omoike and Chorover (2004). *Bacillus subtilis 168 (DSM 402)* was grown to a stationary phase in Luria-Bertani (LB) broth for 24 h at 150 rpm. The bacterial cells were separated from the medium by centrifugation at 12,000 g, 4°C, 30 min. EPS were precipitated from the supernatant solution by adding 3 volumes of cold ethanol (4°C). This suspension was stored at -18°C for 24 h. The precipitated EPS were eventually recovered by centrifugation at 12,000 g, 30 min, 4°C and dialyzed against ultrapure water to remove ethanol and residual media components with water changed

every 24 h for 4 days (molecular weight cutoff: 1 kDa; Spectra/Por7, Spectrum Labs, USA). The EPS solution was stored at -20 °C.

Only the free EPS were isolated and used for the experiments. EPS were characterized by the measuring its total carbon content, total proteins, total carbohydrates, zeta potential and FTIR spectra. The total amount of EPS was measured as its carbon content determined by CNS analyzer (Euro EA, Eurovector, Italy). The protein concentrations were measured by Folin lowery method (Lowry et al., 1951) and the carbohydrate concentrations were measured by the phenol-sulfuric acid method (Dubois et al., 1956). The net charge on the EPS macromolecules was measured by measuring the zeta potential by Malvern Nano ZS (Malvern Instruments, UK). The FTIR spectra was recorded with a Nicolet iS10 spectrometer (Thermo Fisher Scientific, Germany).

Section 2. Colloidal stability and aggregation kinetics of HNP coated with EPS

2.1 Coating of hematite nanoparticles with EPS

Three different mass ratio of carbon to iron (1:5, 2:1 and 5:1) were prepared by adding different quantities of EPS solution (20, 200, 500 mg C, respectively) (pH 6.8) to hematite solution. The final concentration of HNP was kept constant (100 mg/l of Fe) in all the four mixtures. The pH was adjusted to approximate 7 (7.0-7.2) using 0.1M NaOH. The solutions were equilibrated for 2 h on a horizontal shaker at 100 rpm and EPS were allowed to adsorb on HNP.

2.2 Concentrations of EPS sorbed on hematite nanoparticles

The concentration of EPS sorbed on the hematite was estimated by centrifuging the solutions at 10,000 rpm for 10 mins at 4°C. The supernatant and the precipitate were analyzed for carbon and iron concentrations.

2.3 Effect of pH on colloidal stability

The zeta potential of the four colloidal suspensions was monitored over a pH range of 1 to 12 (Malvern Nano ZS, Malvern Instruments, UK). The pH was adjusted using 0.1 M HCl and 0.1 M NaOH. Five measurements were made for each suspension. The isoelectric point (pH_{IEP}) was determined as the pH at which all the particles are aggregated, and the zeta potential of the particles is zero (He et al., 2008).

2.4 Effect of salts on colloidal stability: colloidal aggregation kinetics

The aggregation kinetics of the particles was measured by conducting time resolved dynamic light scattering experiments with increasing concentrations of monovalent (NaCl) and divalent ($CaCl_2$) salts. The concentration of colloids during the experiment was kept constant (100 mg/l of Fe). The aggregation was initiated by adding the salt solution to the HNP suspension in the cuvette. The cuvette was shaken for dispersion and DLS measurements were started immediately (Malvern Nano ZS, Malvern Instruments, UK). The hydrodynamic diameter was recorded at 21°C over a period of 4000 sec (K. L. Chen et al., 2006). The aggregation of HNP suspensions was tested for a battery of ionic strength (1–800 mM NaCl, 1-100 mM CaCl2) over time.

2.5 Calculation of aggregation rate constant and attachment efficiency

The total interaction between the particles result from the balance of repulsive and attractive forces. Two limiting regimes of aggregation have been described in literature (Berg, 2010). When the repulsive forces between the particles are dominant, the aggregation rate is limited by the time required to overcome the repulsive forces. This is termed as reaction-limited aggregation (RLA) or slow aggregation. In contrast, when the repulsive forces are negligible, the aggregation rate is limited by diffusion

of particles. This is termed as diffusion-limited aggregation (DLA) or the fast aggregation (Berg, 2010).

The stability ratio W is used to indicate the stability of the system and can be calculated by monitoring the aggregation over time. W is defined as the ratio of the aggregation rate constant in the fast regime to the aggregation rate constant in the slow regime.

$$W = \frac{k_{fast}}{k} \tag{2-1}$$

The attachment efficiency α is another measure to describe aggregation kinetics. It is the reciprocal of stability ratio W.

$$\alpha = \frac{1}{W} \tag{2-2}$$

When W=1, all the collisions result in to aggregation and DLA dominates. Vice versa, if W>1, only a fraction of collisions leads to aggregation and RLA dominates. In our experiments, the stability ratio for the HNP at different salt concentrations was measured by monitoring the increase in the aggregate size (R_H) with time using DLS.

The rate of increase in the radius of the aggregates (R_H) over time (t) is proportional to the number of particles present initially (n_0) and the initial aggregation rate constant (k)

$$\left(\frac{dR_H}{dt}\right)_{t\to o} \propto kn_0 \tag{2-3}$$

When n_0 is kept constant in all the experiments, the calculation of W reduces to the ratio of the rate constant in the rapid (k_{fast}) aggregation to the rate constant in slow aggregation (k) (Di Marco et al., 2007; He et al., 2008; Holthoff et al., 1996).

$$W = \frac{(dR_H/dt)_{t\to 0\ fast}}{(dR_H/dt)_{t\to 0\ slow}} \tag{2-4}$$

When number of particles are kept constant, the aggregation rate constant k proportional to the slope of R_H vs. time. The rate of increase in the R_H was obtained by determining the slope up to the point of initial stages of coagulation (0-200 s) for each electrolyte concentration. W was calculated by normalizing the slope obtained with different electrolyte solutions by the slope obtained by the fast aggregating electrolyte (equation (2-3)) (K. L. Chen & Elimelech, 2006; He et al., 2008).

2.6 Modeling aggregation kinetics

DLVO theory is a simplified approach that accounts for attractive van der Waals and repulsive electrostatic interactions. However, steric and hydrophobic forces dominate high molecular weight polymers interactions (Grasso et al., 2002; Hiemenz & Rajagopalan, 1997; Kleshchanok & Lang, 2007; Perni et al., 2014). EPS surfaces can exert Lewis acid–base (AB) interaction when present in inert salt solutions (Liu et al., 2000; Somasundaran, 2004). Furthermore, adhesion of biofilms to mineral surfaces has been explained using EDLVO theory with acid base and steric interactions (Azeredo et al., 1999). Hence EDLVO theory with hydrophobic and steric interactions was also used to explain our observations.

Puertas and de las Nieves (1999) described the stability ratio in terms of total interaction energy (or energy barrier) $V_T(H)$ by the following equation (Di Marco et al., 2007)

$$W = \frac{\int_0^\infty \beta\,(H)/(H + 2R_H)^2 . \exp\left(\frac{V_T(H)}{k_B T}\right) dH}{\int_0^\infty \beta\,(H)/(H + 2R_H)^2 . \exp\left(\frac{V_A(H)}{k_B T}\right) dH} \quad (2\text{-}5)$$

Here, H is the distance between the particle surfaces, β(H) is the hydrodynamic correction factor (Overbeek, 1982), $V_T(H)$ is the total potential energy of interaction and $V_A(H)$ is the potential energy of the van der Waals interaction.

2.6.1 DLVO interactions

The total interaction energy between the particles $V_T(H)$ is given by the equation,

$$V_T(H) = V_A(H) + V_E(H) \quad (2\text{-}6)$$

Here $V_E(H)$ is the total potential energy of electrostatic double layer interactions.

The total potential energy of the van der Waals interaction is given by

$$V_A(H) = -\frac{A}{6}\left[\frac{2{R_H}^2}{H(4R_H + H)} + \frac{2{R_H}^2}{(2R_H + H)} + ln\frac{H(4R_H + H)}{(2R_H + H)^2}\right] \quad (2\text{-}7)$$

Where A is the Hamaker constant of particles interacting in the water.

The total potential energy by electrostatic double layer interaction is given by

$$V_E(H) = 2R_H \varepsilon_0 \varepsilon_r \pi \left[\frac{4K_B T}{\mathrm{Z}e}\gamma\right]^2 e^{-\kappa H} \quad (2\text{-}8)$$

where γ is given by

$$\gamma = \frac{e^{\mathrm{Z}e\psi d/2K_B T} - 1}{e^{\mathrm{Z}e\psi d/2K_B T} + 1} \quad (2\text{-}9)$$

ε_o is the permittivity in vacuum, ε_r is the relative permittivity, K_B is the Boltzmann constant, T is the absolute temperature, Z is the valence of the electrolyte, κ is the

Debye parameter, which depends on the ionic strength of the solution, ψ_d is the diffusion potential related to and very close (in value) to the zeta potential (Di Marco et al., 2007).

2.6.2 EDLVO interactions

2.6.2.1 Steric interactions

In the presence of steric forces, additional term is added to the total interaction energy equation (2-6)

$$V_T(H) = V_A(H) + V_E(H) + V_S(H) \quad (2\text{-}10)$$

The steric interaction energy comprised of two energies the osmotic energy V_{osm} and the elastic energy V_{elas}

$$V_S(H) = V_{osm}(H) + V_{elas}(H) \quad (2\text{-}11)$$

When the polymer brushes of the two parties overlap, osmotic pressure is built up due to an increase in the concentration of the polymer resulting in repulsion between the two particles.

$$V_{osm}(H) = 0 \qquad 2\delta \leq H \quad (2\text{-}12)$$

$$V_{osm}(H) = \frac{4\pi a}{v_1}(\phi_2)^2 k_B T \left(\frac{1}{2} - \chi\right)\left(\delta - \frac{H}{2}\right)^2 \qquad \delta \leq H \leq 2\delta \quad (2\text{-}13)$$

$$V_{osm}(H) = \frac{4\pi a}{v_1}(\phi_2)^2 k_B T \left(\frac{1}{2} - \chi\right)\delta^2\left(\frac{H}{2\delta} - \frac{1}{4} - ln\left(\frac{H}{\delta}\right)\right) \qquad H < \delta \qquad (2\text{-}14)$$

Here χ is the Flory-Huggins solvency parameter, ϕ_2 is the volume fraction of the EPS within the brush layer, δ is the thickness of the brush layer and v_1 is the volume of one solvent molecule.

When the two particles are at such a close distance (H=δ), some polymer molecules undergo compression leading to loss of entropy for the polymers, which result, into elastic repulsion between the two particles.

$$V_{elas}(H) = 0 \qquad \delta \leq H \qquad (2\text{-}15)$$

$$V_{elas}(H) = k_B T\left(\frac{2\pi a}{M_w}\phi_2\delta^2\rho\right)\left(\frac{H}{\delta} ln\left(\frac{H}{\delta}\left(\frac{3 - H/\delta}{2}\right)^2\right) - 6\, ln\left(\frac{3 - H/\delta}{2}\right) + 3\left(1 + \frac{H}{\delta}\right)\right) \qquad H< \delta \qquad (2\text{-}16)$$

Here M_w is the molecular weight of the EPS and ρ is the density of the EPS (Romero-Cano et al., 2001)

2.6.2.2 Acid-base interactions

EPS sorption can also affect the surface electron acceptor and electron donor properties. Hence, acid-base interaction can also contribute to the total interaction energy. When acid-base interactions contribute to total energy, the acid-base component is added to the total energy equation (2-6)

$$V_T(H) = V_A(H) + V_E(H) + V_{AB}(H) \quad (2\text{-}17)$$

The acid-base energy between two particles is given by

$$V_{AB}(H) = \pi r \lambda \Delta G_{h_o}^{AB} exp\left(\frac{H_o - H}{\lambda}\right) \quad (2\text{-}18)$$

here λ is the decay length of the molecules of the liquid medium, and $\Delta G_{h_o}^{AB}$ is the polar free interaction energy between the particles at distance H_o which is the minimum equilibrium distance due to Born repulsion which is 0.157 nm (K. Li & Chen, 2012).

Table 2.1 Parameters used for the calculation of VT(H) by DLVO and EDLVO theories

Parameter		Value
Hydrodynamic correction factor (Overbeek, 1982)	β(H)	$\beta(h) = \frac{6\left(\frac{h}{a}\right)^2 + 13\left(\frac{h}{a}\right) + 2}{6\left(\frac{h}{a}\right)^2 + 4\left(\frac{h}{a}\right)}$
Debye parameter (Berg, 2010)	κ	$\frac{1}{\sqrt{\frac{\varepsilon_r \varepsilon_o RT}{2F^2 C_o}}}$
Permittivity in vacuum	εo	8.854 × 10−12 F/m
Relative permittivity	εr	80.1
Absolute temperature	T	293 K
Boltzmann constant	KB	1.3806×10-23 m2 kg s-2 K-1
Gas constant	R	8.3144 J K−1 mol−1
Faraday constant	F	96485.3365 C mol−1

The derivation of equation (2-5) permits the comparison of predicted W values to the experimental data of log W vs electrolyte concentration. Some values such as

Hamaker constant (A), Gibbs free energy of acid/base interaction ($\Delta G_{h_o}^{AB}$), the volume fraction of the EPS with in the brush layer (ϕ_2), the thickness of the brush layer (δ) could not be derived independently. Hence these parameters were fitted to the observed data using the Levenberg-Marquardt algorithm for local optimization (Levenberg, 1944; Marquardt, 1963). The correlation between the fitting parameters was also calculated. All the values used for different parameters are given in Table 2.1. Parameter uncertainty was calculated as the 95 % confidence interval.

Section 3. Closed-flow column transport experiments

A) Transport of uncoated HNP in uncoated, biofilm and EPS-coated porous media

B) Transport of EPS-coated HNP (HNP 5:1, HNP 2:1, HNP 1:5) in uncoated, biofilm and EPS-coated porous media

C) Remobilization of HNP in uncoated porous media with EPS

2.1 Transport experiments: Closed flow column system

Closed flow column systems described by Totsche (2001) and Ritschel and Totsche (2016a) were used to study the transport of nanoparticles. Three different porous media namely, 1: Uncoated 2: EPS-coated 3: Biofilm-coated were studied in duplicated for the transport of four different HNP 1: Uncoated, 2: EPS-coated 1:5, 3: EPS-coated 2:1 and 4: EPS-coated 5:1. Thus, total 24 columns were set up.

2.2 Column set up: Closed flow column system

The working of a closed flow column involves transport of the solute from the mixing vessel through the column against the gravity. In the close flow mode, the column effluent is redirected into the column via the mixing vessel. The solute in the mixing vessel is continuously monitored until an equilibrium concentration is achieved. Thus,

only the mobile fraction of the solute can be exhaustively determined. Also, this type of column experiments allows a full establishment of equilibrium, while at the same time conserving the total mass of the system and minimizing experimental artifacts (Ritschel & Totsche, 2016a, 2016b; Totsche, 2001).

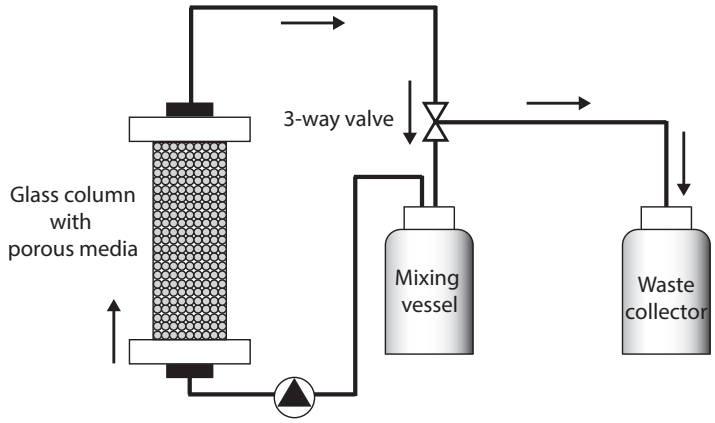

Figure 2.1 Closed flow column setup

The detailed column set up is given in Figure 2.1. Glass columns (L=0.01 m, I.D.=0.04 m,) with stainless steel capping at the two ends were connected to the mixing vessel (DURAN® Laboratory Bottle, with GL 45 thread, Duran, Germany) with Pharmed ®-tubes (Ismatec, Germany). Flow was driven vertically against gravity by a peristaltic pump (Ismatec Reglo Digital MS-2/12, Germany). An additional waste collector was added to collect the waste solutions for washing off solutions after the tracer study or after coating with biofilm. The flow of the solution could be diverted to the waste collector using a 3-way valve. The entire setup was sterilized by autoclaving and assembled under a clean bench to ensure sterility (**Figure 2.2**).

Glass beads (∅= 2.5 mm) (Borosilicate SiLibeads, SiLi GmbH, Germany) were used as the porous media. The bulk density and porosity of the porous medium was 1.35 and 0.48 g/cm^3, respectively. The glass beads were sterilized by autoclaving prior

packing into the columns. All the columns were placed under a clean bench during the entire period of the experiments. The columns were saturated with deionized water at flow rate of 0.5 PV/day.

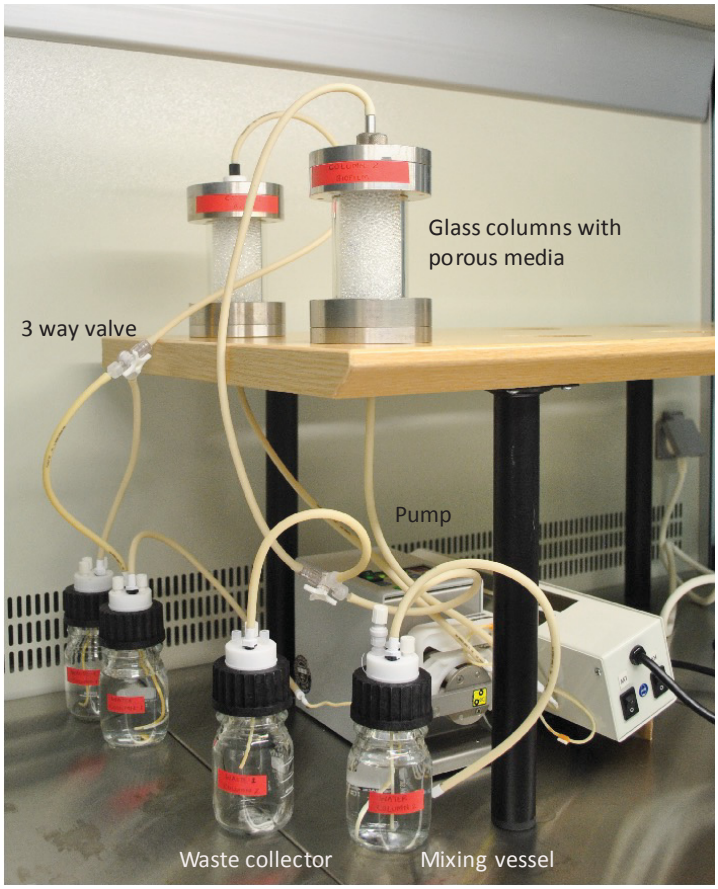

Figure 2.2 Closed flow columns under a clean bench

2.3 Coating of porous media with biofilm and EPS

Three different porous media were studied 1. Uncoated glass beads 2. Biofilm-coated glass beads 3. EPS-coated glass beads, for the transport of HNP. The *Bacillus subtilis 168 (DSM 402)* bacterial culture was grown and maintained on sterile LB (VWR, USA) agar slants. To maintain the osmotic pressure for the bacteria and EPS, all the columns were conditioned by equilibrating with 10mM NaCl before coating with biofilms or EPS. Uncoated glass beads columns were also conditioned with 10 mM NaCl to maintain similar condition.

2.3.1 Biofilm coating on the porous media

The biofilm and EPS coating on the porous media was done as reported in literature (Lerner et al., 2012; Tong et al., 2010; Tripathi et al., 2012). A single colony of 16 h old *Bacillus subtilis 168 (DSM 402)* culture was inoculated into a diluted LB broth (4 g/l) and incubated for 16 h at 150 rpm. This preculture (1 ml) was later inoculated into 100 ml diluted LB broth (4 g/l), which was fed to columns for two days at a flow rate of 1 PV/day (Lerner et al., 2012; Tripathi et al., 2012). The flow direction was switched between upward flow and downward flow every 8 h to ensure equal distribution of biofilm at both ends of the column (Tong et al., 2010). After the biofilm formation, unattached cells, residual media, and EPS were removed by flushing sterile 10 mM NaCl through the columns at a flow rate of 3 PV/day. This was continued until a steady value of cells and dissolved organic carbon (DOC) was reached in the outflow solutions. The viable bacteria were measured using plating technique, and DOC was measured using a DOC/TOC analyzer (Analytic Jena multi N/C 2100s, Germany).

2.3.2 EPS coating on the porous media

For EPS-coated columns, the porous media was coated by the same procedure as biofilm coating. Columns equilibrated with 10 mM NaCl were coated with 100 mg/l EPS. After the coating procedure, sterile 10 mM NaCl was flushed through the columns to remove unattached residual EPS till constant values of dissolved organic carbon (DOC) was reached in the outflow. DOC was measured using DOC/TOC analyzer (Analytic Jena multi N/C 2100s, Germany). The mixing vessel was monitored for bacterial cells and contamination in all the columns, using plating techniques.

2.4 Characterization of the porous media: coated and uncoated

New columns were set up, and the beads were coated by the same procedure as described above. Beads were then harvested for characterization of the porous media.

2.4.1 Measurement of surface charge

The streaming potential of the glass beads (uncoated, biofilm and EPS-coated) was measured using an Electrokinetic Analyzer (Anton Paar, Austria) (Tripathi et al., 2012). When an electrolyte is passed through a charged porous media under a pressure gradient, a streaming potential is generated. The streaming potential is used to measure the surface charge of larger particles.

Coated and uncoated glass beads were packed into the measuring cell and the streaming potential was measured at 1mM NaCl. The streaming potential is determined by measuring the current developed by passing an electrolyte solution over the charged surface at different pressures. The electrolyte disturbs the distribution of ions near the surface of the charged surface generating a potential difference (Abaza, 1966). Due to the large size of the glass beads, high bulk porosity and low the flow resistance, sufficient pressure difference could not be attained. Thus, the values measured were lower than expected. Hence, the results were reconfirmed using glass plates made from the same material (borosilicate). The glass plates were coated with biofilm and EPS and analyzed for the streaming potential. Possible loss of coating due to measurement procedure was also monitored by continuous analysis of total organic carbon (TOC/DOC analyzer, Analytic Jena multi N/C 2100s. Germany).

2.4.2 Visualization of the coatings

The biofilms on the glass beads were visualized using confocal laser scanning microscopy (CLSM) (Zeiss LSM 510 META, Germany), and scanning electron microscopy (SEM) (ultra plus field emission scanning electron microscopy, Zeiss,

Germany). Around 10 beads from each of the three different sections of the columns (top 3 cm, middle 4 cm, and bottom 3cm) were harvested and analyzed for the coatings.

For SEM imaging, the glass beads were fixed on the SEM holders coated with double sided tape and allowed to dry overnight. For CLSM imaging, Chamber slides ™ (Lab- Tek, USA) slide boxes were used. The samples were placed in the chambers and fixed with 2.5% (v/v) formaldehyde (Sigma-Aldrich, USA) and stained simultaneously with 1 mg/l ethidium bromide (Sigma-Aldrich, USA) and 75 mg/l calcofluor white (Sigma-Aldrich, USA) for 20 min (Shih & Huang, 2002). The samples were then immersed in saline and observed using CLSM. The bacterial cells were viewed using 514 nm laser to excite ethidium bromide giving red fluorescence, and the EPS was visualized using 405 nm laser exciting calcofluor white emitting blue fluorescence.

2.4.3 Measurement of the coating thickness

The distribution of the biofilm in the column was determined by measuring the thickness of the biofilm and EPS layers in the three different sections (top, middle and bottom) of the columns using the gravimetric method as described by Staudt et al. (2004). New columns were set up, and the glass beads were coated in the same manner as in the main experiment. After the coating procedure, columns were completely drained of any liquid. The glass beads from the three different sections (bottom: 0-3cm, middle: 3-7cm. top: 7-10cm) were harvested and measured for the wet mass m_{WF}. The sections were then dried at 40ºC for 12 h to dry and preserve the organic matter coating and measured for its dry mass m_d. The beads were then washed to remove the organic coatings and dried at 800 ºC to combust the remaining organic matter and mass of the beads was measured again (m_o). The difference in the weight

of the beads gives the dry weight of the biomass m_{DF} (m_d - m_o). The distribution of the biofilm mass was estimated from the dry weight of the biomass.

The biofilm thickness was calculated with

$$L_F = \frac{m_{WF}}{\rho_{WF} * A_F} \quad (2\text{-}19)$$

here ρ_{WF} is the density of wet biofilm (approx. 1 g/cm^3) (Staudt et al., 2004) and A_F is the surface area of the glass beads.

2.5 Transport experiment: Conservative tracer study

Conservative tracer studies were done before and after coating the glass beads to estimate the effect of the coatings on the transport and the changes in the porosity of the columns. Conservative tracer bromide was used since chloride (most commonly used) was already present in the system (Levy & Chambers, 1987). A 100 ml of 10 mM NaBr (pH 7) was flowing through the columns at the flow rate of 3 PV/day. The samples were taken after 3, 15, 30 and 60 PV. The concentration of bromide was measured with ion chromatography (Thermo Scientific™, Dionex™, USA).

2.6 Transport of uncoated and coated HNP

All the columns were flushed with sterile 10 mM NaCl to remove traces of bromide (from tracer studied) in the column system. The transport of uncoated, and EPS-coated (HNP 1:5, HNP 2:1 and HNP 5:1) (100ml, pH 7) nanoparticles was carried out at a flow rate of 3 PV/day. Samples were collected after 3,15, 30, 60 PV and analyzed for the iron concentration, pH, EC, hydrodynamic diameter and zeta potential. The characteristic reddish orange color of hematite was used for visual observations of the transport studies.

2.7 EPS remobilization study

The effect of EPS on remobilization of HNP was investigated using uncoated porous media columns from the previous transport experiments with uncoated hematite depositions. EPS solution (100 mg/l) and sterile water (for control columns) was fed to the columns at a flow rate of 3 PV/day. The samples were collected from the inflow vessel after 3, 15, 30 PV and measured for the hematite concentration.

2.8 Porous media contact efficiency

The transport data from these experiments are described using the colloidal filtration (CFT) theory (Tufenkji & Elimelech, 2004) with corrections for the closed flow transport regime. It calculates the attachment efficiency of the porous media and the single collector contact efficiency.

The attachment efficiency (α) is the fraction of collisions between the particles and porous media that result in the attachment.

$$\alpha = -\frac{2}{3}\frac{d_c}{(1-f)L\eta_o}\ln\left(\frac{c}{c_i}\right) \qquad (2\text{-}20)$$

Here d_c is the average diameter of the porous media, f is the porosity, L is the length of the column, C/C_i is the ratio of the concentration of nanoparticles in the column at the end of the transport experiment to the concentration of nanoparticles expected after imminent dilution due to the water of saturation in the columns and η_o is the theoretical single collector contact efficiency developed by Tufenkji and Elimelech (2004). All the parameters used for the calculation of attachment efficiency and the single collector contact efficiency is given in Table 2.2.

The actual single collector removal efficiency (η), which is generally lower than the single collector contact efficiency (η_o), is given by

$$\eta = \alpha\eta_0 \tag{2-21}$$

Moreover, the particle deposition rate coefficient k_d is given by

$$k_d = \frac{3}{2}\frac{(1-f)}{d_c f}U\alpha\eta_0 \tag{2-22}$$

Here U is the approach velocity of the medium.

The single collector contact efficiency (η_o) is calculated by

$$\eta_0 = 2.4A_s^{1/3}N_R^{-0.081}N_{Pe}^{-0.715}N_{vdW}^{0.052} + 0.55A_sN_R^{1.675}N_A^{0.125} + 0.22N_R^{-0.24}N_G^{1.11}N_{vdW}^{0.053} \tag{2-23}$$

Here,

$$A_s = 2(1-\gamma^5)/(2-3\gamma+3\gamma^5-2\gamma^6) \tag{2-24}$$

$$\gamma = (1-f)^{1/3} \tag{2-25}$$

$$N_R = {d_p}\Big/{d_c} \tag{2-26}$$

$$N_{Pe} = \frac{Ud_c}{D_\infty} \tag{2-27}$$

$$D_\infty = \frac{k_B T}{3\pi\mu d_c} \tag{2-28}$$

$$N_{vdW=\frac{A_{132}}{k_B T}} \tag{2-29}$$

$$N_A = \frac{A_{132}}{3\pi\mu U d_p^2} \tag{2-30}$$

$$N_G = \frac{1}{9}\frac{d_p^2(\rho_p-\rho_f)g}{2\mu U} \tag{2-31}$$

Table 2.2 Parameters used for the calculation of attachment efficiency and the single collector contact efficiency

Parameter	Values
Porosity (f)	0.4897
Diameter of porous media (d_c)	0.0025 m
Diameter of particles (d_p)	1.81E-07 m
Length of the column (L)	0.1 m
Fluid approach velocity (U)	1.0865E-06 m/s
Boltzmann constant (kB)	1.3806488E-23 m2 kg s-2 K-1
Absolute temperature (T)	298 K
Hamaker constant (glass)A_{132}	1.93E-20
Hamaker constant (biofilm and EPS) A_{132}	3.31E-21 J
Particle density (ρ_p)	2400 kg/m3
Fluid density (ρ_f)	1000 kg/m3

3 Results and Discussion

Section 1. Synthesis and characterization of Hematite nanoparticles and EPS from *Bacillus subtilis*

3.1 Properties of Hematite nanoparticles

3.1.1 Structural and Morphological Properties

The XRD diffractogram and the FTIR spectra of synthesized hematite show all necessary features of well crystalline hematite (Figure 3.1 A). No reflexes except for those produced by hematite were seen in the sample. FTIR is a rapid method of identification of hematite and can detect traces (1-2%) of goethite in the sample of hematite. No such goethite impurity was found in the synthesized HNP.

The size and the distribution of the HNP was measured using SEM images showed small aggregates (100-150 nm) of HNP with individual particle sizes ranging from 10-20 nm. However, aggregates can be formed during sample preparation step (drying) for SEM.

3.1.2 Colloidal properties

HNP were colloidally stable with a zeta potential of +55 ± 6 mV and a hydrodynamic diameter of 171 ± 70 nm at pH of 5.2. Absolute zeta potential larger than 20 mV indicate colloidally stable nanoparticles (Hanaor et al., 2012). DLS and SEM observation together points to presence of colloidally stable HNP aggregates. The hydrodynamic diameter of the HNP is far more than the size of the nanoparticles seen with SEM (10-20 nm). Many researchers have shown a small increase (20-40 nm) in the hydrodynamic diameter compared to the observed size under electron microscope (Bootz et al., 2004; Lim et al., 2013). The hydrodynamic diameter is expected to be greater than the size measured by SEM due to the difference in the measurement

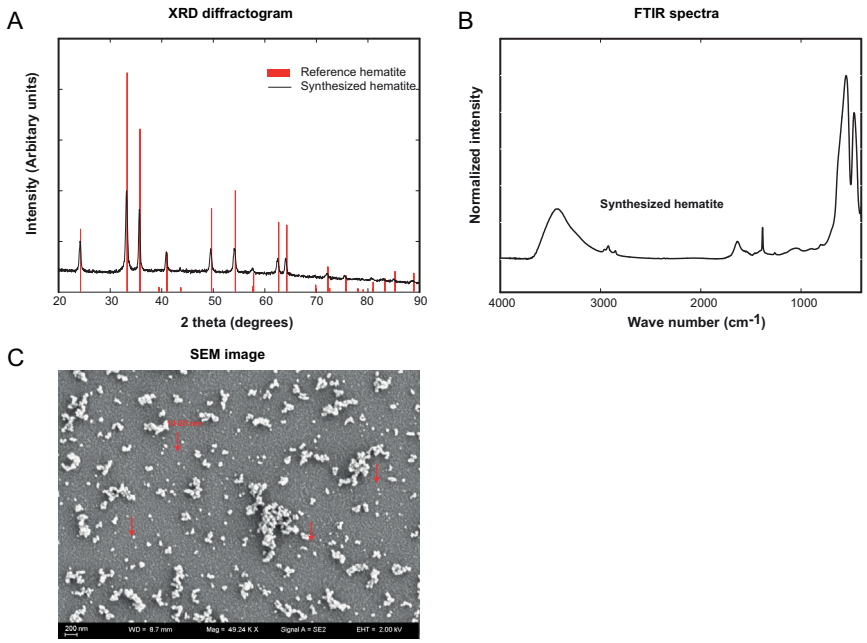

Figure 3.1 Characteristics of synthesized HNP A. X-ray diffraction of synthesized HNP compared with reference hematite (Maslen et al., 1994) (The American Mineralogist Crystal Structure Database) (Downs & Hall-Wallace, 2003) B. FTIR spectra of synthesized HNP C. SEM image of uncoated HNP (The red arrows point to 10-20 nm HNP with larger aggregates)

techniques (Fissan et al., 2014). DLS is an intensity-based observation. It measures solvent molecule layer attached to the outside of the nanoparticle and coatings if any, whereas, SEM is number-based observation. However, the amount of light scattered by a single particle is proportional to the sixth power of its radius (volume square) (Fissan et al., 2014). Thus, the hydrodynamic diameter is also weighted by volume square. Furthermore, DLS measurements cannot distinguish between different sized particles and smaller sizes are screened out in presence of larger particles (Fissan et al., 2014). Thus, the large difference observed individual particles size in SEM and hydrodynamic diameter could be attributed to presence of colloidally stable aggregates.

3.2 Characterization of EPS

About 0.35 mg/L of media (dry weight) soluble fraction of EPS was isolated. The total carbon and nitrogen content estimated was 383.7 ±1.45 mg/g carbon and 45.3 ±1.64 mg/g nitrogen. The concentration of carbohydrates (657 ± 32.52 mg/l) was higher than the protein content (170 ±18.87 mg/l) in the isolated EPS.

The FTIR spectra shows the presence of nucleic acids (1300 to 900 cm-1) and lipids (2930 and 2860 cm-1) along with proteins and polysaccharides (Figure 3.2) (Jiao et al., 2010).

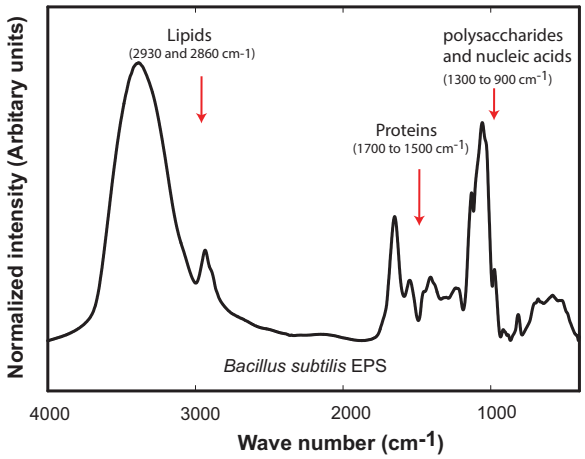

Figure 3.2 FTIR spectrum of isolated EPS showing presence of proteins, carbohydrate, lipids and nucleic acids (red arrows indicate the lipids, proteins, polysaccharides and nucleic acid spectra).

Section 2. Colloidal stability and aggregation kinetics of HNP coated with EPS

3.1 Concentration of EPS sorbed on the hematite nanoparticles

Hematite nanoparticles could not be separated from the solution by centrifugation. Some hematite particles were still found in the supernatant despite high-speed centrifugation (Table 3.1). Colloidally stable HNP 5:1 and HNP 2:1 have many particles in the supernatant in comparison to colloidally unstable HNP 1:5. Hence we could not precisely determine the concentration of EPS sorbed on the HNP.

However, a general increase in the concentration of EPS present on the surface is seen with increasing loadings of EPS. Table 3.1 gives concentration of EPS sorbed on HNP. Other methods of separation such as aggregation of HNP using high concentration of salts was not used since salts can also precipitated colloidal EPS molecules. Also, we cannot rule out the interference of free EPS in the stability of HNP. But, we can relate it to environmental conditions where free EPS will be the medium along with the nanoparticles.

Table 3.1 Amount of EPS sorbed on HNP

EPS: HNP suspension	**Carbon concentrations (mg/l)**		**Iron concentrations (mg/l)**
	Supernatant	Precipitate	Supernatant
HNP 5:1	356.33	103.40	20.63
HNP 2:1	112.62	70.41	6.29
HNP 1:5	53.72	50.21	1.89

3.2 Effect of EPS on the isoelectric point of HNP

The zeta potential of uncoated HNP decreased from positive value (+55 mV) to negative value (-46 mV) with an increase in pH from 1 to 14. The isoelectric point of the nanoparticles is the pH at which the nanoparticles have a net zero charge and are colloidally unstable with a large aggregate size. However, the isoelectric charge depends on the method of synthesis of particles and the size of particles (Suttiponparnit et al., 2011). The isoelectric point (pH_{iep}) for uncoated HNP was at pH 9.8. The experimentally determined pH_{iep} for HNP agrees with the pH_{iep} described in the literature (pH 8-10) (Mączka & Kosmulski, 2014; Plaza et al., 2002).

The influence of EPS on the zeta potential of HNP as a function of pH is shown in Figure 3.3. In the presence of EPS, the entire zeta potential curve shifts in the negative range, resulting in decrease in pH_{iep}. The shift in the zeta potential of HNP

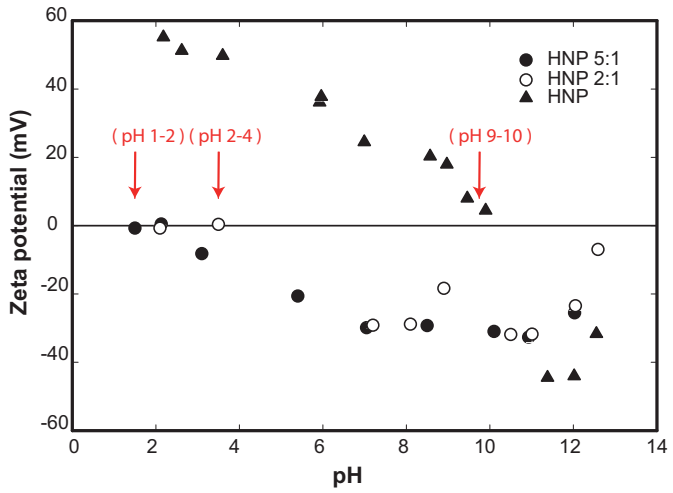

Figure 3.3 Shift in zeta potential of HNP with increasing EPS loading as a function of pH (red arrows indicate the isoelectric point of coated and uncoated HNP)

1:5 at different pH was not be measured since they were aggregated in large chunks at the beginning of the experiment. Thus, the pH_{iep} was considered as the pH at which the mixture was prepared i.e. pH 6.5. The pH_{iep} of HNP 2:1 and HNP 5:1 is around pH 3.5 and pH 2.3 respectively (Table 3.2, Figure 3.3).

EPS are a mixture of positive and negative charged macromolecules with a net negative charge (ZP: -39mV ±14 mV, pH 7) and exhibits strong affinity to iron oxides (Cao et al., 2011),Wang et al. (2012) have reported the pH_{iep} of EPS from *Bacillus megatherium* TF10 to be around pH 4. The shift in the zeta potential curve and the decrease in pH_{iep} with increasing EPS concentrations indicate presence of EPS on the surface of HNP. Werner et al. (1992) and Pena et al. (2006) have explained the shift in pH_{iep} with the formation of inner-sphere surface complexes (direct bonding to surface) between the adsorbate and surface of the nanoparticles which can change the surface charge. On the other hand, outer sphere complexes (aqua-ion surrounded by

water molecules and held to the surface of the sorbent by electrostatic attraction) are formed with no chemical reactions between the adsorbent and surface of the nanoparticles. Hence there should be no change in the surface charge of the nanoparticles (Fang et al., 2012). Considering the strong shift in pH_{iep}, we conclude that EPS forms negatively charged inner sphere complexes modifying the surface properties of HNP.

3.3 Colloidal stability of EPS-coated HNP

No significant change was observed in the size of HNP 5:1 (217 nm) and HNP 2:1 (204 nm) in comparison to uncoated HNP (210 nm) (Table 3.2). However, HNP 1:5 exhibited a very large size which could not be measured effectively by DLS measurements. The particles in HNP 1:5 were aggregated at the bottom of the medium, whereas, in the case of HNP 5:1 and HNP 2:1, the particles were suspended in the medium (Table 3.2).

As mentioned above, zeta potential also decreased with increasing EPS concentrations shifting from positive to negative potential (Table 3.2). The absolute zeta potential values higher than 20 mV indicate colloidally stable solutions (Hanaor et al., 2012; Hunter, 1981a). Thus at neutral pH (experimental pH), HNP uncoated, HNP 5:1 and HNP 2:1 were colloidally stable while HNP 1:5 was colloidally unstable and completely aggregated which could also be visually observed.

The negatively charged EPS balances the positively charged hematite particles thus reducing the zeta potential. At low concentrations (HNP 1:5), the amount of EPS are just enough to neutralize the positively charged functional groups of HNP by electro-static attraction resulting in net neutral surface charge causing aggregation of particles. While at high concentration (HNP 2:1 and HNP 5:1), the EPS functional groups can neutralize more positive charges on hematite surfaces and the excess

Table 3.2 Colloidal properties of uncoated and coated HNP

Colloidal properties	HNP	HNP 1:5	HNP 2:1	HNP 5:1
Size (DLS) [nm]	210±70	-#	204 ± 86	217 ± 47
Zeta potential [mV]	+35 ± 7	+4 ± 8	-26 ± 7	-33 ± 6
pH of solution	6.9	7.3	7.3	7.2
Isoelectric point	9-10	6-7	1-3	1-3
Critical coagulation concentration (CCC) [mM NaCl]	95	0	196	250
Critical coagulation concentration (CCC) [mM $CaCl_2$]	30	0	4.6	1.9
Visual observation				

 # Aggregating particles cannot be measured using DLS

results in net negative surface charge causing colloidal stability. A similar decrease in ZP values of magnetite was observed with increasing concentrations of humic acid and dissolved organic matter. It was attributed to an increased screening of positive charges on HNP by humic acid with negatively charged functional groups (Hu et al., 2010; Illes & Tombacz, 2006).

3.4 Effect of EPS on aggregation Kinetics of HNP

3.4.1 Aggregation with NaCl

With increasing concentration of NaCl, uncoated HNP, coated HNP 2:1 and HNP 5:1 showed an increase in the hydrodynamic diameter with time (Figure 3.4). Coated HNP- 1:5 were unstable and aggregated soon after formation, hence were not included in these measurements.

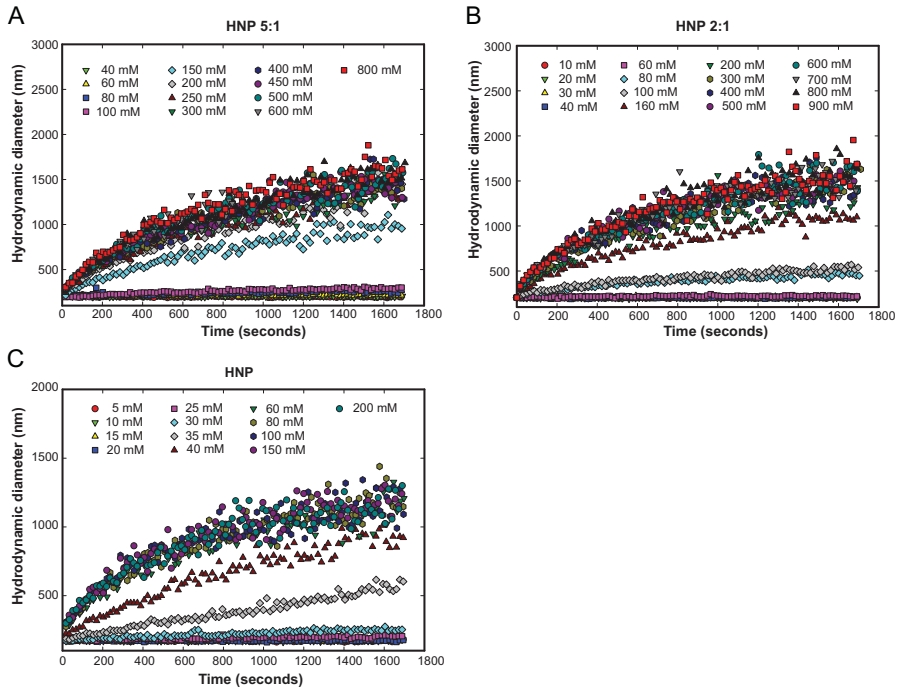

Figure 3.4 Aggregation profiles of A) HNP 5:1 B) HNP 2:1 C) HNP with different NaCl concentrations.

The two aggregation regimes i.e. the slow, reaction limited (RLA) and the fast diffusion limited aggregation (DLA) were observed at different salt concentrations for all the three HNP suspensions. In the RLA regime, the electrolyte concentration is not enough to screen the surface charge, while in DLA regime the electrolyte concentration is high enough to screen the surface charge on the particles, thus eliminating the kinetic energy barrier, leading to fast aggregation (K. L. Chen & Elimelech, 2007; Di Marco et al., 2007; He et al., 2008). Uncoated HNP particles exhibit a slow aggregation up to 40 mM NaCl concentration, whereas coated HNP 5:1 and 2:1 showed slow aggregation up to 200 mM NaCl. The fast aggregation was observed above 100 mM NaCl for uncoated particles, but the coated particles 5:1 and 2:1 showed fast aggregation only above 400 mM NaCl.

The energy at which the kinetic energy barrier disappears, and aggregation sets in, is defined as the critical coagulation concentration (CCC). With increasing electrolyte

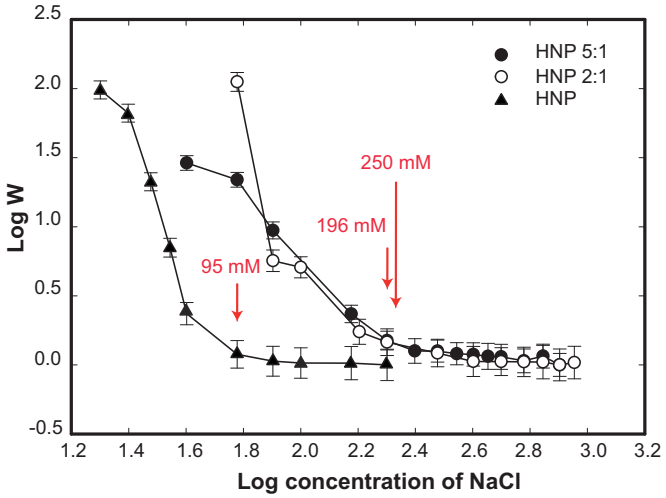

Figure 3.5 Stability ratio W as a function of NaCl concentration for coated and uncoated HNP (Red arrows indicate the CCC).

concentration, the stability ratio W decreases as the electrolyte concentration increases until CCC is reached. After this point, increasing salt concentration has no effect on the stability ratio (Figure 3.5). The CCC was determined from the graph of the stability ratio W versus electrolyte concentration (stability ratio graph). This graph typically displays two linear regions, a steep part for low electrolyte concentrations with dominant RLA regime and an almost horizontal part for higher electrolyte concentrations with dominant DLA regime. The point of intersection of the two regions is taken as the CCC (K. L. Chen & Elimelech, 2007; He et al., 2008). From Figure 3.5, the CCCs were determined to be 95 mM NaCl for HNP-uncoated, 250 mM NaCl for HNP-5:1, and 196 mM NaCl for HNP-2:1. Our results agree with the CCC values reported in literature for uncoated HNP (Amal et al., 1992; He et al., 2008; Mylon et al., 2004).

The increase in the CCC of the HNP on coating with EPS demonstrates the stabilizing effect of EPS on HNP due to the formation of more complete EPS coating on the HNP. The stronger inter-particle repulsion in HNP 5:1 and HNP 2:1 may be due to steric forces and electrostatic repulsion (Di Marco et al., 2007; Hu et al., 2010). When

the double layer electrostatic charges on the hematite and EPS polymers are screened by the cations, the polymer reduces the available volume for particle interaction, resulting into repulsive steric forces, stabilizing the attractive forces (Di Marco et al., 2007). Similar trends were observed for humic acid coatings on fullerene nanoparticles (K. L. Chen & Elimelech, 2007) and on magnetite nanoparticles (Hu et al., 2010) which were attributed to steric and electrostatic forces playing an important role in colloidal stabilization.

3.4.2 Aggregation kinetics with $CaCl_2$

Aggregation of coated and uncoated HNP with increasing concentrations of $CaCl_2$ was in general much faster than compared to NaCl. For HNP-uncoated particles, slow aggregation was observed up to 20 mM $CaCl_2$ (Figure 3.6), and fast aggregation was seen from 40 mM $CaCl_2$. However, for coated HNP-5:1 and HNP-2:1, fast aggregation was observed at very low concentrations of $CaCl_2$ (1.5 mM).

The CCC values also showed an opposite pattern in comparison to that shown by NaCl (HNP>HNP 2:1>HNP 5:1). For the uncoated HNP the CCC was 30 mM $CaCl_2$ and coated HNP 2:1 was 4.6 mM $CaCl_2$ and for HNP 5:1 was 1.9 mM $CaCl_2$. A slightly higher CCC of HNP 2:1 (with low EPS content) as compared to HNP 5:1 points towards an aggregation mechanism involving EPS (Huynh & Chen, 2011). Divalent ions such as calcium are known to bridge negatively charged groups of EPS and bring about flocculation (Bitton, 2010). Consequently, a drastic decrease in the CCC in presence of Ca^{2+} is due to formation of calcium bridges between the EPS molecules. Thus, HNP 5:1 with the highest concentration of EPS has the least CCC. Decrease in CCC due to formation of Ca bridges has also been reported for humic substances (Amirbahman & Olson, 1995; K. L. Chen & Elimelech, 2007; Kretzschmar & Sticher, 1997) and alginate polymers (Abe et al., 2011; K. L. Chen &

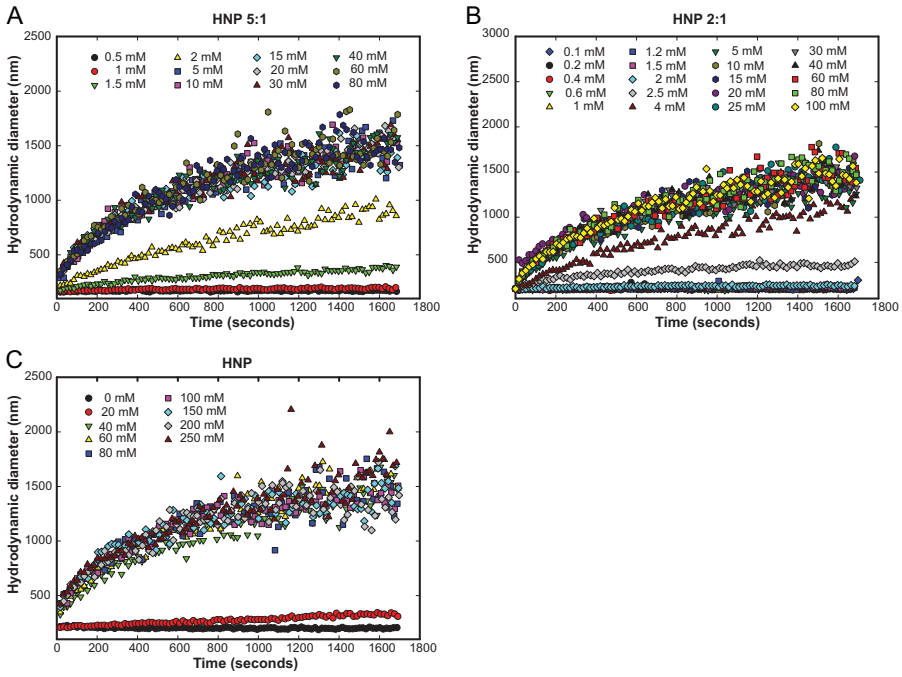

Figure 3.6 Aggregation profiles of A) HNP 5:1 B) HNP 2:1 C) HNP with different $CaCl_2$ concentrations.

Elimelech, 2006), fulvic acids (Abe et al., 2011; Amal et al., 1992) and polysaccharides (Labille et al., 2005).

3.5 Evaluation of interactions between the particles

The reconstructed W values using the DLVO model matched the experimental data (Supporting information, section no. S.9). The only parameter subjected to fitting was the Hamaker constant. However, not all data points were within the calculated range of model uncertainty. This can either be caused by the uncertainty in measured parameters, (especially the zeta potential might not represent ψ_d properly) or electrostatic and van der Waals forces are not enough to cannot explain the interactions between the particles. Many researchers have observed discrepancies with the DLVO prediction for organic coatings and have used the EDLVO to explain their results (K. Li & Chen, 2012; Romero-Cano et al., 2001). Hence, to increase the goodness of fit, we added different equations for interactions like acid/base and steric

interactions to the DLVO equation. Acid-base interactions have been successfully used to describe colloidal aggregation with natural organic matter (Hu et al., 2010; K. Li & Chen, 2012). Since it is not possible to individually measure certain parameters, parameter fitting was carried out for Hamaker constant and the Gibbs free energy of acid/base interaction. However, no increase in the quality of the fit could be achieved, since the effect of acid/base interactions on the shape of the log W vs. log concentration curve is identical to the effect caused by the changes in the Hamaker constant. Therefore, since none of these parameters can be measured adequately, the addition of acid/base interactions can only provide a strong parameter correlation between the Hamaker constant and the Gibbs free energy of acid/base interaction.

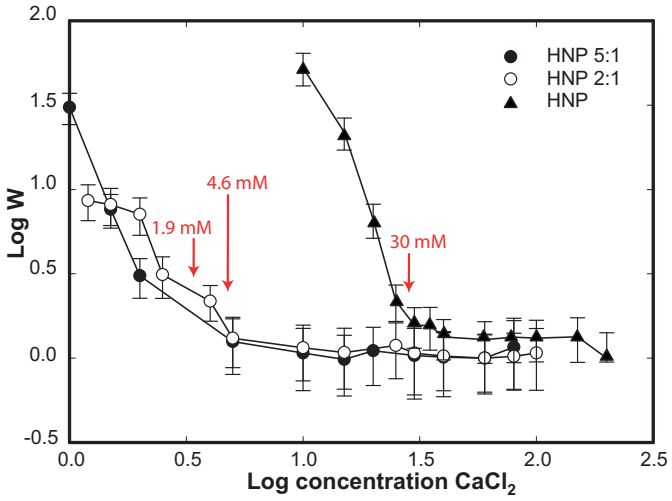

Figure 3.7 Stability ratio as a function of electrolyte concentration ($CaCl_2$) for uncoated and coated HNP (the red arrow indicate the CCC)

An analogous situation was encountered when using steric interactions in place of acid-base interactions. The values for Hamaker constant, the volume fraction of the EPS within the brush layer (ϕ_2) and the thickness of the brush layer (δ) were fitted. However, no increase in the goodness of fit could be achieved due to a strong correlation between the Hamaker constant and the parameters needed to represent steric interaction. Although the presence of steric interaction/ acid base interactions is

plausible from a physical point of view, the addition of further process models to the basic DLVO did not provide an increase in the goodness of fit and, therefore, renders unnecessary from a mathematical point of view. If these processes are present in the experimental data, they could not be identified properly using the EDLVO model due to severe parameter correlation. A thorough and precise determination of the Hamaker constant and the zeta potential would be needed to inversely fit parameters from the E-DVLO in a meaningful way. However due to the complexity of EPS samples and extremely small size of the nanoparticles it was not possible to do so.

Section 3. Closed-flow column transport experiments

3.1 Characterization of uncoated, biofilm-coated and EPS-coated porous media

3.1.1 Visualization of biofilm and EPS coating

SEM and CLSM combined with fluorescent staining were used to visualize the coatings on the porous media (Figure 3.8). The fluorescent dye ethidium bromide binds the DNA of bacteria and emits red light while calcofluor white binds the carbohydrates in the EPS and emits blue light. Thus, it was possible to differentiated between bacteria and EPS in the coatings on the porous media.

However, it was not possible to view the entire surface of the porous media at a magnification of 10x/ 40x due to the large size of the beads. Hence, 20 beads from each coating were analyzed for different surfaces. For CLSM, Z-stack images were made to observe the coated surfaces. The uncoated porous media was also observed for reference. Uniform coatings were observed on both biofilm and EPS-coated porous media (Figure 3.8 B,C,E,F). Also, bacteria were not observed in EPS-coated porous media.

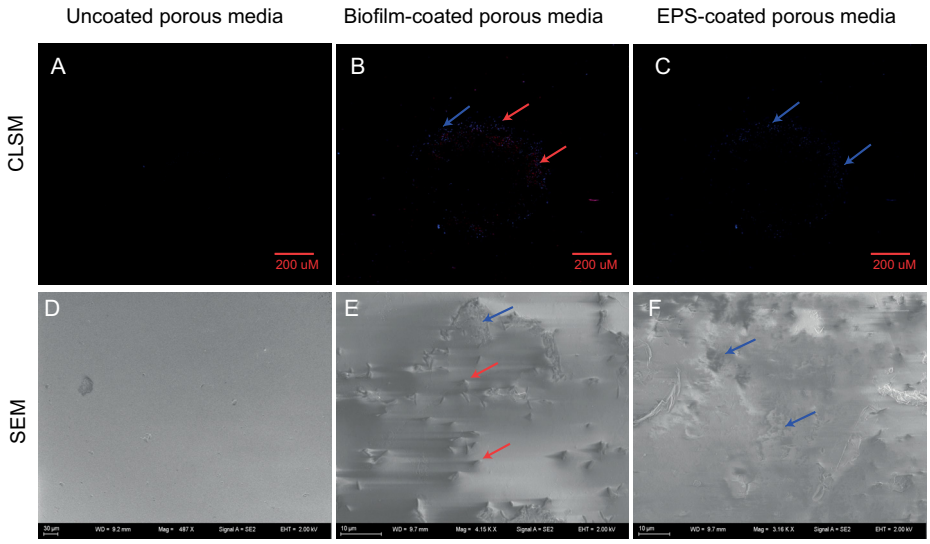

Figure 3.8 Coatings on the glass beads. A, B, C: CLSM image of uncoated glass bead, biofilm-coated glass bead and EPS-coated glass bead respectively. D, E, F: SEM image of uncoated glass bead, biofilm-coated glass bead and EPS-coated glass bead respectively.
(Red arrows indicate bacteria and blue arrows indicate EPS)

3.1.2 Thickness of the biofilm and EPS coating

Since CLSM visualized only a small area, the thickness of the coatings was indirectly measured by gravimetric analysis. The average thickness of the biofilm (22.7 ± 2.2 μm) was twice as large as EPS (12.3 ± 0.9 μm). The thickness of the coatings was uniform throughout the columns (Figure 3.9) with a slightly greater thickness of the

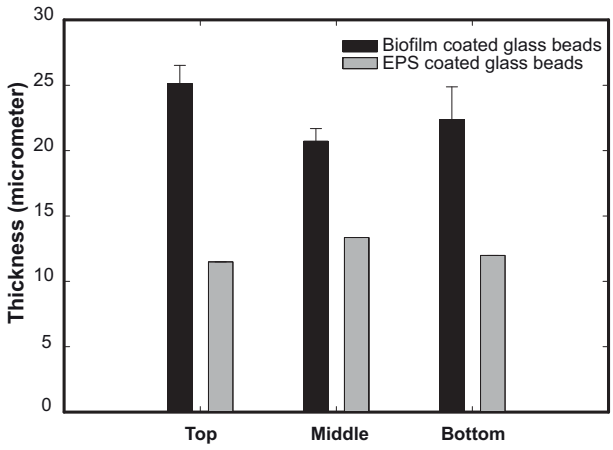

Figure 3.9 Thickness of the biofilm and EPS layers on the glass beads determined by gravimetric analysis

biofilm at the inflow end. This increase can be attributed to several reasons such as straining or physiochemical filtration, or higher availability of nutrients at the column influent (Tripathi et al., 2012). The distribution of the biofilms and EPS in the different layers was also equal. Gravimetric experiments along with CLSM and SEM confirmed the presence of a uniform layer of biofilms and EPS on the porous media.

3.1.3 Surface charge of uncoated, biofilm-coated and EPS-coated porous media

All the three surfaces tested have a net negative surface charge in the experimental pH range (pH~7). EPS and biofilm coating result in a decrease in the streaming potential of the porous media over a pH range 2-12 (Figure 3.10 B). The isoelectric point of the glass beads also changes on coating with EPS and biofilm. This shift in the surface charge is due to the modification of the functional group on the surface of the glass beads. EPS contains weakly acidic functional groups like carboxyl, phosphoryl, and hydroxyl that will cause a weakly acidic surface potential (Wang et al., 2012).

Furthermore, the biofilm and EPS-coated surfaces exhibit similar surface charge, suggesting analogous surface moieties or charged functional groups. Some prior

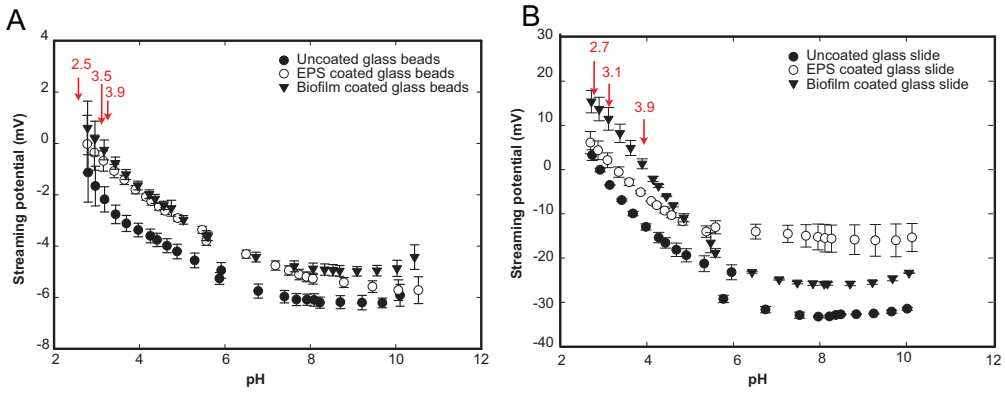

Figure 3.10 A. Streaming potential of coated and uncoated glass slides B. Streaming potential of coated and uncoated glass beads (red arrows indicate the isoelectric point for the coated and uncoated glass beads)

studies also show a decrease in the streaming potential of a surface after coating with

biofilms (Z. Li et al., 2013; Tripathi et al., 2012; Truesdail et al., 1998). This change in the surface potential by EPS/biofilm coating may have implications on the sorption of the nanoparticles (Tripathi et al., 2012).

Table 3.3 Isoelectric point of the glass bead with different surface coatings

Surface	Isoelectric point (pH)
Uncoated glass beads	2.5
EPS-coated glass beads	3.5
Biofilm-coated glass beads	3.9

However, the absolute streaming potential for borosilicate glass is far too large than the literature value of around -40 mV at pH 7 (Hunter, 1981a; Lameiras et al., 2008). As already explained in the method section, this is due to the large size of the glass beads which results in a decrease in the pressure difference achieved between the two electrodes during the measurement. To circumvent these artifacts, we conducted an analog experiment with borosilicate glass slides with similar coatings. A comparable trend of the streaming potential was observed (Uncoated > EPS-coated ≥ biofilm-coated) (Figure 3.10 A).

Table 3.4 Carbon content (mg C/l) of the electrolyte after streaming potential measurements (HCl and NaOH were used to adjust the pH of the solution)

Sample	After HCl	After NaOH
Glass	-	6.5
EPS-coated glass beads	-	6.6
Biofilm-coated glass beads	1.0	5.5

To ensure the stability of the coatings during the measurement procedure, DOC of the solution passed through the beads was measured after the experiment. There were no significant differences in carbon content (Table 3.4). The increase in the DOC content

after alkaline titration is caused by the high carbon content of the added base at the start of the experiment.

3.2 Concentration of organic matter and microbial cells released from the biofilm and EPS-coated columns

The release of

bacteria and organic components from the EPS and biofilm-coated porous media was monitored over time. The total number of viable bacteria and the DOC in the effluent is given in the Table 3.5. Both, bacteria and released organic substances form the biofilm and EPS may serve as mobile bio-colloids and organic colloids respectively. Once released, they are subject to interactions with the HNP.

3.3 Transport of conservative tracer

In closed flow columns, a typical breakthrough in the mixing vessel consists of oscillations (a continuous increase and decrease) in the concentration of the solute,

Table 3.5 Total concentration of bacteria and EPS resealed from coated porous media

HNP suspension	Biofilm-coated porous media		EPS-coated porous media
	Total bacterial count CFU/ml Colony forming units/ml	DOC mg/L	DOC mg/L
HNP 5:1	4.9 X 107	11.93 ± 2.1	19.96 ±0.8
HNP 2:1	9.6 X 107	12.56 ±0.6	27.9 ±2.03
HNP 1:5	6.55 X 108	15.7 ± 3.3	25.6 ±7.9
HNP	3.6 X 107	10.6 ±1.6	29.7± 4.1

which finally stabilizes at equilibrium stage (Figure 3.11). This is due to flow of the solute through the column until the dispersion, diffusion and mixing leads to a stable concentration in the mixing vessel (Ritschel & Totsche, 2016a). The mobility of the solute can be interpreted by comparing the concentration of the solute in the mixing vessel with the volumetric dilution at equilibrium. The volumetric dilution line

(Figure 3.12) depicts the expected decrease in the concentration of the solution due to water-filled pore space present in the columns (Ritschel & Totsche, 2016a).

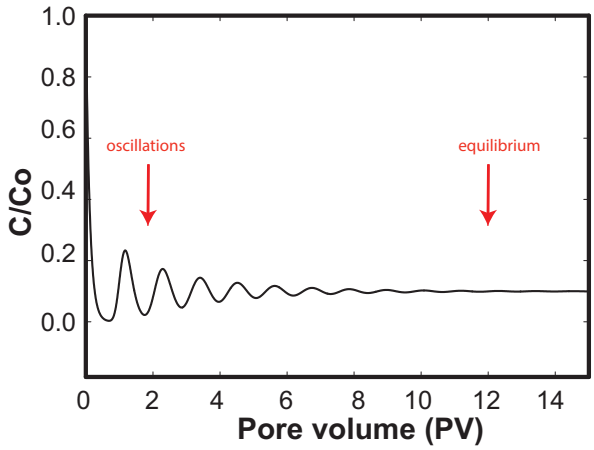

Figure 3.11 A typical breakthrough curve obtained by simulations (Ritschel & Totsche, 2016a)

The transport of the non-reactive tracer bromide showed no significant difference between the coated and the uncoated porous media at the equilibrium state (60 PV) (Figure 3.12). The decrease in the bromide concentration at equilibrium was in the range of volumetric dilution, indicating non-reactive transport of bromide in both coated and uncoated porous media. Also, no significant change was observed in the final concentration of the conservative tracer at equilibrium (60 PV) in uncoated and coated columns. Effects such as non-uniform flow or preferential flow due to complete/ partial clogging by extensive growth of biofilm have been reported by some researchers (Engesgaard et al., 2006; Kone et al., 2014; Taylor & Jaffe, 1990; Wanner et al., 1995). Such effects were not observed in our experiments since biofilms were grown only for two days, and no more growth media was provided.

Section 3.3 A Transport of uncoated HNP in uncoated, biofilm and EPS-coated porous media

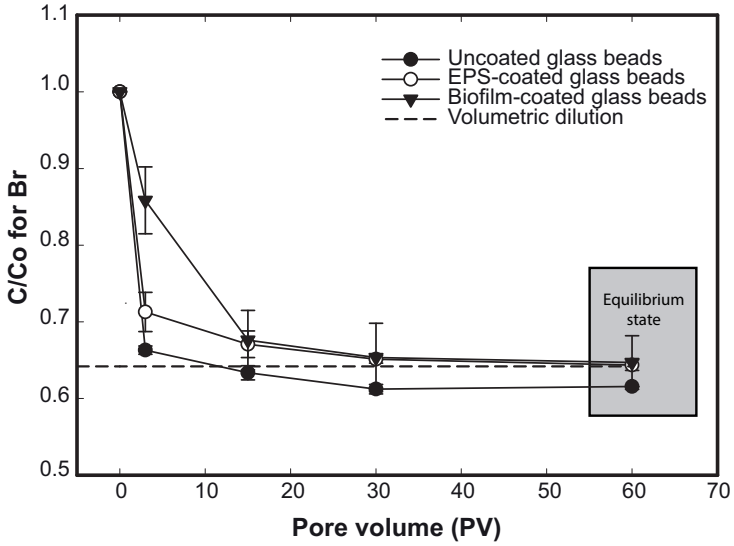

Figure 3.12 Transport of conservative tracer (Equilibrium state is highlighted with a box)

A significantly different mobility of HNP was observed in the three different porous media tested (Figure 3.13). At the end of 60 PV, uncoated HNP were completely retained in the uncoated columns, and no particles were seen in mixing vessel. However, in coated columns the retention of HNP was comparatively weak as qualitatively indicated by the weak staining of the porous media and the still strong color in the mixing vessel. The pH of the system was constant at neutral pH and not much change was observed in the electrical conductivity of the system (fluctuation of 10 μS/cm).

The change in the relative concentration of HNP in the mixing vessel over pore volume is given in Figure 3.14. In uncoated columns, the concentration of HNP drops drastically below the volumetric dilution and reaches zero. Combining this observation with the visual observation we can attribute the decrease in the HNP

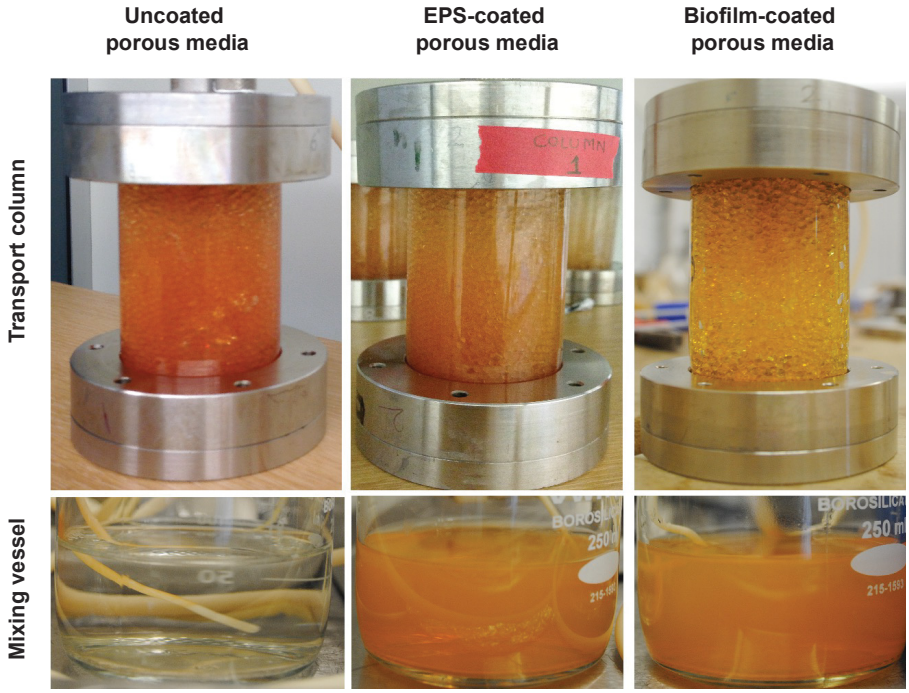

Figure 3.13 Visual observation of transport of HNP through uncoated, EPS-coated and biofilm-coated porous media at equilibrium (60 PV) A,B,C,: glass columns for uncoated, EPS-coated and biofilm-coated porous media respectively. D,E,F: mixing vessel for uncoated, EPS-coated and biofilm-coated porous media respectively)

concentration to an attachment of HNP to the surface of the glass beads. In the case of EPS and biofilm-coated columns, the concentration of the HNP drops below the volumetric dilution but does not reach zero. Therefore, a fraction of HNPs are mobile in biofilm and EPS-coated porous media at equilibrium.

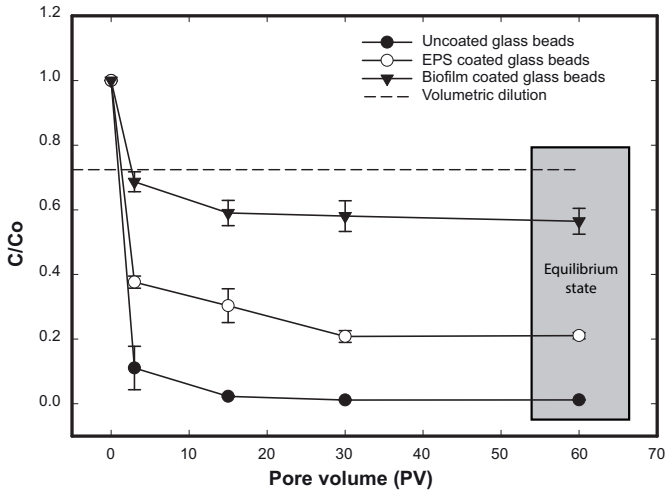

Figure 3.14 Transport of uncoated HNP through uncoated, EPS-coated and Biofilm-coated porous media

3.1 Colloidal stability during transport

Colloidal properties the nanoparticles before and after the transport experiments are given in Table 3.6. The zeta potential values of the HNP suspension after passing through EPS or biofilm-coated porous media indicate colloidal stable HNP (|ZP|> 20 mV; (Hanaor et al., 2012; Hunter, 1981b)) with a net negative zeta potential. The charge reversal of the HNP from positive to negative suggests a possible coating of the HNP with organic matter released from biofilms (Abudalo et al., 2010; Chekli et al., 2013; Zhuang & Yu, 2002) forming organo-mineral colloids. A steady amount of organic colloids are released from the coating of the porous media over time (Table

Table 3.6 Colloidal stability of HNP before and after transport in uncoated, EPS-coated and Biofilm-coated porous media

Porous media ->	**Uncoated**		**EPS-coated**		**Biofilm-coated**	
	0 PV	60 PV	0 PV	60 PV	0 PV	60 PV
Hydrodynamic diameter (nm)	210 ± 70	- #	210 ± 70	443±120	210 ± 70	372± 572
Zeta potential (mV)	+35 ± 7	- #	+35 ± 7	-19± 14	+35 ± 7	-23± 16

no hematite particles were present in the solution. Hence measurements could not be done

3.5). Once released, the organic matter can interact with uncoated HNP forming colloidally stable organo-mineral colloids with a net negative zeta potential as observed.

We also observed the charge reversal of HNP on coating with different concentration of EPS in earlier section. Charge reversal on coating with an opposite charged material is also reported in literature for, e.g., iron oxides coated with humic acids (Chekli et al., 2013), coating of clay minerals (kaolinite, montmomorillinite and illite) with iron oxides and organic matter (Zhuang & Yu, 2002).

3.2 Porous media attachment efficiency

The calculated single collector contact efficiency and the porous media attachment efficiency are given in Table 3.7. The attachment efficiency of HNP to the glass beads decreased on coating with EPS and biofilm. Hence low retention of HNP was

Table 3.7 Contact efficiency, removal efficiency, attachment efficiency and deposition efficiency calculated for transport of uncoated HNP in uncoated, biofilm and EPS-coated porous media

Porous media	Alpha (α)	n_o	C/Co	k_d
Uncoated	0.72	0.18	0.02	2.20E-05
EPS-coated	0.18	0.21	0.29	6.58E-06
Biofilm-coated	0.04	0.17	0.77	1.32E-06

observed on EPS and biofilm-coated porous media. The deposition coefficient k_d also points to higher deposition of uncoated hematite.

The calculated theoretical single collector contact efficiency (η_o) however contradicts the observed results. The η_o calculated for EPS-coated porous media and is slightly higher than the uncoated HNP suggesting a higher retention of coated HNP in the EPS-coated porous media. The equations described by Tufenkji and Elimelech (2004) for calculating the η_o does not take into account the surface charge of the particles and

the collector surfaces. And in this case the surface charge of the particles changes during transport. Hence, we cannot use the relative values of η_o for predicting the difference between oppositely charged particles.

3.3 Mechanism of transport of HNP in uncoated, EPS-coated and biofilm-coated porous media

The retention of the HNP in the uncoated columns can be due to strong sorption of the HNP on the glass beads by electrostatic interactions between the positively charged HNP and negatively charged silica (Schwertmann & Cornell, 2000) at the experimental pH ~7. Other factors such as straining can be overruled due to extremely small ratio of (7.2E-05) of particles size to collector size. Straining is considered a feasible mechanism for retention of nanoparticles only when the size ratio is greater than 0.05 (Bradford et al., 2003).

As shown by the streaming potential, the coated glass beads exhibit negative surface potentials. The fraction of HNP mobile in the coated columns exhibit net negative zeta potential. Moreover, the retention and attachment efficiency of the HNP to the coated surfaces is rather small. These all results suggest electro-steric repulsion between the HNP and the coated surfaces as observed by Mitzel and Tufenkji (2014). Mitzel and Tufenkji (2014) reported a low attachment efficiency of biofilm-coated surfaces for PVP stabilized silver nanoparticles, which was attributed to steric repulsion between the nanoparticles and the coated surfaces.

A high fraction of HNP were mobile in biofilm-coated porous media in comparison to EPS-coated porous media despite similar surface potential of both biofilm and EPS-coated porous media. We explain this with the different thickness of the coatings as established by the gravimetric analysis of the surface layer thickness. Also, the density and the charge on EPS depend upon its local concentration and the number of

linkages between adjacent polymer chains (Ikuma et al., 2015) thus affecting its reactive sites and consequently its attachment efficiency.

Section 3.3 B Transport of EPS-coated HNP (HNP 5:1, HNP 2:1, HNP 1:5) in uncoated, biofilm and EPS-coated porous media

Transport of EPS-coated HNP through uncoated porous media

EPS-coated HNP (HNP 5:1, HNP 2:1, HNP 1:5) were flown through columns with uncoated glass beads as porous media at neutral pH and electrical conductivity of 61 µS/cm. Significantly different mobility of the uncoated and coated HNP suspensions were observed after exchange of 60 PV (Figure 3.15). HNP 5:1 and HNP 2:1 were seen in the column as well as the mixing vessel. However, HNP 1:5 were aggregated and sediment in the mixing vessel and no color of hematite was observed in the columns. The transport of uncoated HNP is already explained in the section above and is used for comparison in this section.

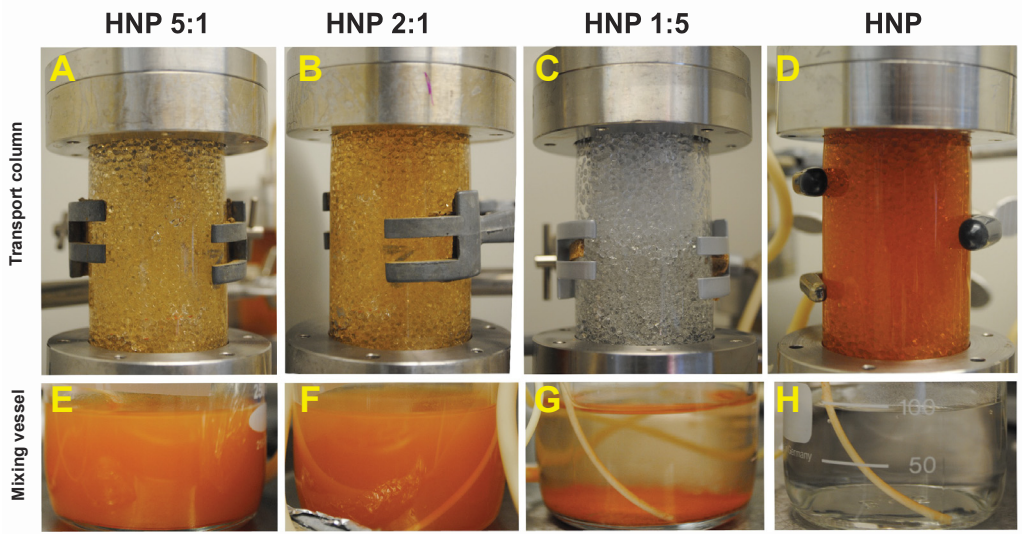

Figure 3.15 Visual observation of transport of EPS-coated HNP through uncoated porous media at 60 PV (A,B,C,D: glass columns for HNP 5:1, HNP 2:1. HNP 1:5 and HNP respectively. E,F,G,H: mixing vessel for HNP 5:1, HNP 2:1. HNP 1:5 and HNP respectively)

The change in the relative concentration of the HNP in the supply vessel over pore volume is given in (Figure 3.16). The concentration of HNP 5:1 and HNP 2:1 decreased below the volumetric dilution and stabilized at equilibrium. Thus, about 60% of particles (HNP 5:1 and HNP 2:1) were mobile in uncoated porous media. However, decrease in the concentration of colloidally unstable HNP 1:5 is nearly equal to the volumetric dilution. Also, visual observations show aggregates of colloidally unstable coated 1:5 nanoparticles in the mixing vessel. Hence we conclude that the decrease in the concentration is due to water of saturation from the columns and the particles are immobile and aggregated in the mixing vessel.

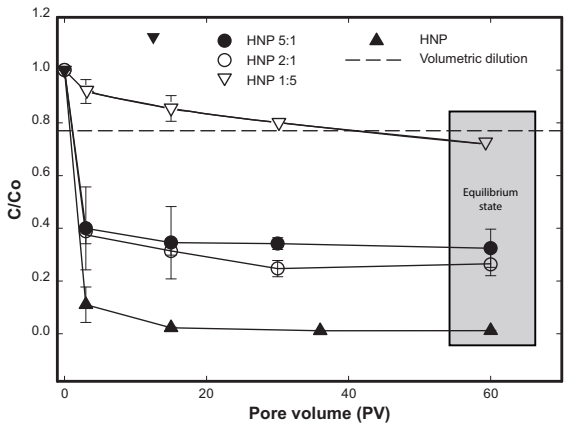

Figure 3.16 Transport of EPS-coated HNP through uncoated porous media columns

3.1 Colloidal stability of the nanoparticles during transport

Under saturated, conditions colloidal stability is an important factor determining the mobility of the colloids (Mccarthy & Zachara, 1989). The hydrodynamic diameter and zeta potential of the HNP suspensions before and after the transport experiments are given in Table 3.8. As seen from the results, HNP 2:1 and HNP 5:1 retain their colloidal stability after the transport experiments and HNP 1:5 are still colloidally unstable (|ZP|< 20 mV).

Table 3.8 Colloidal stability of EPS-coated HNP before and after transport experiments in uncoated porous media

HNP suspensions	Hydrodynamic diameter (nm)		Zeta potential (mV)	
	0 PV	60 PV	0 PV	60 PV
HNP 5:1	217 ± 47	134 ± 50	-33 ± 6	-29 ± 9
HNP 2:1	204 ± 86	256 ± 49	-26 ± 7	-31 ± 7
HNP 1:5	1552 ± 924	2584 ± 761	+4 ± 8	-10 ± 4
HNP	210 ± 70	#	+35 ± 7	#

 # all the particles were retained in the column

3.2 Porous media attachment efficiency

The calculated single collector contact efficiency and the porous media attachment efficiency are given in Table 3.9. The porous media attachment efficiency (α) of HNP 1:5 is higher than coated particles HNP 5:1 and HNP 2:1. Hence coated particles HNP 5:1 and 2:1 exhibited a lower retention in the uncoated porous media. The calculated theoretical single collector contact efficiency (η_o) calculated for HNP 2:1 and HNP 5:1 is lower than HNP 1:5 suggesting a higher retention of HNP 1:5 in the porous media. However, we cannot compare the single collector contact efficiency of uncoated HNP with the coated HNP as explained in the earlier section (Page no 62)

Table 3.9 Contact efficiency, removal efficiency, attachment efficiency and deposition efficiency for transport of EPS-coated HNP through uncoated porous media columns

HNP suspensions	Alpha (α)	η_o	C/Co	k_d
HNP 5:1	0.11	0.23	0.45	4.28E-06
HNP 2:1	0.12	0.26	0.37	5.34E-06
HNP1:5	2.30E-05	13.08	0.99	4.91E-08
HNP	0.72	0.18	0.02	2.20E-05

3.3 Mechanism of transport

Colloidally stable coated particles HNP 5:1 and HNP 2:1 are negatively charged at the experimental pH (ZP: -33, -26 mV respectively). The decrease in retention of the HNP 5:1 and HNP 2:1 in uncoated porous media is due to repulsion between negatively charged nanoparticles and the porous media. In a comparative study, a similar decrease in the deposition rate of humic acid coated HNP (Amirbahman & Olson, 1995; Kretzschmar & Sticher, 1997) and negatively charged zinc-oxide nanoparticles (Jiang et al., 2012) in negatively charged porous media is reported.

Transport of EPS-coated HNP through EPS-coated glass columns

The concentration of EPS-coated HNP 2:1 and HNP 5:1 decreased below the volumetric line but did not reach zero (Figure 3.17). Thus a fraction of EPS-coated HNP 2:1 and HNP 5:1 were mobile in EPS-coated porous media. However, colloidally unstable HNP 1:5 remain aggregated in the supply vessel and were immobile in EPS-coated columns. The high error in measurements is due to the aggregates formed in the suspension, which produce variation in the sampling.

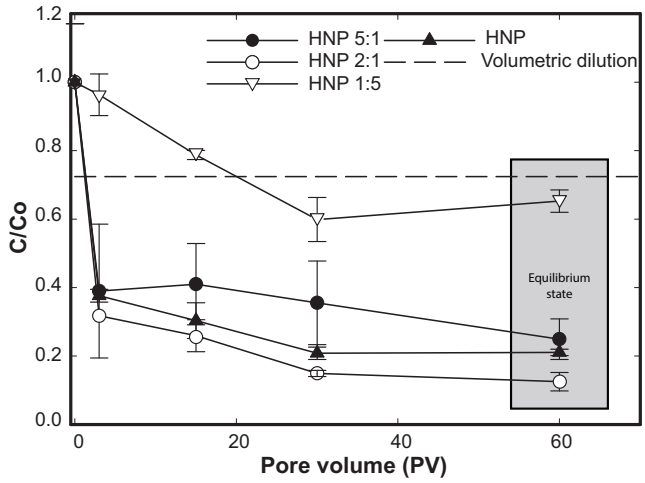

Figure 3.17 Transport of EPS-coated HNP through EPS-coated porous media columns

3.4 Colloidal stability during transport

The zeta potential values of HNP 5:1 and HNP 2:1 indicated colloidally stable HNP even after transport experiments (Table 3.10). A small decrease in the zeta potential value was observed for HNP 1:5. This reduction in the zeta potential can be associated to the interactions of the HNP with the organic matter discharged from EPS-coated columns.

Table 3.10 Colloidal stability of EPS-coated HNP before and after transport experiments in EPS-coated porous media

HNP suspensions	Hydrodynamic diameter (nm)		Zeta potential (mV)	
	0 PV	60 PV	0 PV	60 PV
HNP 5:1	217 ± 47	347 ± 95	-33 ± 6	-30 ± 5
HNP 2:1	204 ± 86	265 ± 72	-26 ± 7	-36 ± 11
HNP1:5	1552 ± 924	764 ± 180	+4 ± 8	-10 ± 5
HNP	210 ± 70	443 ± 120	+35 ± 7	-19 ± 14

3.5 Porous media attachment efficiency

EPS-coated HNP 5:1, HNP 2:1 exhibited the low attachment efficiency to the EPS-coated porous media (Table 3.11). Furthermore, HNP 5:1 has the lowest attachment efficiency of all. This indicates a decrease in retention of particles in the porous media in comparison to HNP 2:1 and uncoated HNP. However, the difference is not experimentally significant. Moreover, the single collector contact efficiency is comparable in this case, due to similar charge (negative) on all the nanoparticles (zeta

Table 3.11 Contact efficiency, removal efficiency, attachment efficiency and deposition efficiency for transport of EPS-coated HNP through EPS-coated porous media columns

HNP suspensions	Alpha (α)	η_o	C/Co	k_d
HNP 5:1	0.16	0.21	0.34	5.68E-06
HNP 2:1	0.23	0.24	0.17	9.34E-06
HNP 1:5	0.28E-03	0.11	0.90	5.53E-07
HNP	0.18	0.21	0.29	6.58E-06

potential of uncoated HNP shifts to negative charge). The single collector contact efficiency for HNP 5:1, HNP 2:1 is nearly same due to comparable deposition on the EPS-coated surfaces.

3.6 Mechanism of mobility

The mobility of coated HNP 2:1 and HNP 5:1 can be explained by electrosteric repulsion between EPS-coated HNP and EPS-coated porous media. The net surface charge on the coated porous media and the surface of coated HNP is negative. Mitzel and Tufenkji (2014) also described a low attachment efficiency of biofilm-coated surfaces for PVP stabilized silver nanoparticles, which was credited to steric repulsion between the nanoparticles and the coated surfaces. At pH 7, EPS are amphoteric and form of a random network of coiled polymeric chains (Wang et al., 2012). The protein components of EPS can contribute to the hydrophobic and steric repulsion (Hwang et al., 2012; Zhao et al., 2014). The hydrophobic and steric repulsion can act as a critical factor to reduce the attachment efficiency when both the porous media and the particle are coated with a steric stabilizing polymer (Lin et al., 2012; Mitzel & Tufenkji, 2014). Therefore, the presence of EPS on the HNP and the porous media surfaces may lead to electrosteric repulsive forces resulting into less deposition on the coated surfaces.

Transport of EPS-coated hematite nanoparticles through biofilm-coated glass columns

Relative concentrations of EPS-coated HNP flow through biofilm-coated porous media are given in Figure 3.18. Colloidally stable EPS-coated HNP 5:1 and HNP 2:1 exhibit a mobile fraction of nanoparticles. Remarkably, around 40 % of colloidally unstable HNP 1:5 were also mobile in biofilm-coated porous media. Uncoated HNP

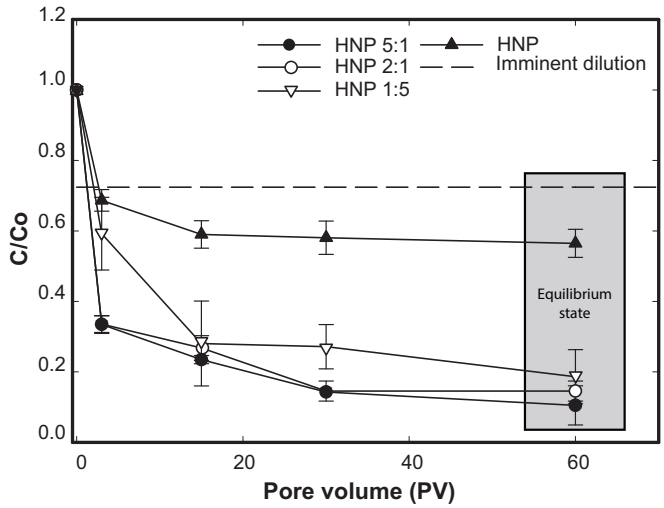

Figure 3.18 Transport of EPS-coated HNP through Biofilm-coated porous media columns

exhibited a higher fraction of mobile particles in comparison to coated HNP 5:1 and 2:1 were less mobile and aggregating in the supply vessel.

3.7 Colloidal stability during transport

Coated HNP 2:1 and HNP 5:1 retained their colloidal stability (|ZP| > 20 mV) with a small increase in their hydrodynamic diameter. However, HNP 1:5 nanoparticles were also colloidally stable (|ZP| > 20 mV) after transport experiments. The decrease in zeta potential of HNP 1:5 was also observed in EPS-coated porous media (Table 3.12).

Table 3.12 Colloidal stability of EPS-coated HNP before and after transport experiments in Biofilm-coated porous media

HNP suspensions	Hydrodynamic diameter (nm)		Zeta potential (mV)	
	0PV	60 PV	0PV	60 PV
HNP 5:1	217 ± 47	538±87	-33 ± 6	-29 ± 18
HNP 2:1	204 ± 86	423±130	-26 ± 7	-32± 11
HNP1:5	1552±924	431±217	+4 ± 8	-32± 6
HNP	210±70	372± 72	+35±7	-23± 16

Biofilm-coated porous media released a higher concentration of organic colloids compared to EPS-coated porous media (Table 3.5), which might have resulted in colloidal stability. We have shown in the previous chapter that increasing concentration of EPS can change the colloidal stability of the nanoparticles. Therefore, the shift in the colloidal stability may have played a role in the mobility of the particles.

3.8 Porous media attachment efficiency

The attachment efficiency of EPS-coated HNP 5:1 and HNP 2:1 is higher than the HNP 1:5 (Table 3.13). This contradicts the observed results. This is due to the large particle size of HNP 1:5 used in the calculation. As seen from the zeta potential measurements, some particles regained colloidal stability and were no longer aggregated. However, DLS is not a competent technique to measure suspension with different particle size. In presence of larger particles, it cannot measure smaller sized particles. Hence we could not measure the effective particle size of the colloidally stable fraction after the transport experiments. Hence we cannot use the CFT model to explain the result obtained for HNP 1:5 in biofilm-coated porous media.

Table 3.13 Contact efficiency, removal efficiency, attachment efficiency and deposition efficiency for transport of EPS-coated HNP through biofilm-coated porous media columns

HNP suspensions	Alpha (α)	η_o	C/Co	k_d
HNP 5:1	0.29	0.22	0.144	1.03E-05
HNP 2:1	0.21	0.24	0.20	8.54E-06
HNP1:5	3.72E-03	11.92	0.25	7.23E-06
HNP	0.04	0.17	0.77	1.32E-06

3.9 Mechanism of mobility

The transport of EPS-coated HNP in biofilm-coated porous media can be explained by electro-steric repulsion between similar surface coatings on the porous media and

biofilms as already explained earlier for EPS-coated columns (Page no: 69)(Amirbahman & Olson, 1995; Kretzschmar & Sticher, 1997)

A small fraction of EPS-coated particles were mobile in biofilm and EPS-coated porous media in comparison to uncoated coated porous media. This reduction in the mobility can be explained by various reasons. The biofilm/EPS-coated surfaces are less negative charge in comparison to uncoated surfaces (Figure 3.10). Thus, biofilm-coated surfaces will exert less electro-steric repulsion on the negatively charged coated HNP compared to uncoated surfaces (Tripathi et al., 2012). Hence, EPS-coated HNP observed more retention in the biofilm-coated porous media as compared to uncoated porous media. However, other mechanisms such as filtration of the coated nanoparticles due to increased aggregation cannot be overruled. Jung et al. (2014) have reported a small decreased in the transport of polymer coated zero-valent iron with high concentrations of humic acids, which was associated to hetero-aggregation. Mitzel and Tufenkji (2014) reported a decrease in the repulsive charge experience by the nanoparticles due to increased separation distance between the surface of porous media and origin of charge on the nanoparticles.

Furthermore, the difference in the mobility of the particles in EPS and biofilm-coated surfaces can be attributed to different reasons. It can be due to the different thickness of the coatings as established by the gravimetric analysis of the surface layer thickness. Also, it can be difference in density and the charge on EPS which depend upon its local concentration and the number of linkages between adjacent polymer chains (Ikuma et al., 2015).

Section 3.3 C Remobilization of hematite nanoparticles

Remobilization of the uncoated hematite retained in the uncoated porous media is presented in Figure 3.19. EPS remobilized about 8% of the sorbed hematite forming

negatively charged HNP (ZP: -21 ± 4 mV). The shift in zeta potential suggested formation of EPS-HNP colloids. However, no remobilization was observed when sterile water was flown through the columns.

EPS are complex mixtures with a wide variety of charges and functional groups present on them (Wang et al., 2012). Hence, they have a varying binding affinity to different molecules or mineral surfaces. It has been established that hematite has a stronger affinity towards EPS in comparison with kaolinite (Poorni & Natarajan, 2014). While goethite has a stronger affinity towards EPS than clay minerals (Cao et al., 2011) and can bind to Fe center via inner sphere complexation of phosphate containing macromolecules (Fang et al., 2012; Omoike & Chorover, 2004). From the observed results, we can conclude that hematite molecules have a higher affinity to EPS in comparison to glass. This also explains transformation of uncoated HNP when flown through EPS and biofilm-coated porous media.

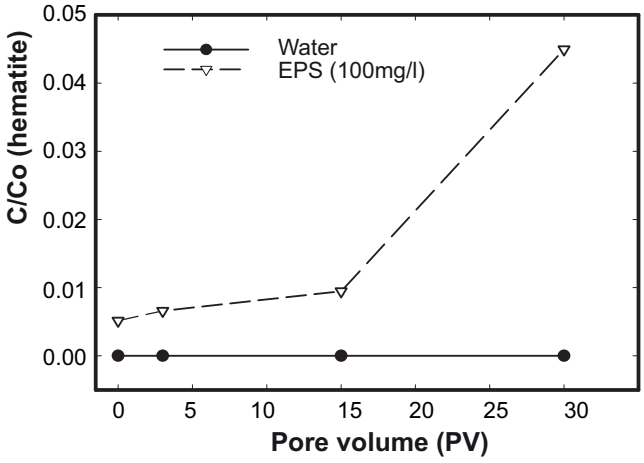

Figure 3.19 Remobilization of HNP with EPS

4 Conclusions and outlook

4.1 General conclusion

Due the heterogeneous and unpredictable properties of biofilms and EPS (i.e., variable composition and structure, complex surface groups), it is challenging to ensure the its role on the fate and mobility of nanoparticles. The results presented in this thesis demonstrate the influence of biofilms and EPS on the transport of nanoparticles considering three major scenarios 1) Biofilms/EPS present on porous media 2) EPS present on nanoparticles 3) Combined 1and 2 i.e. Biofilm/EPS present on both, porous media and nanoparticles. A pictorial representation of the important processes influencing the transport of hematite nanoparticles in the three cases studied is shown in Figure 4.1.

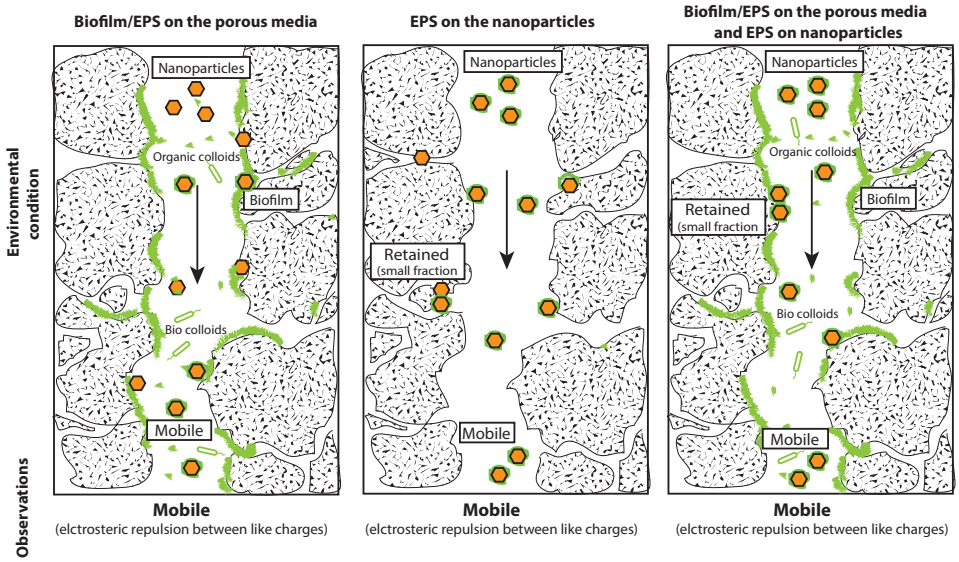

Figure 4.1 Representation of observations for influence of biofilms/EPS on transport of HNP

In the first case study, the presence of biofilm and EPS coatings on the porous media enhanced the transport of HNP. Contrarily, in the control experiment, uncoated HNP were retained inside the uncoated porous media. The zeta potential values of the

outflow solution show presence of organic matter coated HNP in biofilm and EPS-coated columns. This transformation of HNP is due to the organic colloids formed by the coating on the porous media. Also, the attachment efficiency of the positively charged uncoated HNP to negatively charged coated surfaces is low. Thus, pointing out that electrokinetic properties like surface charge are not always good predictors of transport. These results negate our hypothesis that "Biofilm on the porous media will act as trap and reduce the mobility of uncoated HNP, due to the electrostatic attraction between the positively charged hematite and negatively charged biofilm surfaces". Biofilm-coated porous media are not always the collectors of nanoparticles as proposed by many studies (Xiao and Wiesner 2013, Tripathi et al. 2011, Li et al. 2013). It is vital to consider the organic colloids formed, surface charge, the concentration and the binding affinity of the biofilm components to the inorganic/organic compounds.

In the second scenario, we established the significance of increasing concentrations of EPS in conferring colloidal stability to HNP. Low concentrations of EPS can aggregate HNP, but higher concentrations of EPS can colloidally stabilize HNP forming organo-mineral colloids. The zeta potential of the HNP and the isoelectric point decreased with increasing concentration of EPS. This points to a complete coverage of EPS on HNP with increasing loadings of EPS. Also, the shift in the isoelectric point of hematite indicates inner-sphere surface complexes of EPS on hematite. The CCC studies with NaCl and $CaCl_2$, also indicates colloidal stability with increasing loadings of EPS. Furthermore, colloidally stable EPS-coated nanoparticles were mobile in uncoated porous media while colloidally unstable EPS-coated nanoparticles were immobile. Therefore, we can conclude that at higher concentrations EPS can transform HNP forming organo-mineral colloids rendering

them mobile in uncoated porous media tested. Thus, proving our hypothesis for this section of the study. This study also highlights the significance of colloidal stability for transport of nanoparticles as reported in the literature (Kretzschmar & Schafer, 2005).

Furthermore, the carbon to iron ratio for most natural colloids is in the range of 0.5 to 2 (Fritzsche et al., 2015; Kögel-Knabner et al., 2008; Quik et al., 2012). Consequently, transport behaviors of HNP 2:1 and HNP 1:5 mimic the natural conditions while HNP 5:1 exhibit an extreme situation. Hence this study can be extrapolated to natural conditions and used to predict the behavior of HNP in biofilm rich zones in the environment.

Lastly, in a combined scenario, colloidally stable EPS-coated HNP were mobile in both biofilm and EPS-coated porous media. Surprisingly, colloidally unstable HNP, regained its colloidal stability (|ZP|>20 mV) and were mobile in biofilm-coated porous media. This may be due to the excess organic colloids released by biofilm-coated porous media. This once again demonstrates the significance of organic colloids released from the biofilms in transport of hematite nanoparticles.

We also studied remobilization of HNP in uncoated porous media. Uncoated HNP were desorbed by EPS solution forming EPS-hematite organo-mineral colloids. This indicates the high bonding affinity between hematite and EPS. This observation also helps to explain the transformation of uncoated hematite in EPS and biofilm-coated porous media. EPS due to its high bonding affinity to HNP, forms negatively charged EPS:HNP colloids which are mobile in all the three porous media tested.

Other environmental factors such as increase in ionic concentration and composition due to sea water infiltration, rain events will also affect the colloidal stability and transport of the such organic colloids. Organic coatings offer some degree of

tolerance to aggregation by changes in the ionic strength. However, it depends on the type of organic matter, the thickness of coatings, etc. In this study, we only examined EPS-coated HNP could resist aggregation to high concentrations of NaCl (250 mg/l), however, small amount of $CaCl_2$ resulted into aggregation due to Ca ion bridging between the EPS molecules. Such factors must be taken into account when predicting the fate of organo-mineral colloids.

Furthermore, the concentration of EPS coating present on the HNP particles could not be precisely determined. Due to extreme small size of the particles it was not possible to separate the coated HNP particles from the free EPS by centrifugation or filtration. Advanced techniques such as AFM combined with SIMS were planned to visualize the spatial distribution of the adsorbed EPS and its components (insular versus patchy versus full/complete coverage) on the nanoparticles. However again, due to extreme small size and magnetization of hematite particles it was impossible to analyze the samples by AFM. Also, it was not possible to identify the controlling mechanisms that dominate the interactions between EPS and HNP. Based on literature, we expect both electrostatic and steric stabilization of EPS-coated HNP particles. However, we could not prove it using DLVO and EDLVO equations. Detailed studies with AFM force microscopy between EPS and hematite can help in determining the forces between EPS and hematite bonding.

In conclusion, organic colloids formed by biofilms can play an important role in transport of nanoparticles in the environment. Formation of EPS-hematite organo-mineral colloids, substantially alter the fate and transport of hematite nanoparticles in the three different porous media tested.

4.2 Outlook

This study highlights one of the multiple interactions between biofilm and inorganic colloids decide the fate and transport of colloidal nanoparticles. Organic colloids formed by biofilms play an important role in inorganic colloidal transport. Bacterial micro-colonies and biofilms are found nearly everywhere in the environment. Hence presence of organic matter of bacterial origin is imminent. In natural environments with saturated conditions such as water logging due to extreme rain events, deicing or hydromorphic soils in wet lands, riverine/ lake sediments/ swamps presence of bacterial organic matter can trigger transport of EPS-coated inorganic hematite nanoparticles.

Even though this study is mainly done in saturated conditions, bacterial biofilms can also influence transport in unsaturated conditions. EPS are generally hydrophobic in nature. It consist of a mixture of substances such as fimbria, flagella, mycolic acids, LPS which impart varying degrees of hydrophobicity and are generally hydrophobic in nature (Donlan, 2002). As seen in this study, organic colloids from the biofilms can modify the surface properties of the nanoparticles forming hydrophobic colloids. Hydrophobicity of the colloids can affect the attachment of the colloids to the solid matrix (Xiao & Wiesner, 2013) as well as the air-water interface (Zevi et al., 2005; Zhang et al., 2014). Thus, influencing transport under unsaturated conditions. Microorganism as well as the organic matter can also attach at the Soil- Water-Air interface (Keller & Auset, 2007). Thus, influencing the hydrophobic properties of the system which can ultimately affect the transport of colloids.

Organo-mineral colloids seem to be rather the rule than the exception in natural systems given that environmental aqueous solutions have high amounts of dissolved and colloidal organic matter. The effect of such organo-mineral geosorbents is not

comparable to that of pure inorganic colloids. The effect of natural organic matter such as humic acids have been extensively studied for the transport of nanoparticles. However, the microbial biomass also contributes to the natural organic matter pool (Miltner et al., 2012). Hence experimental results on carrier assisted transport must be revisited given the effect of organic colloids from biofilms on the stability and mobility of inorganic colloids.

A few researches have worked on deciphering the interactions between EPS and inorganic mineral surfaces (Cao et al., 2011; Mikutta et al., 2012; Omoike & Chorover, 2004; Wei et al., 2011). Nonetheless, the high diversity in the chemical and physical properties of biofilm and EPS complicates the study outcomes. Future studies should comprise spatially explicitly, submicron scale surface sensitive techniques such as AFM, SIMS that will allow visualize the spatial distribution of the adsorbed EPS and its components and nature of bonding between the mineral surface and EPS, since it has been established to have significant implications for the colloidal stability. Also, additional knowledge of the chemical composition of EPS will help in understanding the interaction between bacterial organic matter and inorganic mineral to get a holistic understanding of the biogeochemical process involved in the transport of colloids.

Summary

"At the surface of the liquid, the rods adhere together by their sides after the manner of the elements of columnar epithelium, but there is, I think, strong reason to believe that this adhesion is not direct, i.e., that they are not in actual contact but glued together by a vicious intermediary substance." (Sanderson, 1870)

Since the first likely description of *Bacillus* biofilm by Burton-Sanderson in 1870, bacterial biofilms have been vastly studied due to their unique microbial development and their implications in various fields such as medical, environmental, food and packaging, historical artifact conservation, waste-water treatment plants, marine engineering plants and many more (Costerton et al., 1987; Hall-Stoodley et al., 2004; Vlamakis et al., 2013). Biofilms are colonies of microorganism encased in self-produced extracellular polymeric substances (EPS), and are found on almost all natural and artificial surfaces (Costerton et al., 1987). EPS are a vast mixture of biopolymers that have a high affinity to mineral surfaces and help in attachment of microbial cells to the surfaces. EPS also aids in protection of the microbial cells from harsh environmental conditions and predators, maintaining the structural integrity of the biofilm, sequestration and degradation of harmful compounds and nutrition (Flemming & Wingender, 2010).

The transport of nanoparticles through biofilm in porous media has been garnering interest for diverse research goals such as waste-water treatment, soil remediation, facilitated transport of contaminants and nanoparticle contamination in groundwater (Jian-Zhou et al., 2015; Kurlanda-Witek et al., 2015; Leon-Morales et al., 2004; Lerner et al., 2012; Z. Li et al., 2013; Mitzel & Tufenkji, 2014; Tong et al., 2010; Tripathi et al., 2012; Xiao & Wiesner, 2013). Bacterial biofilms and their components

such as the EPS, can affect colloidal stability, reactivity and transport of colloidal nanoparticles by

1. Modifying the surface of the porous media by coating it; thereby altering the interaction between the nanoparticles and the porous media

2. Modifying the surface properties and colloidal stability of the nanoparticles due to direct interactions with organic matter such as EPS released from the biofilm (organic colloids). High molecular weight hydrated biopolymers such as EPS can sorb on mineral surfaces altering the charge and hydrophobicity of the minerals. This can affect the colloidal stability of the minerals, which is crucial for envisaging their fate and mobility.

However, only the effect of biofilms on the surface of porous media has been studied so far with contrasting results for the mobility of different nanoparticles (Jian-Zhou et al., 2015; Kurlanda-Witek et al., 2015; Leon-Morales et al., 2004; Lerner et al., 2012; Z. Li et al., 2013; Mitzel & Tufenkji, 2014; Tong et al., 2010; Tripathi et al., 2012; Xiao & Wiesner, 2013). No comprehensive studies are done to date on the effect of EPS on the colloidal stability of the nanoparticles. Also, the combined effect of biofilms/EPS on the porous media and on the nanoparticles, has not been interrogated so far.

The main aim of this study was to explore the role of bacterial biofilm and EPS in the colloidal stability and transport of nanoparticles in synthetic porous media. Using complementary experimental approaches, we investigated (1) the effect of microbial EPS on the colloidal stability of nanoparticles, (2a.) the transport of uncoated colloidal nanoparticles in biofilm and EPS-coated porous media, (2b.) the transport of EPS-coated colloidal nanoparticles in uncoated porous media (2c), the combined effect: transport of EPS-coated colloids in biofilm and EPS-coated porous media, and

finally (3) the remobilization of deposited colloidal nanoparticles by EPS. Laboratory synthesized hematite nanoparticles (HNP) and *Bacillus subtilis 168 (DSM 402)* were used as nanoparticles and biofilm forming bacterium respectively.

The first study was aimed to quantify the effect of increasing EPS loading on the colloidal stability and aggregation kinetics of hematite colloids (HNP). To do so, HNP were equilibrated with increasing concentrations of EPS (20, 200 and 500mg/l carbon). This procedure resulted in EPS-coated HNP with carbon: iron ratios 1:5, 2:1 and 5:1, respectively. With increasing EPS loadings, the isoelectric point of HNP changed from 9.8 (uncoated) to ~2 (EPS-coated). The zeta potential (ZP) of HNP also shifted from positive to negative values due to sorption of EPS on HNP surfaces. EPS binds to HNP by inner surface bonding, thus changing the surface properties of HNP. At neutral pH, low concentration of EPS (20 mg/l carbon, HNP 1:5) result in aggregation of HNP due to partial neutralization of the positive charges on HNP. In contrast, at higher concentrations (200 mg/l and 500 mg/l carbon, HNP2:1, HNP5:1), EPS:HNP associations were colloidally stable (|ZP| >20 mV). The values of the critical coagulation concentration (CCC) in NaCl increased with increasing concentration of EPS (CCC: HNP < HNP 2:1 < HNP 5:1). However, in the presence of $CaCl_2$, CCC decreased with increasing concentration of EPS (CCC: HNP > HNP 2:1 > HNP 5:1) which can be attributed to the formation of calcium bridges between EPS and HNP. In conclusion, high concentration of EPS colloidally stabilize HNP while low concentrations of EPS aggregated HNP.

The transport behavior of the HNP was studied using column experiments run in closed-flow mode. Three types of porous media were used in this study: uncoated, biofilm-coated and EPS-coated glass beads. The uncoated, biofilm and EPS-coated porous media were characterized by confocal laser scanning microscopy, scanning

electron microscopy, electro-kinetic measurements, and total biomass quantification. The porous media had a relatively uniform and equal distribution of biofilm and EPS coatings throughout the columns. Both coated and uncoated porous media exhibited a net negative surface potential at pH 7. Transport properties of the porous media obtained with an inert tracer revealed a moderate advection dominated transport regime with no observable preferential flow. Interesting, a low but continuous release of biofilm and EPS components including microbial cells was observed as dissolved organic matter in the column effluent. About 13 mg/L DOC (dissolved organic carbon) of organic matter was released from biofilm-coated columns and the 36mg/L DOC from EPS-coated columns. This can be attribute to mechanical strain (shear forces) and local change in ionic concentrations.

The transport of uncoated hematite in uncoated, biofilm-coated and EPS-coated porous media was evaluated over a period of 15 days (60 PV). The uncoated hematite nanoparticles were strongly retarded in uncoated porous media due to electrostatic attraction between the positive charges on HNP and negative charges on porous media. Contrarily, in biofilm and EPS-coated porous media, a considerable fraction of uncoated HNP were mobile and colloidally stable. Also, the ZP of the particles changed from positive to negative (ZP: -23 mV). This shift implies EPS coating on the hematite surfaces. As one important consequence, the organic matter released from the coating on the porous media may adsorb on the HNP forming organo-mineral associations with negative zeta potential. Hence, the biofilms/EPS present on the porous media influences the transport of HNP where normally HNP would be immobile if biofilms were not present.

The transport of EPS-coated HNP in uncoated porous media highlighted the essential role of colloidal stability in transport of nanoparticles under saturated conditions.

Higher concentrations of EPS loadings forming colloidally stable EPS-coated HNP (EPS:HNP 2:1, 5:1) exhibited a mobile fraction of colloids in uncoated porous media. While, colloidally unstable HNP1:5 were immobile and remained in the mixing vessel as sediment. Thus, EPS coatings on the HNP imparted colloidal stability and mobility to HNP in uncoated porous media.

In the last case, with biofilm/EPS present on porous media and EPS present on the nanoparticles, colloidally stable EPS-coated HNP were mobile in both biofilm and EPS-coated porous media. The colloidal stability of the particles is maintained ($|ZP| > 20$ mV) even after the transport experiments. Colloidally unstable EPS-coated HNP (HNP 1:5) were immobile in uncoated, and EPS-coated porous media. However, a fraction of HNP 1:5 gained colloidal stability ($|ZP| > 20$ mV) and were mobile in biofilm-coated porous media over time. This shift in the colloidal stability may be due the interaction with the organic colloids produced in the biofilm-coated porous media. The organic matter released from biofilms favor colloidal stability and remobilization of HNP. Moreover, the overall surface charge on coated nanoparticles and the coated porous media is net negative. This leads to electro-steric repulsion and in turn maintains mobility.

Remobilization of uncoated HNP sorbed on uncoated porous media was observed on flushing the porous media with an EPS solution. About 8% sorbed HNP were remobilized forming colloidally stable HNP with a negative zeta potential. EPS has a high bonding affinity to iron oxide minerals (Cao et al., 2011; Poorni & Natarajan, 2014) and can re mobilize hematite by forming negatively charged EPS-hematite colloids. The remobilization studies point towards a higher affinity of HNP to EPS molecules than to the surface of the glass beads. This also explains transformation of

uncoated HNP to negatively charged HNP during transport in biofilm and EPS-coated porous media.

Conclusively, this study highlights the importance of organo-mineral colloids formed by the interaction of biofilm and EPS in the transport of nanoparticles in uncoated (mineral) or biofilm-coated porous media. Moreover, microbial biofilms do not always act as traps for nanoparticles. Microbial biofilms act as a source of organic colloids which under suitable environment with saturate conditions such as water logging due to extreme rain events, wetlands, hydric soils, riverine/ lake sediments can trigger transport of immobile inorganic hematite nanoparticles by forming colloidally stable organo mineral colloids. This can have serious implications on the transport of contaminants associated with hematite nanoparticles as well as EPS.

The applications of this study are not only limited to colloid facilitated transport. This study can be extrapolated to understanding the influence of engineered nanoparticles used in bioremediation as well as fate of toxic nanoparticles in waste water treatment plants which are also dominated by presence of biofilms. A good understanding of the interactions between metal nanoparticles and naturally occurring bacterial EPS may also help in design of engineered systems for remediation from contaminated soils. This will also help in more accurate risk assessment of contaminated sites as well as nanotechnology in general.

References

Abaza, M. M. I. (1966). *Streaming current and streaming potential induced by water flow rough porous media.* Utah State University, All Graduate Theses and Dissertations. Paper 1628. Retrieved from http://digitalcommons.usu.edu/etd/1628

Abe, T., Kobayashi, S., & Kobayashi, M. (2011). Aggregation of colloidal silica particles in the presence of fulvic acid, humic acid, or alginate: Effects of ionic composition. *Colloids and Surfaces a-Physicochemical and Engineering Aspects, 379*(1-3), 21-26. doi:10.1016/j.colsurfa.2010.11.052

Abudalo, R. A., Ryan, J. N., Harvey, R. W., Metge, D. W., & Landkamer, L. (2010). Influence of organic matter on the transport of cryptosporidium parvum oocysts in a ferric oxyhydroxide-coated quartz sand saturated porous medium. *Water Res, 44*(4), 1104-1113. doi:10.1016/j.watres.2009.09.039

Allard, A. S., & Neilson, A. H. (1997). Bioremediation of organic waste sites: A critical review of microbiological aspects. *International Biodeterioration & Biodegradation, 39*(4), 253-285. doi:Doi 10.1016/S0964-8305(97)00021-8

Amal, R., Raper, J. A., & Waite, T. D. (1992). Effect of fulvic-acid adsorption on the aggregation kinetics and structure of hematite particles. *J Colloid Interface Sci, 151*(1), 244-257. doi:Doi 10.1016/0021-9797(92)90255-K

Amirbahman, A., & Olson, T. M. (1995). Deposition kinetics of humic matter-coated hematite in porous-media in the presence of Ca2+. *Colloids and Surfaces a-Physicochemical and Engineering Aspects, 99*(1), 1-10. doi:Doi 10.1016/0927-7757(95)03134-Y

Azeredo, J., Visser, J., & Oliveira, R. (1999). Exopolymers in bacterial adhesion: Interpretation in terms of dlvo and xdlvo theories. *Colloids and Surfaces B-Biointerfaces, 14*(1-4), 141-148. doi:Doi 10.1016/S0927-7765(99)00031-4

Banfield, J. F., & Zhang, H. Z. (2001). Nanoparticles in the environment. *Nanoparticles and the Environment, 44*(1), 1-58.

Basnet, M., Gershanov, A., Wilkinson, K. J., Ghoshal, S., & Tufenkji, N. (2016). Interaction between palladium-doped zerovalent iron nanoparticles and biofilm in granular porous media: Characterization, transport and viability. *Environmental Science-Nano, 3*(1), 127-137. doi:10.1039/c5en00109a

Baumann, T. (2010). Nanoparticles in groundwater – occurrence and applications. In H. F. Frimmel & R. Niessner (Eds.), *Nanoparticles in the water cycle: Properties, analysis and environmental relevance* (pp. 23-34). Berlin, Heidelberg: Springer Berlin Heidelberg.

Bazaka, K., Crawford, R. J., Nazarenko, E. L., & Ivanova, E. P. (2011). Bacterial extracellular polysaccharides. In D. Linke & A. Goldman (Eds.), *Bacterial adhesion: Chemistry, biology and physics* (pp. 213-226). Dordrecht: Springer Netherlands.

Berg, J. C. (2010). *An introduction to interfaces & colloids : The bridge to nanoscience*. Hackensack, N.J.: World Scientific.

Bhaskar, P. V., & Bhosle, N. B. (2005). Microbial extracellular polymeric substances in marine biogeochemical processes. *Current Science, 88*(1), 45-53.

Bitton, G. (2010). Introduction to wastewater treatment *Wastewater microbiology* (pp. 267-280): Wiley.

Bootz, A., Vogel, V., Schubert, D., & Kreuter, J. (2004). Comparison of scanning electron microscopy, dynamic light scattering and analytical ultracentrifugation for the sizing of poly(butyl cyanoacrylate) nanoparticles. *Eur J Pharm Biopharm, 57*(2), 369-375. doi:10.1016/S0939-6411(03)00193-0

Bradford, S. A., Simunek, J., Bettahar, M., Van Genuchten, M. T., & Yates, S. R. (2003). Modeling colloid attachment, straining, and exclusion in saturated porous media. *Environ Sci Technol, 37*(10), 2242-2250. doi:10.1021/es025899u

Brannen-Donnelly, K., & Engel, A. S. (2015). Bacterial diversity differences along an epigenic cave stream reveal evidence of community dynamics, succession, and stability. *Front Microbiol, 6*, 729. doi:10.3389/fmicb.2015.00729

Braydich-Stolle, L. K., Schaeublin, N. M., Murdock, R. C., Jiang, J., Biswas, P., Schlager, J. J., & Hussain, S. M. (2009). Crystal structure mediates mode of cell death in tio2 nanotoxicity. *Journal of Nanoparticle Research, 11*(6), 1361-1374. doi:10.1007/s11051-008-9523-8

Brydie, J. R., Wogelius, R. A., Merrifield, C. M., Boult, S., Gilbert, P., Allison, D., & Vaughan, D. J. (2005). The μ2m project on quantifying the effects of biofilm growth on hydraulic properties of natural porous media and on sorption equilibria: An overview. *Geological Society, London, Special Publications, 249*(1), 131-144. doi:10.1144/gsl.sp.2005.249.01.11

Burmolle, M., Hansen, L. H., & Sorensen, S. J. (2007). Establishment and early succession of a multispecies biofilm composed of soil bacteria. *Microb Ecol, 54*(2), 352-362. doi:10.1007/s00248-007-9222-5

Cao, Y., Wei, X., Cai, P., Huang, Q., Rong, X., & Liang, W. (2011). Preferential adsorption of extracellular polymeric substances from bacteria on clay minerals and iron oxide. *Colloids Surf B Biointerfaces, 83*(1), 122-127. doi:10.1016/j.colsurfb.2010.11.018

Chekli, L., Phuntsho, S., Roy, M., & Shon, H. K. (2013). Characterisation of fe-oxide nanoparticles coated with humic acid and suwannee river natural organic matter. *Sci Total Environ, 461-462*, 19-27. doi:10.1016/j.scitotenv.2013.04.083

Chen, G., Liu, X., & Su, C. (2012). Distinct effects of humic acid on transport and retention of tio2 rutile nanoparticles in saturated sand columns. *Environ Sci Technol, 46*(13), 7142-7150. doi:10.1021/es204010g

Chen, G., & Walker, S. L. (2012). Fecal indicator bacteria transport and deposition in saturated and unsaturated porous media. *Environ Sci Technol, 46*(16), 8782-8790. doi:10.1021/es301378q

Chen, J. H., Czajka, D. R., Lion, L. W., Shuler, M. L., & Ghiorse, W. C. (1995). Trace metal mobilization in soil by bacterial polymers. *Environ Health Perspect, 103 Suppl 1*, 53-58. doi:Doi 10.2307/3432013

Chen, K. L., & Elimelech, M. (2006). Aggregation and deposition kinetics of fullerene (C60) nanoparticles. *Langmuir, 22*(26), 10994-11001. doi:10.1021/la062072v

Chen, K. L., & Elimelech, M. (2007). Influence of humic acid on the aggregation kinetics of fullerene (C60) nanoparticles in monovalent and divalent electrolyte solutions. *J Colloid Interface Sci, 309*(1), 126-134. doi:10.1016/j.jcis.2007.01.074

Chen, K. L., & Elimelech, M. (2008). Interaction of fullerene (C60) nanoparticles with humic acid and alginate coated silica surfaces: Measurements, mechanisms, and environmental implications. *Environ Sci Technol, 42*(20), 7607-7614. doi:10.1021/es8012062

Chen, K. L., Mylon, S. E., & Elimelech, M. (2006). Aggregation kinetics of alginate-coated hematite nanoparticles in monovalent and divalent electrolytes. *Environ Sci Technol, 40*(5), 1516-1523. doi:Doi 10.1021/Es0518068

Christian, P., Von der Kammer, F., Baalousha, M., & Hofmann, T. (2008). Nanoparticles: Structure, properties, preparation and behaviour in environmental media. *Ecotoxicology, 17*(5), 326-343. doi:10.1007/s10646-008-0213-1

Coombs, P., Wagner, D., Bateman, K., Harrison, H., Milodowski, A. E., Noy, D., & West, J. M. (2010). The role of biofilms in subsurface transport processes. *Quarterly Journal of Engineering Geology and Hydrogeology, 43*(2), 131-139. doi:10.1144/1470-9236/08-029

Costerton, J. W., Cheng, K. J., Geesey, G. G., Ladd, T. I., Nickel, J. C., Dasgupta, M., & Marrie, T. J. (1987). Bacterial biofilms in nature and disease. *Annu Rev Microbiol, 41*, 435-464. doi:10.1146/annurev.mi.41.100187.002251

Cullimore, D. R. (2010). Common bacteriologically initiated events. In B. R. FL (Ed.), *Practical atlas for bacterial identification, second edition* (pp. 11-22): CRC Press.

Cunningham, A. B., Characklis, W. G., Abedeen, F., & Crawford, D. (1991). Influence of biofilm accumulation on porous-media hydrodynamics. *Environmental Science & Technology, 25*(7), 1305-1311. doi:DOI 10.1021/es00019a013

Cunningham, A. B., Sharp, R. R., Hiebert, R., & James, G. (2003). Subsurface biofilm barriers for the containment and remediation of contaminated groundwater. *Bioremediation Journal, 7*(3-4), 151-164. doi:10.1080/713607982

Di Marco, M., Guilbert, I., Port, M., Robic, C., Couvreur, P., & Dubernet, C. (2007). Colloidal stability of ultrasmall superparamagnetic iron oxide (USPIO) particles with different coatings. *International Journal of Pharmaceutics, 331*(2), 197-203. doi:10.1016/j.ijpharm.2006.11.002

Donlan, R. M. (2002). Biofilms: Microbial life on surfaces. *Emerging Infectious Diseases, 8*(9), 881-890. doi:10.3201/eid0809.020063

Downs, R. T., & Hall-Wallace, M. (2003). The american mineralogist crystal structure database. *American Mineralogist, 88*(1), 247-250.

Dubois, M., Gilles, K. A., Hamilton, J. K., Rebers, P. A., & Smith, F. (1956). Colorimetric method for determination of sugars and related substances. *Analytical Chemistry, 28*(3), 350-356. doi:DOI 10.1021/ac60111a017

Ebihara, T., & Bishop, P. L. (2002). Effect of acetate on biofilms utilized in PAHs bioremediation. *Environmental Engineering Science, 19*(5), 305-319. doi:Doi 10.1089/10928750260418944

Engesgaard, P. K., Seifert, D., & Herrera, P. (2006). Bioclogging in porous media: Tracer studies *Nato science series, iv. Earth and environmental sciences* (pp. 93-118).

Fang, L., Cao, Y., Huang, Q., Walker, S. L., & Cai, P. (2012). Reactions between bacterial exopolymers and goethite: A combined macroscopic and spectroscopic investigation. *Water Res, 46*(17), 5613-5620. doi:10.1016/j.watres.2012.07.046

Fang, L., Wei, X., Cai, P., Huang, Q., Chen, H., Liang, W., & Rong, X. (2011). Role of extracellular polymeric substances in Cu(II) adsorption on bacillus subtilis and pseudomonas putida. *Bioresour Technol, 102*(2), 1137-1141. doi:10.1016/j.biortech.2010.09.006

Farnleitner, A. H., Wilhartitz, I., Ryzinska, G., Kirschner, A. K., Stadler, H., Burtscher, M. M., . . . Mach, R. L. (2005). Bacterial dynamics in spring water of alpine karst aquifers indicates the presence of stable autochthonous microbial endokarst communities. *Environ Microbiol, 7*(8), 1248-1259. doi:10.1111/j.1462-2920.2005.00810.x

Fissan, H., Ristig, S., Kaminski, H., Asbach, C., & Epple, M. (2014). Comparison of different characterization methods for nanoparticle dispersions before and after aerosolization. *Analytical Methods, 6*(18), 7324-7334. doi:10.1039/c4ay01203h

Flemming, H. C., & Wingender, J. (2010). The biofilm matrix. *Nat Rev Microbiol, 8*(9), 623-633. doi:10.1038/nrmicro2415

Fontes, D. E., Mills, A. L., Hornberger, G. M., & Herman, J. S. (1991). Physical and chemical factors influencing transport of microorganisms through porous-media. *Applied and Environmental Microbiology, 57*(9), 2473-2481.

Francis, A. J., Gillow, J. B., Dodge, C. J., Dunn, M., Mantione, K., Strietelmeier, B. A., . . . Papenguth, H. W. (1998). Role of bacteria as biocolloids in the transport of actinides from a deep underground radioactive waste repository. *Radiochimica Acta, 82*, 347-354.

Fritz, G., Schadler, V., Willenbacher, N., & Wagner, N. J. (2002). Electrosteric stabilization of colloidal dispersions. *Langmuir, 18*(16), 6381-6390. doi:10.1021/la015734j

Fritzsche, A., Schroder, C., Wieczorek, A. K., Handel, M., Ritschel, T., & Totsche, K. U. (2015). Structure and composition of fe-om co-precipitates that form in soil-derived solutions. *Geochimica et Cosmochimica Acta, 169*, 167-183. doi:10.1016/j.gca.2015.07.041

Fu, F., Dionysiou, D. D., & Liu, H. (2014). The use of zero-valent iron for groundwater remediation and wastewater treatment: A review. *Journal of Hazardous Materials, 267*, 194-205. doi:10.1016/j.jhazmat.2013.12.062

Gehrke, I., Geiser, A., & Somborn-Schulz, A. (2015). Innovations in nanotechnology for water treatment. *Nanotechnology, Science and Applications, 8*, 1-17. doi:10.2147/NSA.S43773

Golmohamadi, M., Clark, R. J., Veinot, J. G. C., & Wilkinson, K. J. (2013). The role of charge on the diffusion of solutes and nanoparticles (silicon nanocrystals, ntio2, nau) in a biofilm. *Environmental Chemistry, 10*(1), 34. doi:10.1071/en12106

Grasso, D., Subramaniam, K., Butkus, M., Strevett, K., & Bergendahl, J. (2002). A review of non-dlvo interactions in environmental colloidal systems. *Reviews in Environmental Science and Bio/Technology, 1*(1), 17-38. doi:10.1023/a:1015146710500

Gwinn, M. R., & Vallyathan, V. (2006). Nanoparticles: Health effects—pros and cons. *Environmental Health Perspectives, 114*(12), 1818-1825. doi:10.1289/ehp.8871

Hall-Stoodley, L., Costerton, J. W., & Stoodley, P. (2004). Bacterial biofilms: From the natural environment to infectious diseases. *Nat Rev Microbiol, 2*(2), 95-108. doi:10.1038/nrmicro821

Hama, T. (1997). Primary productivity and photosynthetic products in the northwest pacific ocean. *Biogeochemical processes in the North Pacific*, 187-191.

Hanaor, D., Michelazzi, M., Leonelli, C., & Sorrell, C. C. (2012). The effects of carboxylic acids on the aqueous dispersion and electrophoretic deposition of zro2. *Journal of the European Ceramic Society, 32*(1), 235-244. doi:10.1016/j.jeurceramsoc.2011.08.015

Hassellov, M., & von der Kammer, F. (2008). Iron oxides as geochemical nanovectors for metal transport in soil-river systems. *Elements, 4*(6), 401-406. doi:10.2113/gselements.4.6.401

He, Y. T., Wan, J. M., & Tokunaga, T. (2008). Kinetic stability of hematite nanoparticles: The effect of particle sizes. *Journal of Nanoparticle Research, 10*(2), 321-332. doi:10.1007/s11051-007-9255-1

Herbold-Paschke, K., Straub, U., Hahn, T., Teutsch, G., & Botzenhart, K. (1991). Behaviour of pathogenic bacteria, phages and viruses in ground water during transport and adsorption. *Water Science and Technology, 24*(2), 301.

Hiemenz, P. C., & Rajagopalan, R. (1997). *Principles of colloid and surface chemistry* (3 ed.). New york: Marcel Dekker.

Hochella, M. F. (2008). Nanogeoscience: From origins to cutting-edge applications. *Elements, 4*(6), 373-379. doi:10.2113/gselements.4.6.373

Holthoff, H., Egelhaaf, S. U., Borkovec, M., Schurtenberger, P., & Sticher, H. (1996). Coagulation rate measurements of colloidal particles by simultaneous static and dynamic light scattering. *Langmuir, 12*(23), 5541-5549. doi:DOI 10.1021/la960326e

Hu, J. D., Zevi, Y., Kou, X. M., Xiao, J., Wang, X. J., & Jin, Y. (2010). Effect of dissolved organic matter on the stability of magnetite nanoparticles under different ph and ionic strength conditions. *Sci Total Environ, 408*(16), 3477-3489. doi:10.1016/j.scitotenv.2010.03.033

Huang, Y. (2012). Temperature effect on the aggregation kinetics of CeO_2 nanoparticles in monovalent and divalent electrolytes. *Journal of Environmental & Analytical Toxicology, 02*(07). doi:10.4172/2161-0525.1000158

Hunter, R. J. (1981a). Chapter 1 - introduction. In R. J. Hunter (Ed.), *Zeta potential in colloid science* (pp. 1-10): Academic Press.

Hunter, R. J. (1981b). Chapter 2 - charge and potential distribution at interfaces. In R. J. Hunter (Ed.), *Zeta potential in colloid science* (pp. 11-58): Academic Press.

Huynh, K. A., & Chen, K. L. (2011). Aggregation kinetics of citrate and polyvinylpyrrolidone coated silver nanoparticles in monovalent and divalent electrolyte solutions. *Environ Sci Technol, 45*(13), 5564-5571. doi:10.1021/es200157h

Hwang, G., Kang, S., El-Din, M. G., & Liu, Y. (2012). Impact of an extracellular polymeric substance (EPS) precoating on the initial adhesion of burkholderia cepacia and pseudomonas aeruginosa. *Biofouling, 28*(6), 525-538. doi:10.1080/08927014.2012.694138

Ikuma, K., Decho, A. W., & Lau, B. L. (2015). When nanoparticles meet biofilms-interactions guiding the environmental fate and accumulation of nanoparticles. *Front Microbiol, 6*, 591. doi:10.3389/fmicb.2015.00591

Illes, E., & Tombacz, E. (2006). The effect of humic acid adsorption on ph-dependent surface charging and aggregation of magnetite nanoparticles. *J Colloid Interface Sci, 295*(1), 115-123. doi:10.1016/j.jcis.2005.08.003

Israelachvili, J. N. (1982). Forces between surfaces in liquids. *Advances in Colloid and Interface Science, 16*(Jul), 31-47. doi:Doi 10.1016/0001-8686(82)85004-5

Jain, R., Jordan, N., Weiss, S., Foerstendorf, H., Heim, K., Kacker, R., . . . Lens, P. N. (2015). Extracellular polymeric substances govern the surface charge of biogenic elemental selenium nanoparticles. *Environ Sci Technol, 49*(3), 1713-1720. doi:10.1021/es5043063

Jian-Zhou, H., Cheng-Cheng, L., Deng-Jun, W., & Zhou, D. M. (2015). Biofilms and extracellular polymeric substances mediate the transport of graphene oxide nanoparticles in saturated porous media. *Journal of Hazardous Materials, 300*, 467-474. doi:10.1016/j.jhazmat.2015.07.026

Jiang, X. J., Tong, M. P., Lu, R. Q., & Kim, H. (2012). Transport and deposition of zno nanoparticles in saturated porous media. *Colloids and Surfaces a-Physicochemical and Engineering Aspects, 401*, 29-37. doi:10.1016/j.colsurfa.2012.03.004

Jiao, Y., Cody, G. D., Harding, A. K., Wilmes, P., Schrenk, M., Wheeler, K. E., . . . Thelen, M. P. (2010). Characterization of extracellular polymeric substances from acidophilic microbial biofilms. *Appl Environ Microbiol, 76*(9), 2916-2922. doi:10.1128/AEM.02289-09

Jung, B., O'Carroll, D., & Sleep, B. (2014). The influence of humic acid and clay content on the transport of polymer-coated iron nanoparticles through sand. *Sci Total Environ, 496*, 155-164. doi:10.1016/j.scitotenv.2014.06.075

Kaste, J. M., Bostick, B. C., Friedland, A. J., Schroth, A. W., & Siccama, T. G. (2006). Fate and speciation of gasoline-derived lead in organic horizons of the

northeastern USA. *Soil Science Society of America Journal, 70*(5), 1688-1698. doi:10.2136/sssaj2005.0321

Keller, A. A., & Auset, M. (2007). A review of visualization techniques of biocolloid transport processes at the pore scale under saturated and unsaturated conditions. *Advances in Water Resources, 30*(6-7), 1392-1407. doi:10.1016/j.advwatres.2006.05.013

Khaydarov, R., & Gapurova, O. (2010). Application of carbon nanoparticles for water treatment. In M. Václavíková, K. Vitale, G. P. Gallios, & L. Ivaničová (Eds.), *Water treatment technologies for the removal of high-toxicity pollutants* (pp. 253-258). Dordrecht: Springer Netherlands.

Kimball, B. A., Callender, E., & Axtmann, E. V. (1995). Effects of colloids on metal transport in a river receiving acid mine drainage, upper arkansas river, colorado, u.S.A. *Applied Geochemistry, 10*(3), 285-306. doi:10.1016/0883-2927(95)00011-8

Kinzler, K., Gehrke, T., Telegdi, J., & Sand, W. (2003). Bioleaching - a result of interfacial processes caused by extracellular polymeric substances (EPS). *Hydrometallurgy, 71*(1-2), 83-88. doi:10.1016/S0304-368x(03)00176-2

Kirkland, C. M., Herrling, M. P., Hiebert, R., Bender, A. T., Grunewald, E., Walsh, D. O., & Codd, S. L. (2015). In situ detection of subsurface biofilm using low-field nmr: A field study. *Environ Sci Technol, 49*(18), 11045-11052. doi:10.1021/acs.est.5b02690

Kleshchanok, D., & Lang, P. R. (2007). Steric repulsion by adsorbed polymer layers studied with total internal reflection microscopy. *Langmuir, 23*(8), 4332-4339. doi:10.1021/la062607k

Kögel-Knabner, I., Guggenberger, G., Kleber, M., Kandeler, E., Kalbitz, K., Scheu, S., . . . Leinweber, P. (2008). Organo-mineral associations in temperate soils: Integrating biology, mineralogy, and organic matter chemistry. *Journal of Plant Nutrition and Soil Science, 171*(1), 61-82. doi:10.1002/jpln.200700048

Kone, T., Golfier, F., Orgogozo, L., Oltean, C., Lefevre, E., Block, J. C., & Bues, M. A. (2014). Impact of biofilm-induced heterogeneities on solute transport in porous media. *Water Resources Research, 50*(11), 9103-9119. doi:10.1002/2013wr015213

Kretzschmar, R., & Schafer, T. (2005). Metal retention and transport on colloidal particles in the environment. *Elements, 1*(4), 205-210. doi:DOI 10.2113/gselements.1.4.205

Kretzschmar, R., & Sticher, H. (1997). Transport of humic-coated iron oxide colloids in a sandy soil: Influence of ca2+ and trace metals. *Environmental Science & Technology, 31*(12), 3497-3504. doi:DOI 10.1021/es970244s

Kurlanda-Witek, H., Ngwenya, B. T., & Butler, I. B. (2015). The influence of biofilms on the mobility of bare and capped zinc oxide nanoparticles in saturated sand and glass beads. *J Contam Hydrol, 179*, 160-170. doi:10.1016/j.jconhyd.2015.06.009

Labille, J., Thomas, F., Milas, M., & Vanhaverbeke, C. (2005). Flocculation of colloidal clay by bacterial polysaccharides: Effect of macromolecule charge and structure. *J Colloid Interface Sci, 284*(1), 149-156. doi:10.1016/j.jcis.2004.10.001

Labrenz, M., Druschel, G. K., Thomsen-Ebert, T., Gilbert, B., Welch, S. A., Kemner, K. M., . . . Banfield, J. F. (2000). Formation of sphalerite (zns) deposits in natural biofilms of sulfate-reducing bacteria. *Science, 290*(5497), 1744-1747.

Lameiras, F. S., de Souza, A. L., de Melo, V. A. R., Nunes, E. H. M., & Braga, I. D. (2008). Measurement of the zeta potential of planar surfaces with a rotating disk. *Materials Research-Ibero-American Journal of Materials, 11*(2), 217-219. doi:Doi 10.1590/S1516-14392008000200018

Lanphere, J. D., Rogers, B., Luth, C., Bolster, C. H., & Walker, S. L. (2014). Stability and transport of graphene oxide nanoparticles in groundwater and surface water. *Environ Eng Sci, 31*(7), 350-359. doi:10.1089/ees.2013.0392

Leon-Morales, C. F., Leis, A. P., Strathmann, M., & Flemming, H. C. (2004). Interactions between laponite and microbial biofilms in porous media: Implications for colloid transport and biofilm stability. *Water Res, 38*(16), 3614-3626. doi:10.1016/j.watres.2004.05.009

Lerner, R. N., Lu, Q., Zeng, H., & Liu, Y. (2012). The effects of biofilm on the transport of stabilized zerovalent iron nanoparticles in saturated porous media. *Water Res, 46*(4), 975-985. doi:10.1016/j.watres.2011.11.070

Levenberg, K. (1944). A method for the solution of certain non-linear problems in least squares. *Quarterly Journal of Applied Mathmatics, II*(2), 164-168. doi:citeulike-article-id:10796881

Levy, B. S., & Chambers, R. M. (1987). Bromide as a conservative tracer for soil-water studies. *Hydrological Processes, 1*(4), 385-389. doi:DOI 10.1002/hyp.3360010406

Li, K., & Chen, Y. (2012). Effect of natural organic matter on the aggregation kinetics of CeO_2 nanoparticles in kcl and cacl2 solutions: Measurements and modeling. *Journal of Hazardous Materials, 209-210*, 264-270. doi:10.1016/j.jhazmat.2012.01.013

Li, Z., Aly Hassan, A., Sahle-Demessie, E., & Sorial, G. A. (2013). Transport of nanoparticles with dispersant through biofilm coated drinking water sand filters. *Water Res, 47*(17), 6457-6466. doi:10.1016/j.watres.2013.08.026

Likos, C. N., Vaynberg, K. A., Lowen, H., & Wagner, N. J. (2000). Colloidal stabilization by adsorbed gelatin. *Langmuir, 16*(9), 4100-4108. doi:DOI 10.1021/la991142d

Lim, J., Yeap, S. P., Che, H. X., & Low, S. C. (2013). Characterization of magnetic nanoparticle by dynamic light scattering. *Nanoscale Res Lett, 8*(1), 381. doi:10.1186/1556-276X-8-381

Lin, S., Cheng, Y., Liu, J., & Wiesner, M. R. (2012). Polymeric coatings on silver nanoparticles hinder autoaggregation but enhance attachment to uncoated surfaces. *Langmuir, 28*(9), 4178-4186. doi:10.1021/la202884f

Liu, Q., Zhang, Y. H., & Laskowski, J. S. (2000). The adsorption of polysaccharides onto mineral surfaces: An acid/base interaction. *International Journal of Mineral Processing, 60*(3-4), 229-245. doi:Doi 10.1016/S0301-7516(00)00018-1

Lowry, O. H., Rosebrough, N. J., Farr, A. L., & Randall, R. J. (1951). Protein measurement with the folin phenol reagent. *J Biol Chem, 193*(1), 265-275.

Lüttge, A., Zhang, L., & Nealson, K. H. (2005). Mineral surfaces and their implications for microbial attachment: Results from monte carlo simulations and direct surface observations. *American Journal of Science, 305*(6-8), 766-790. doi:10.2475/ajs.305.6-8.766

MacKay, A. A., & Gschwend, P. M. (2001). Enhanced concentrations of PAHs in groundwater at a coal tar site. *Environmental Science & Technology, 35*(7), 1320-1328. doi:Doi 10.1021/Es0014786

Mączka, E., & Kosmulski, M. (2014). Time-dependent particle aggregation in SDS — hematite dispersions. *Colloids and Interface Science Communications, 1*, 10-13. doi:10.1016/j.colcom.2014.06.004

Marquardt, D. W. (1963). An algorithm for least-squares estimation of nonlinear parameters. *Journal of the Society for Industrial and Applied Mathematics, 11*(2), 431-441. doi:10.1137/0111030

Marvasi, M., Visscher, P. T., & Casillas Martinez, L. (2010). Exopolymeric substances (EPS) from bacillus subtilis: Polymers and genes encoding their synthesis. *Fems Microbiology Letters, 313*(1), 1-9. doi:10.1111/j.1574-6968.2010.02085.x

Maslen, E. N., Streltsov, V. A., Streltsova, N. R., & Ishizawa, N. (1994). Synchrotron x-ray study of the electron-density in alpha-Fe_2O_3. *Acta Crystallographica Section B-Structural Science, 50*(4), 435-441. doi:Doi 10.1107/S0108768194002284

Matthess, G., Pekdeger, A., & Schroeter, J. (1988). Persistence and transport of bacteria and viruses in groundwater - a conceptual evaluation. *Journal of Contaminant Hydrology, 2*(2), 171-188. doi:10.1016/0169-7722(88)90006-X

Mccarthy, J. F., & Zachara, J. M. (1989). Subsurface transport of contaminants - mobile colloids in the subsurface environment may alter the transport of contaminants. *Environmental Science & Technology, 23*(5), 496-502. doi:DOI 10.1021/es00063a602

Mikutta, R., Baumgartner, A., Schippers, A., Haumaier, L., & Guggenberger, G. (2012). Extracellular polymeric substances from bacillus subtilis associated with minerals modify the extent and rate of heavy metal sorption. *Environ Sci Technol, 46*(7), 3866-3873. doi:10.1021/es204471x

Miltner, A., Bombach, P., Schmidt-Brucken, B., & Kastner, M. (2012). SOM genesis: Microbial biomass as a significant source. *Biogeochemistry, 111*(1-3), 41-55. doi:10.1007/s10533-011-9658-z

Miot, J., Benzerara, K., Obst, M., Kappler, A., Hegler, F., Schadler, S., . . . Morin, G. (2009). Extracellular iron biomineralization by photoautotrophic iron-oxidizing bacteria. *Appl Environ Microbiol, 75*(17), 5586-5591. doi:10.1128/AEM.00490-09

Mitzel, M. R., & Tufenkji, N. (2014). Transport of industrial PVP-stabilized silver nanoparticles in saturated quartz sand coated with pseudomonas aeruginosa

pao1 biofilm of variable age. *Environ Sci Technol, 48*(5), 2715-2723. doi:10.1021/es404598v

Mylon, S. E., Chen, K. L., & Elimelech, M. (2004). Influence of natural organic matter and ionic composition on the kinetics and structure of hematite colloid aggregation: Implications to iron depletion in estuaries. *Langmuir, 20*(21), 9000-9006. doi:10.1021/la049153g

Nashaat , N. N. (2013). The application of nanoparticles for wastewater remediation *Applications of nanomaterials for water quality* (pp. 52-65): Future Science Ltd.

Nevers, M. B., & Boehm, A. B. (2011). Modeling fate and transport of fecal bacteria in surface water *The fecal bacteria*: American Society of Microbiology.

Novikov, A. P., Kalmykov, S. N., Utsunomiya, S., Ewing, R. C., Horreard, F., Merkulov, A., . . . Myasoedov, B. F. (2006). Colloid transport of plutonium in the far-field of the mayak production association, russia. *Science, 314*(5799), 638-641. doi:10.1126/science.1131307

O'Toole, G., Kaplan, H. B., & Kolter, R. (2000). Biofilm formation as microbial development. *Annu Rev Microbiol, 54*(1), 49-79. doi:10.1146/annurev.micro.54.1.49

Omoike, A., & Chorover, J. (2004). Spectroscopic study of extracellular polymeric substances from bacillus subtilis: Aqueous chemistry and adsorption effects. *Biomacromolecules, 5*(4), 1219-1230. doi:10.1021/bm034461z

Overbeek, J. T. G. (1982). Monodisperse colloidal systems, fascinating and useful. *Advances in Colloid and Interface Science, 15*(3-4), 251-277. doi:Doi 10.1016/0001-8686(82)80003-1

Pang, L., Close, M. E., Noonan, M. J., Flintoft, M. J., & van den Brink, P. (2005). A laboratory study of bacteria-facilitated cadmium transport in alluvial gravel aquifer media. *J Environ Qual, 34*(1), 237-247.

Pena, M., Meng, X., Korfiatis, G. P., & Jing, C. (2006). Adsorption mechanism of arsenic on nanocrystalline titanium dioxide. *Environ Sci Technol, 40*(4), 1257-1262. doi:Doi 10.1021/Es052040e

Perni, S., Preedy, E. C., & Prokopovich, P. (2014). Success and failure of colloidal approaches in adhesion of microorganisms to surfaces. *Adv Colloid Interface Sci, 206*, 265-274. doi:10.1016/j.cis.2013.11.008

Philippe, A., & Schaumann, G. E. (2014). Interactions of dissolved organic matter with natural and engineered inorganic colloids: A review. *Environ Sci Technol, 48*(16), 8946-8962. doi:10.1021/es502342r

Plaza, R. C., Quirantes, A., & Delgado, A. V. (2002). Stability of dispersions of colloidal hematite/yttrium oxide core-shell particles. *J Colloid Interface Sci, 252*(1), 102-108. doi:10.1006/jcis.2002.8459

Poorni, S., & Natarajan, K. A. (2014). Flocculation behaviour of hematite-kaolinite suspensions in presence of extracellular bacterial proteins and polysaccharides. *Colloids Surf B Biointerfaces, 114*(0), 186-192. doi:10.1016/j.colsurfb.2013.09.049

Puertas, A. M., & de las Nieves, F. J. (1999). Colloidal stability of polymer colloids with variable surface charge. *J Colloid Interface Sci, 216*(2), 221-229. doi:10.1006/jcis.1999.6294

Quik, J. T., Stuart, M. C., Wouterse, M., Peijnenburg, W., Hendriks, A. J., & van de Meent, D. (2012). Natural colloids are the dominant factor in the sedimentation of nanoparticles. *Environ Toxicol Chem, 31*(5), 1019-1022. doi:10.1002/etc.1783

Redman, J. A., Grant, S. B., Olson, T. M., & Estes, M. K. (2001). Pathogen filtration, heterogeneity, and the potable reuse of wastewater. *Environ Sci Technol, 35*(9), 1798-1805. doi:10.1021/es0010960

Ritschel, T., & Totsche, K. U. (2016a). Closed-flow column experiments-insights into solute transport provided by a damped oscillating breakthrough behavior. *Water Resources Research, 52*(3), 2206-2221. doi:10.1002/2015wr018317

Ritschel, T., & Totsche, K. U. (2016b). Closed-flow column experiments: A numerical sensitivity analysis of reactive transport and parameter uncertainty. *Water Resources Research, 52*(8), 6094-6110. doi:10.1002/2015wr018388

Rittmann, B. E. (1993). The significance of biofilms in porous-media. *Water Resources Research, 29*(7), 2195-2202. doi:Doi 10.1029/93wr00611

Romero-Cano, M. S., Martin-Rodriguez, A., & de las Nieves, F. J. (2001). Electrosteric stabilization of polymer colloids with different functionality. *Langmuir, 17*(11), 3505-3511. doi:10.1021/la001659l

Saleh, N., Kim, H. J., Phenrat, T., Matyjaszewski, K., Tilton, R. D., & Lowry, G. V. (2008). Ionic strength and composition affect the mobility of surface-modified

fe0 nanoparticles in water-saturated sand columns. *Environ Sci Technol, 42*(9), 3349-3355.

Sand, W., & Gehrke, T. (2006). Extracellular polymeric substances mediate bioleaching/biocorrosion via interfacial processes involving iron(iii) ions and acidophilic bacteria. *Res Microbiol, 157*(1), 49-56. doi:10.1016/j.resmic.2005.07.012

Sanderson, J. B. (1870). *Appendix no. 5 in 13th report of the medical officer of the privy council* (J. Simon Ed.). Her Majesty's Stationery Office, London, 1871.

Saywell, L. G., & Cunningham, B. B. (1937). Determination of iron: Colorimetric o-phenanthroline method. *Industrial & Engineering Chemistry Analytical Edition, 9*(2), 67-69. doi:10.1021/ac50106a005

Schwertmann, U., & Cornell, R. M. (2000). Coating of SiO_2 sand (quartz; cristobalite) with iron oxides *Iron oxides in the laboratory* (pp. 153-156): Wiley-VCH Verlag GmbH, Weinheim, Germany.

Shabarova, T., Villiger, J., Morenkov, O., Niggemann, J., Dittmar, T., & Pernthaler, J. (2014). Bacterial community structure and dissolved organic matter in repeatedly flooded subsurface karst water pools. *FEMS Microbiol Ecol, 89*(1), 111-126. doi:10.1111/1574-6941.12339

Shih, P. C., & Huang, C. T. (2002). Effects of quorum-sensing deficiency on pseudomonas aeruginosa biofilm formation and antibiotic resistance. *J Antimicrob Chemother, 49*(2), 309-314.

Simmons, A. M., & Neymark, L. A. (2012). Conditions and processes affecting radionuclide transport. *Geological Society of America Memoirs, 209*, 277-362. doi:10.1130/2012.1209(06)

Somasundaran, P. (2004). Encyclopedia of surface and colloid science *Encyclopedia of surface and colloid science* (Vol. 5): CRC Press.

Soni, D., Naoghare, P. K., Saravanadevi, S., & Pandey, R. A. (2015). Release, transport and toxicity of engineered nanoparticles. In D. M. Whitacre (Ed.), *Reviews of environmental contamination and toxicology* (pp. 1-47). Cham: Springer International Publishing.

Sorum, C. H. (1928). The preparation of chloride free colloidal ferric oxide from ferric chloride1,2. *Journal of the American Chemical Society, 50*(5), 1263-1267. doi:10.1021/ja01392a004

Spath, R., Flemming, H., & Wuertz, S. (1998). Sorption properties of biofilms. *Water Science and Technology, 37*(4-5), 207-210. doi:10.1016/s0273-1223(98)00107-3

Staudt, C., Horn, H., Hempel, D. C., & Neu, T. R. (2004). Volumetric measurements of bacterial cells and extracellular polymeric substance glycoconjugates in biofilms. *Biotechnol Bioeng, 88*(5), 585-592. doi:10.1002/bit.20241

Strathmann, M., Leon-Morales, C. F., & Flemming, H.-C. (2007). Influence of biofilms on colloid mobility in the subsurface. In F. H. Frimmel, F. Kammer, & H.-C. Flemming (Eds.), *Colloidal transport in porous media* (pp. 143-173). Berlin, Heidelberg: Springer Berlin Heidelberg.

Suttiponparnit, K., Jiang, J., Sahu, M., Suvachittanont, S., Charinpanitkul, T., & Biswas, P. (2011). Role of surface area, primary particle size, and crystal phase on titanium dioxide nanoparticle dispersion properties. *Nanoscale Res Lett, 6*(1), 27. doi:10.1007/s11671-010-9772-1

Tadros, T. (2006). General principles of colloid stability and the role of surface forces *Colloid stability* (pp. 1-22): Wiley-VCH Verlag GmbH & Co. KGaA.

Taylor, S. W., & Jaffe, P. R. (1990). Substrate and biomass transport in a porous-medium. *Water Resources Research, 26*(9), 2181-2194. doi:DOI 10.1029/WR026i009p02181

Theng, B. K. G., & Yuan, G. (2009). Nanoparticles in the soil environment. *Elements, 4*(6), 395.

Thullner, M., Zeyer, J., & Kinzelbach, W. (2002). Influence of microbial growth on hydraulic properties of pore networks. *Transport in Porous Media, 49*(1), 99-122. doi:Doi 10.1023/A:1016030112089

Tong, M., Ding, J., Shen, Y., & Zhu, P. (2010). Influence of biofilm on the transport of fullerene (C60) nanoparticles in porous media. *Water Res, 44*(4), 1094-1103. doi:10.1016/j.watres.2009.09.040

Totsche, K. U. (2001). *Reaktiver stofftransport in böden: Optimierte experimentdesigns zur prozessidentifikation.* (75 ed.): Chair of Soil Science and Soil Geography, University of Bayreuth, Germany.

Totsche, K. U., Jann, S., & Kogel-Knabner, I. (2007). Single event-driven export of polycyclic aromatic hydrocarbons and suspended matter from coal tar-contaminated soil. *Vadose Zone Journal, 6*(2), 233-243. doi:10.2136/vzj2006.0083

Tourney, J., & Ngwenya, B. T. (2014). The role of bacterial extracellular polymeric substances in geomicrobiology. *Chemical Geology, 386*, 115-132. doi:10.1016/j.chemgeo.2014.08.011

Tripathi, S., Champagne, D., & Tufenkji, N. (2012). Transport behavior of selected nanoparticles with different surface coatings in granular porous media coated with pseudomonas aeruginosa biofilm. *Environ Sci Technol, 46*(13), 6942-6949. doi:10.1021/es202833k

Truesdail, S. E., Westermann-Clark, G. B., & Shah, D. O. (1998). Apparatus for streaming potential measurements on granular filter media. *Journal of Environmental Engineering-Asce, 124*(12), 1228-1232. doi:Doi 10.1061/(Asce)0733-9372(1998)124:12(1228)

Tufenkji, N., & Elimelech, M. (2004). Correlation equation for predicting single-collector efficiency in physicochemical filtration in saturated porous media. *Environ Sci Technol, 38*(2), 529-536. doi:10.1021/es034049r

Vlamakis, H., Chai, Y., Beauregard, P., Losick, R., & Kolter, R. (2013). Sticking together: Building a biofilm the bacillus subtilis way. *Nat Rev Microbiol, 11*(3), 157-168. doi:10.1038/nrmicro2960

Wagner, S., Gondikas, A., Neubauer, E., Hofmann, T., & von der Kammer, F. (2014). Spot the difference: Engineered and natural nanoparticles in the environment—release, behavior, and fate. *Angewandte Chemie International Edition, 53*(46), 12398-12419. doi:10.1002/anie.201405050

Wang, L. L., Wang, L. F., Ren, X. M., Ye, X. D., Li, W. W., Yuan, S. J., . . . Wang, X. K. (2012). pH dependence of structure and surface properties of microbial EPS. *Environ Sci Technol, 46*(2), 737-744. doi:10.1021/es203540w

Wanner, O., Cunningham, A. B., & Lundman, R. (1995). Modeling biofilm accumulation and mass transport in a porous medium under high substrate loading. *Biotechnol Bioeng, 47*(6), 703-712. doi:10.1002/bit.260470611

Waychunas, G. A., & Zhang, H. (2009). Structure, chemistry, and properties of mineral nanoparticles. *Elements, 4*(6), 381.

Wei, X., Fang, L., Cai, P., Huang, Q., Chen, H., Liang, W., & Rong, X. (2011). Influence of extracellular polymeric substances (EPS) on Cd adsorption by bacteria. *Environ Pollut, 159*(5), 1369-1374. doi:10.1016/j.envpol.2011.01.006

Werner, S., Sigg, L., & Sulzberger, B. (1992). *Chemistry of the solid-water interface: Processes at the mineral-water and particle-water interface in natural systems*. New York: Wiley.

Wilson, S. C., & Jones, K. C. (1993). Bioremediation of soil contaminated with polynuclear aromatic hydrocarbons (PAHs): A review. *Environ Pollut, 81*(3), 229-249. doi:10.1016/0269-7491(93)90206-4

Xiao, Y., & Wiesner, M. R. (2013). Transport and retention of selected engineered nanoparticles by porous media in the presence of a biofilm. *Environ Sci Technol, 47*(5), 2246-2253. doi:10.1021/es304501n

Xu, Y., & Zhao, D. (2007). Reductive immobilization of chromate in water and soil using stabilized iron nanoparticles. *Water Res, 41*(10), 2101-2108. doi:10.1016/j.watres.2007.02.037

Yucel, M., Gartman, A., Chan, C. S., & Luther, G. W. (2011). Hydrothermal vents as a kinetically stable source of iron-sulphide-bearing nanoparticles to the ocean. *Nature Geoscience, 4*(6), 367-371. doi:10.1038/Ngeo1148

Zänker, H., Moll, H., Richter, W., Brendler, V., Hennig, C., Reich, T., . . . Hüttig, G. (2002). The colloid chemistry of acid rock drainage solution from an abandoned zn–pb–ag mine. *Applied Geochemistry, 17*(5), 633-648. doi:10.1016/s0883-2927(01)00126-3

Zevi, Y., Dathe, A., McCarthy, J. F., Richards, B. K., & Steenhuis, T. S. (2005). Distribution of colloid particles onto interfaces in partially saturated sand. *Environmental Science & Technology, 39*(18), 7055-7064. doi:10.1021/es048595b

Zhang, Q., Hassanizadeh, S. M., Liu, B., Schijven, J. F., & Karadimitriou, N. K. (2014). Effect of hydrophobicity on colloid transport during two-phase flow in a micromodel. *Water Resources Research, 50*(10), 7677-7691. doi:10.1002/2013WR015198

Zhao, W., Walker, S. L., Huang, Q., & Cai, P. (2014). Adhesion of bacterial pathogens to soil colloidal particles: Influences of cell type, natural organic matter, and solution chemistry. *Water Res, 53*, 35-46. doi:10.1016/j.watres.2014.01.009

Zhuang, J., & Yu, G. R. (2002). Effects of surface coatings on electrochemical properties and contaminant sorption of clay minerals. *Chemosphere, 49*(6), 619-628. doi:http://dx.doi.org/10.1016/S0045-6535(02)00332-6

Acknowledgment

First and foremost, I would like to thank my supervisor Prof. Dr. Kai Uwe Totsche for his guidance and encouragement during my Ph.D. Thank you very much for giving me this opportunity to do Ph.D. in your group with a very little geology background I came with. You believed in me when I had lost faith. Your continuous motivation and valuable hints kept me going through all the challenges during my Ph.D.

I would also like to acknowledge Prof. Dr. Kirsten Küsel for all the assistance with the microbiology aspect for my work. I am very grateful for all the valuable inputs she gave me during our discussions. I also appreciate the support received from the lab members of the Küsel lab during my time there.

I am very grateful to research training group GRK 1257 for supporting this research. Multiple seminars, workshops and colloquiums conducted in this group help me a lot to learned different aspects in bio-geosciences.

This work would not have been achievable without the cooperation of many people. Special thanks are due to Dr Cornellia Bellmann and Mrs Anja Caspari from Leibniz-Institute für Polymerforschung Dresden for electrokinetic measurements and Ms Hella Schmidt from Leibniz Institute for Natural Product Research, Jena for her inputs in CLSM microscopy. I am also indebted to my lab mates Akardius, Karin, and Mathias for helping me with SEM imaging, FTIR and XRD analysis. Also, would never forget the help I was given from the lab personals Gundel, Katy and Christel for numerous aspects in the lab despite our language barriers. I also appreciate Thomas for his mathematic wizardry in assisting me work out the DLVO and EDLVO equations. I am also thankful to Andreas for his inputs during writing and his help in translation of the abstract. Also, thanks are due to all the lab members for a positive working environment.

This fresh beginning in Germany would not have been feasible without support from Sabina, Katharina, Robert and Benny who made me feel at home in this county far away from home. A special mention to all my friends in different countries and back home who always spoke to me at unearthly hours just because I was feeling lonely.

And finally, I owe a lot to Aie, Baba, Dada and Mothiaie for inculcating great values and making me who I am today. Also, I would like to mention my Aunt Seema for standing behind me when I needed her the most and giving me a push to move forward to achieve my dreams. I am also grateful to my in-laws Aie and Nana for accepting me and continuing to stand by my side. And finally, my loving husband Nilesh for being the best anti-stress punching bag and continuing to support me.

Tabellarischer Lebenslauf

Sneha Narvekar
Birth date: 19/12/1985
Birth place: Dombivli, India

Work experience

May 2011-till today	Scientific co-worker at Friedrich Schiller University of Jena, Institute of Geosciences, Jena Germany
June 2008 – March 2011	Full time lecturer at University of Mumbai, Department of Microbiology and Biotechnology, B.N. Bandodkar College of Science, Thane, India

Education

June 2006 - May 2008	Masters of science (Microbiology), University of Mumbai, India
June 2003 - May 2006	Bachelors in science (Microbiology and Biochemistry), University of Mumbai, India.
June 2001 - May 2003	Higher Secondary schooling from Maharashtra State Board of Secondary and Higher Secondary Education, India
June 1991 - May 2001	Secondary Schooling from Maharashtra State Board of Secondary and Higher Secondary Education, India

…… …….

Place, Date Sneha Pradip Narvekar

Selbstständigkeitserklärung

Ich erkläre, dass ich die vorliegende Arbeit selbstständig und unter Verwendung der angegebenen Hilfsmittel, persönlichen Mitteilungen und Quellen angefertigt habe.

. . . .

Ort, Datum. Unterschrift des Verfassers